BOUC-WEN MODEL PARAMETER IDENTIFICATION FOR A NEW MAGNETO-RHEOLOGICAL FLUID DAMPER USING PARTICLE SWARM OPTIMIZATION

MOHD AZRAAI BIN MOHD RAZMAN

MASTER OF ENGINEERING (MANUFACTURING)

UNIVERSITY MALAYSIA PAHANG

UNIVERSITI MALAYSIA PAHANG

DECLARATIONOF THESIS AND COPYRIGHT

Author's full name	:	Mohd Azraai bin Mohd Razman
Date of birth	:	21 Jun 1987
Title	:	Bouc-Wen model parameter identification for a new Magneto-rheological fluid damper using Particle Swarm Optimization
Academic Session	:	2013/2014

I declare that this thesis is classified as:

☐ **CONFIDENTIAL** (Contains confidential information under the Official Secret Act 1972)*

☐ **RESTRICTED** (Contains confidential information as specified by the organization where research was done)*

☐ **OPEN ACCESS** I agree that my thesis to be published as online open access (full text)

I acknowledge that Universiti Malaysia Pahang reserve the right as follows:

1. The Thesis is the Property of Universiti Malaysia Pahang
2. The Library of Universiti Malaysia Pahang has the right to make copies for the purpose of research only.
3. The Library has the right to make copies of the thesis for academic exchange.

Certified By:

(Student's Signature)	(Signature of Supervisor)
870621-14-5405	Dr. Gigih Priyandoko
New IC/ Passport Number	Name of Supervisor
Date: 5 Septmber 2014	Date: 5 September 2014

BOUC-WEN MODEL PARAMETER IDENTIFICATION FOR A NEW MAGNETO-RHEOLOGICAL FLUID DAMPER USING PARTICLE SWARM OPTIMIZATION

MOHD AZRAAI BIN MOHD RAZMAN

Thesis submitted in fulfilment of the requirements
for the award of the degree of
Master of Engineering (Manufacturing)

Faculty of Manufacturing Engineering
UNIVERSITI MALAYSIA PAHANG

SEPTEMBER 2014

SUPERVISOR'S DECLARATION

I hereby declare that I have checked this thesis and in my opinion, this thesis is adequate in terms of scope and quality for the award of the degree of Master of Engineering in Manufacturing Engineering

Signature:

Name of Supervisor: DR. GIGIH PRIYANDOKO
Position: SENIOR LECTURER
Date: 05/09/14

Signature:

Name of Co-supervisor: DR. AHMAD RAZLAN BIN YUSOFF
Position: SENIOR LECTURER / DEPUTY DEAN
Date: 05/09/14

STUDENT'S DECLARATION

I hereby declare that the work in this thesis is my own except for quotations and summaries which have been duly acknowledged. The thesis has not been accepted for any degree and is not concurrently submitted for award of other degree.

Signature:

Name: MOHD AZRAAI BIN MOHD RAZMAN
ID Number: MMF11006
Date: 05/09/14

ACKNOWLEDGEMENTS

Grasping the years of knowledge embankment, diverse perception has been receive upon completing this thesis. My highest appreciation to the Creator of science and technology, He who is sole invent it for mankind to explore.

To my supervisor I would show my deepest gratitude for the guidance and knowledge transfer. Professional ethics on the task given has shown me the life of an academician and researcher. In depth knowledge and the exposure have made me aware of the ever yearning on the current trend in technology development.

Thanks to the Faculty of Manufacturing Engineering and University Malaysia Pahang for granting me this opportunity to encounter the academic and research world with the involvement by the staff and students.

To my parents and family for the encouragement in pursuing my studies and the conviction they have lent for me to achieve my goal. To my beloved wife who has been my backbone in completing this thesis and for the future outcome towards becoming a successful engineer.

In hope that what I have benefited will flourish and disseminate for the future sustenance.

ABSTRACT

In constructing a reliable semi-active suspension system, the modelling of the damper is imperative as it produces the controllability on the suspension system. The modelling of Magneto-rheological (MR) fluid damper for the control device has been major focuses throughout the decades as semi-active systems are deems to be efficient in vibration suppression for various applications. MR fluid damper is abided by the behaviour of hysteresis model that not just predict the subsequent impact, but has the ability to retract the motion by the model internal memory. Acquiring a suitable model comes a setback from the natural existence of non-linearity from the MR fluid damper as the parameters of the hysteresis model may requires tuning as the response time for the absorber to response are in milliseconds. Hence, Particle Swarm Optimization (PSO) was introduced for altering significant parameters for Bouc-Wen hysteresis model to replicate the MR fluid damper performance in real-time. The objectives are succinct in three main criteria starting with the development of MR fluid damper, then a representation of hysteresis model and lastly optimizing these parameters by inducing PSO algorithm. Validations by physical experiment and simulation were conducted to enhance the justification of the present model. These performances are measured in force against displacement and force against displacement for the hysteresis model to depict MR fluid damper behaviour. The average marginal error was presented to strengthen the model along with analysis and discussion in deliberating the outcome. Approximation of the model demonstrates dependable fitting compared to the experimental data with the average marginal error ranging from 6.0 % to 8.3 %. The findings suggest that several parameters of the hysteresis systems requires boundary and by imposing the known sensitive variables to the model can emulated into near perfect model.

ABSTRAK

Dalam pembinaan sebuah sistem pergantungan separa-aktif, pembikinan struktur terhadap penyerap adalah penting untuk menghasilkan sistem pergantungan yang boleh dikawal. Untuk membikin struktur peredam cecair MR sebagai bahan kawalan telah menjadi tumpuan utama sejak kebelakangan dekad apabila sistem separa-aktif ini dikatakan berfungsi secara telus dalam mengagihkan gegaran bagi aplikasi yang meluas. peredam cecair MR ini mengandungi tingkah laku yang diperoleh dari struktur histeresis yang bukan sahaja boleh mengagak impak di masa hadapan, malah mempunyai kebolehan untuk menjejak kembali pergerakkan dengan kehadiran imbasan dalaman. Memenuhi sebuah modal yang sesuai, datangnya kekurangan dari lumrah azali pengkadaran yang tidak melurus dari peredam cecair MR di mana parameter-parameter histeresis modal mugkin memerlukan penalaan pada tindak balas masa yang berlaku dalam masa yang singkat milisaat. Jadi, Pengoptimuman Kawan Partikel (PSO) digunakan untuk mengubah parameter-parameter yang terbabit bagi struktur histeresis bagi menghasilkan struktur peredam cecair MR dalam waktu semasa. Objektif-objektif utama terbahagi kepada tiga bermula dari penghasilan peredam cecair MR, penyerupaan struktur hysteresis dan akhir sekali mengoptimumkan parameter-parameter dengan mengunakan algoritma PSO. Bukti dari eksperimen secara fizikal dan simulasi di jalankan untuk memperkukuhkan bukti penggunaan stuktur yang dilancarkan. Prestasi ini diukur melalui daya melawan kelajuan dan daya melawan ralat kedudukan. Purata beza dibentangkan bagi memperkuatkan analisa serta perbincangan atas hasil yang dikeluarkan. Anggaran dari struktur ini menunjukkan kebergantungannya terhadap eksperimen di dalam lingkungan 6.0 % ke 8.3 % purata perbezaan. Penemuan berasaskan atas dasar parameter-parameter daripada hysteresis memerlukan lingkungan dan dengan menyeterai pemalar yang sensitif untuk menghasilkan modal yang telus.

TABLE OF CONTENTS

LIST OF TABLES

LIST OF FIGURES

LIST OF SYMBOLS

ΔP	Pressure drop
ΔP_n	Viscous component
ΔP_τ	Field dependent induced yield stress component
Q	Pressure driven of MR fluid flow
L	Length
g	Fluid gap
w	Width of Annular Orifice
η	Plastic Viscosity of MR Fluid
τ_y	Field Dependant Yield Stress
C	Ratio of $\Delta P_\tau/\Delta P_n$
F_{shear}	Force Generated by Two Poles Plates
F_η	Viscous Shear Force
F_τ	Magnetic Field Dependant Shear Force
A	Pole Plate Area
S_{shear}	Relative Velocity between Pole Plates
V	Volume of Activated MR Fluid
λ	Desired Control Ratio
W_m	Mechanical Power Dissipation
S	Displacement of the Valve
H	Magnetic Field
l	Length of The Wire
N	Number of Coil Turn

i	Current Supplied to the Coil
μ	Relative Permeability of the Material
μ_0	Free Space Permeability
B_c	Magnetic Strength For The Core
B_w	Magnetic Strength At The Wall
ϕ	Magnetic Flux
B_g	Magnetic Strength At Fluid Gap
A_g	Cross Sectional Areas of the Fluid Gap
A_c	Cross Sectional Areas of the Core
A_w	Cross Sectional Areas of the Cylinder Wall
t_g	Fluid Gap
l_c	Core Length
l_w	Wall Length
c	Viscous coefficient
k	Stiffness Coefficient
α	Scaling factor of hysteresis
z	Hysteresis Displacement
β	Hysteresis Parameter
γ	Hysteresis Parameter
δ	Hysteresis Parameter
m	Mass
$u(t)$	Displacement
$F(t)$	Restoring Force
$f(t)$	Excitation Force
F_y	Yield Force

u_y	Yield Displacement
$z(t)$	Dimensionless Hysteretic Parameter
$sgn(\bullet)$	Signum Function
n	Exponential Parameter
k_e	Initial Stiffness
k_p	Post-Yielding Stiffness
f	Damping Force
f_0	Damper Force Offset
$\tau_{y(field)}$	Yield Stress Induced by the Magnetic Field
$\dot{x}$	Nonzero Piston Velocities
f_c	The Magnitude of Hysteresis
$pbest$	Best Position
$gbest$	Best Global Value
$lbest$	Best link
x_k^i	Initial Swarm Particles of Positions
v_k^i	Initial Swarm Particles of Velocity
i^{th}	Number Of Particle
$rand$	Uniformly Distributed Random Variable
p_k^g	Best Global Value
$vmax$	Maximum Velocity
φ	Constant Acceleration
c_1	Constant Acceleration
c_2	Constant Acceleration
w	Inertia Weight
$D1$	Wire Hole inside The Hollow Shaft

D2	Internal Diameter of The Piston Ring
D3	Inner Diameter of Internal Piston
D4	Outer Diameter of Piston Ring
D5	Height of Magnetic Choke
G	Fluid Gap
W	Flange Thickness
A	Ampere
F_{exp}	Experimental Data
F_{sim}	Simulation Data

LIST OF ABBREVIATIONS

2D	Two dimensional
3D	Three dimensional
ANFIS	Adaptive Neuro Fuzzy Inference System
BW	Bouc-Wen
DAQ	Data Acquisition
DS	Design Space
EH	Electro-Hydraulic
ER	Electro-rheological
GA	Genetic Algorithm
LVDT	Linear Variable Differential Transformer
MR	Magneto-rheological
MTS	Material Testing System
PSO	Particle Swarm Optimization
RMSE	Root-mean-square error
SGA	Standard Genetic Algorithm

CHAPTER 1

INTRODUCTION

1.1 RESEARCH BACKGROUND

Semi-active suspension application throughout the decades has seen promising potential predominantly on the stability and robust nature for controlling exerted vibrations in automotive particularly. Hence, the role of influencing the vibration is obliged by the damper. Magneto-rheological (MR) fluid is alleged to be a smart material that able to alter its resistivity with pertinent operation. In despite of the adaptable condition designated for the MR fluid damper, the sophistication on modeling the behavior has been scrutinized ever since.

Orientation of iron particles inside the MR fluid is influenced by the strength of the magnetic field that is dignified from the amount of current induced. Hence the resistive force that constraint the flow of fluid through orifice inside the piston is competent to regulate viscosity for the entire MR fluid damper system. In spite of having the feature to manipulate the restrictive force, the development of MR fluid damper ought to be realized. In drafting the suitable MR fluid damper in synchronizing with parametric identification, several factors are required to perform the investigation in intention for modeling and parameter identification. These aspects include the dimension of damper, geometric structural and magnetic design.

Identification methods withal have endured the modeling of MR fluid damper as an alternative source in replicating its performance. Supplementary, the bearing of MR fluid damper possesses hysteresis model systems. It relies on the current state inclusively with prediction of the forthcoming situation. Various techniques were applied in order to realize onto a leading model. Methods that are frequently associated with modeling are categorized either parametric or non-parametric. The importance of prototyping is to formulate the groundwork for applying into control strategies before extending the execution for semi-active suspension. Nevertheless, the complexity of modeling the MR fluid damper is erratic knowing the fact that absorber has nonlinearity feature. Furthermore, the drawback of hysteresis model is the presence of dynamic halt during intermission of input and output. An explicit hysteresis system called Bouc-Wen model suggested by Kwok demonstrates substantial quality as a modeling method to match the behavior of MR fluid damper (Kwok et al., 2006). It was modified from initial models discovered by Bouc in 1971 and further enhanced by (Wen, 1976) up till now it is well recognized as Bouc-Wen model. Kwok et al. (2006) revised certain traits from Bouc-Wen to ensure the stability of the hysteresis and performances to depict the MR fluid damper were consented.

In furtherance of imitating the MR fluid damper, Particle Swarm Optimization (PSO) method was introduced to enhance the parameter search for identification. The concept of PSO is emulating the social behaviors of wildlife interaction primarily in a clustered movement for instance in a flock of birds or swarming ants. The collaboration between (Kennedy and Eberhart, 1995) had leaded a renowned optimization method and has been seen in diverse application ever since. Subsequent to the motion of these groups, it has similar analogy to acquire best parameter value, for instance a flock of birds finding source of food in randomize formation until the location is found by another bird hence the position is predicted as an optimized position. This analogy is then applied onto the hysteresis model to locate the finest possible value in imitating the MR fluid damper characteristics.

Parametric modeling have arisen several drawbacks during processing as the domain of control force range is larger than the passive absorber. Subsequently the development of MR fluid damper has subjective limitations especially on the properties of amending the viscosity which rely on the amount of applied magnetic field. Thus the accuracy of modeling the hysteresis model has become major dispute amidst existing identification approaches. In addition to emerging complications, PSO has to endeavor the assignments of recalculating the utmost suitable parameters values for curve fitting of MR fluid damper model. Under these circumstances, extensive researches are required to increase the performances of hysteresis model that represents MR fluid damper. This is by the agency of implementing PSO algorithm to optimize the parameters values subsequently enhancing hysteresis model in replicating the MR fluid damper.

The main purpose of this research is to implement PSO to optimize the parameter values of the Bouc-Wen hysteresis model proposed by Kwok et al. (2006) that depicts the behavior of MR fluid damper.

1.2 PROBLEM STATEMENT

To acquire data from MR fluid damper and to be manipulated for optimization, a number of interjections must be sorted out prior to finalizing the end results.

1) The foremost predicament would be raised from designing the modular MR fluid damper that can satisfy emulating the behavior for parametric identification. In specific would be the coil design correlates to viscosity changes for given current input.
2) Modeling the MR fluid damper in hysteresis structure may result in uncertainties and augmented noise.
3) Optimizing using PSO carries the setback of depicting the hysteresis models in which the PSO parameters need to consider tolerance result and account the hysteresis parameters that are adjustment sensitive.

1.3 RESEARCH OBJECTIVE

Based on the research motivation, raised several queries:

1) Determine the functional and practical MR fluid damper that qualifies to be tested and compared with simulation from the structural and magnetic design.

2) Suggest an algorithm of PSO that is able to optimize the parameter value for hysteresis model that represents the MR fluid damper behavior using Bouc-Wen hysteresis model.
3) Determine the receptive hysteresis parameters that alter the behavior of MR fluid damper.

In this research, three hypotheses have been reached which are:

1) The structural design of MR fluid damper has distinctive specifications as the relation of resistive force and magnetic field strength influenced by current input.
2) Parameter values of Bouc-Wen hysteresis model proposed by Kwok capable of being optimized by using the advocated PSO algorithm.
3) There will be several hysteresis parameters that delicate towards the MR fluid damper modeling which leads to fluctuating results

The objectives of research are realized as:

1) To compose a control algorithm that proficient in enhancing the best parameters value by integrating experimental and simulation study consequently reproducing a noteworthy model of MR fluid damper to be utilize as a model controller of semi-active suspension device.
2) To prove that several hysteresis parameters are certainly requires regulation to generate agreeable MR fluid damper model and by deducing these boundaries the replication of a more realistic hysteresis model are practicable.

1.4 RESEARCH SCOPE

To reach the objectives as mentioned, the research scope has been clarified:

1) This research only focuses on mono-tube damper that has one reservoir for the fluid to flow. The structural and magnetic design is solely on the magnetic choke, the area of fluid passing through the orifice.

2) An original equipment of shock absorber was employed to enclose the primary objective of designing the dimension at magnetic choke to generate a bounded force and permitted operating current. The data collected from MR fluid damper performance was classified under distinguished test condition.

3) The parameter identification method proposed only on the algebraic function. The comparison of models was done within this subject to validate the leading model and subsequently the main reason is to optimize an existing model.

4) PSO algorithm was employed to enhance the performance of hysteresis Bouc-Wen models. The findings of the hysteresis parameters were amplified to depict the experimental data of the MR fluid damper for various test condition. The algorithm is preset to a reduce uncertainties of parameter search and was employed only as a method of parameter enhancer.

1.5 RESEARCH METHODOLOGY

The research activities were done in four stages. Firstly, the reviews on the development of MR fluid damper, hysteresis model and parameter identification were done. It was done for the comprehension on the current technology expansion with respect to MR fluid damper modeling using parametric identification and the algorithm PSO.

Next is the structural and magnetic design modification on the original damper. The proposed MR fluid damper is based on the operating platform for collecting data by experiment. When the design was finalized, the data was collected in various test conditions and stored for impending modeling verification.

Third, parametric identification was imposed beforehand in replicating the behavior of MR fluid damper. The algebraic function from a number of hysteresis models was steered by comparing selected models, Bingham, Bouc-Wen and Bouc-Wen by Kwok. Simulation method was operated in investigating these models either by employing MATLAB or Simulink reliant from the model intricacy. Significant parameters that initiate the modeling of hysteresis model profile were identified. The assessment was preceded to PSO algorithm for optimizing the suitable model for reproducing the MR fluid damper performance. Optimization method was done via MATLAB code parallel to the hysteresis model acquired by parametric identification stage.

Lastly the verification of the simulation results with reference to the experimental data was attained by elementary statistics procedure. Parameters acquired from the enhanced hysteresis models are examined. The validation on the best fitting model is investigated through the marginal error and further justified by the percentage error on each point between retrieving records experimentally and the numerals results from simulation. For every test condition the outcome was observed and justification for the results was deliberated.

The flowchart of research activities is done by the following steps as in Figure 1.1

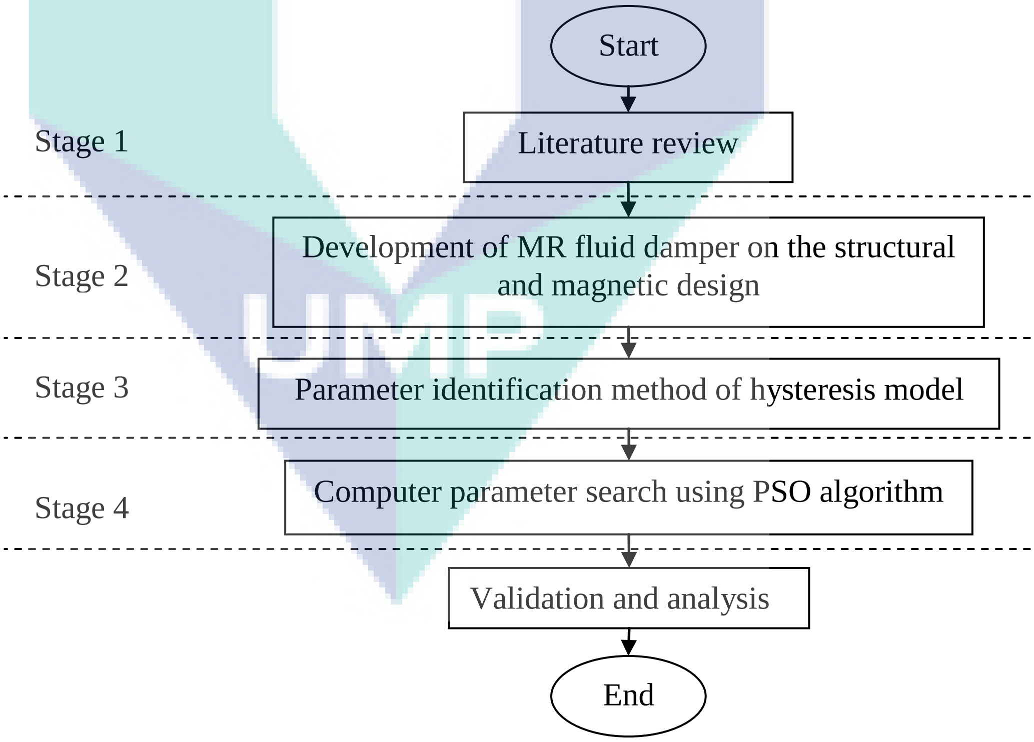

Figure 1.1: Flowchart of research activities

1.6 THESIS STRUCTURE

This thesis is structured as follows:

Chapter 2: Literature review – discussion on the MR fluid damper development, parametric hysteresis modeling, PSO algorithm in the perspective of background and research literature.

Chapter 3: Research methodology – the outline of research development is extracted into hardware and simulation phases from elaborating on the MR fluid damper design and collecting damper performances the simulation synthesizing and overall evaluation results can be achieved.

Chapter 4: Results and discussion – results obtained from previous chapter was deliberated for analysis apprehension. The prime hysteresis model was determined from hysteresis comparison, implementation of PSO has enhanced the model and optimized parameters were resolved. The justification was done by underlining the error between experimental and simulated results.

And lastly **Chapter 5: Conclusion** – conclusion of the entire experiment based on the construction of this research and proposed improvements for future research work.

CHAPTER 2

LITERATURE REVIEW

2.1 INTRODUCTION

In this chapter, a review on the MR fluid damper design, hysteresis model comparison and PSO operation is discussed. The review follows the basis of this research according to practical realization of this project. Three main aspects on this review will sum up extending to the scope for generalizing the research project.

MR fluid damper is a type of controllable device which has the property to change its viscosity depending on the applied magnetic field. Hysteresis model depicts the behaviour of the damper correlates to the input/output relationship. Parametric model are based on mechanical principle including interpretation by arranging springs and dashpot. PSO)is an optimizing technique based on population and individual search finding from emulating social interaction (i.e. bird flocks) (Kennedy and Eberhart, 1995).

2.2 MR FLUID DAMPER

The MR fluid is defined as a smart material that can shift its property and early discovery was dated back in the 1940's (Rabinow, 1948; Winslow, 1947; Winslow, 1949). The manipulative system allows vibrations suppression ploughed on the performance in civil and mechanical structures. A survey was conducted where MR fluid damper as a semi-active devices, in which a property can be accustomed immediately but the system cannot receive energy (Dyke and Spencer, 1997). The versatility and adaptability of active systems are maintained by these device and act as dependant passive devices denote recognition for MR fluid damper to be unswerving.

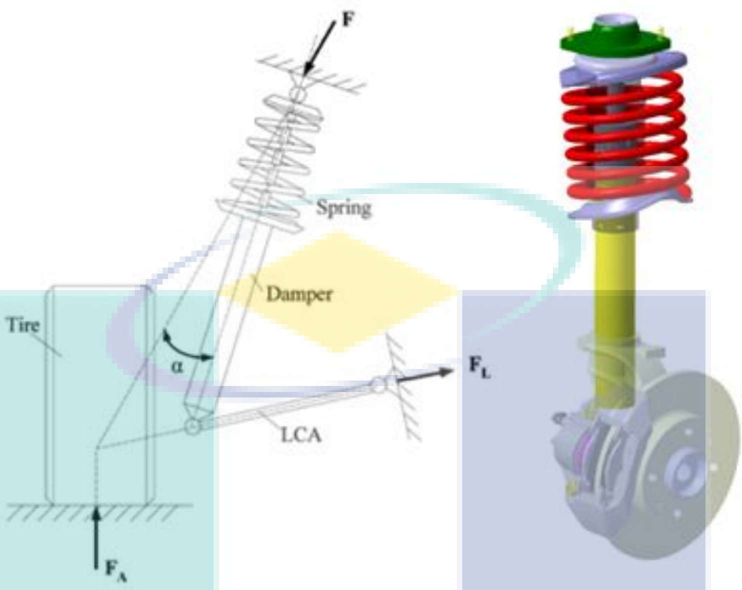

Figure 2.1: Suspension schematic

Source: Liu et al. (2006)

Figure 2.1 shows a representation of a suspension system. It consists of spring, damper, mountings, knuckle and linkage (arm). The stiffness of the system is carried by the spring which isolates the vehicle body from disturbances, thus energy is released and supply vibration to the system. This is where shock absorber dissipates the energy supplied. By applying the damping coefficient into the system equation, it equalise the vibration from releasing and dissipating energy.

The elastic element usually a coil spring carries the static load from the suspension system. It conveys forces proportional and opposed to the suspension elongation. The damping element however is the absorber or damper which differs from user's specification. Hydraulics shock absorber, electro-hydraulic (EH), magneto-rheological (MR) or electro-rheological (ER) often seen on applications and technologies of semi active suspensions. The reason is because dynamic behaviour of the system is controlled by these dampers to enhance the stability of the body and delivers negligible force at steady-state. The mechanical linkage element primarily links up the suspension system to the body in other words sprung body to the unsprung mass.

2.2.1 Damper advancement and classification

Recent technologies on suspension systems have expanded to a new approach that categorize each suspension technology on its significant characteristics (Hrovat, 1997; Guglielmo et al., 2008; Isermann, 2003). The first case of active suspension, it can be narrowed down to three well executed applications on the active field; load-levelling, slow-active and fully-active. The difference between all of these is the actuation framework of the bandwidth that the suspension can withstand. For load-levelling the bandwidth is at the fine underline of the main suspension dynamics, however bandwidth between body and wheel dynamics, and full-bandwidth is the slow-active and fully-active suspensions respectively.

There are two criterion to elaborate electronically controlled suspensions; energy input and bandwidth. The main comparison to notify the differences between active and semi-active is by energy insertion into the system. It is classified as 'Active' when energy is 'supplied' to the system, on the other hand it is considered as 'semi-active' when the suspension system is electronically customized to exclude energy insertion apart from the energy to steer the electronic parts. If the suspension can 'lift' the vehicle it said to be active or else it is semi-active systems.

Bandwidth is the other feature that characterizes the suspension system. It is the element in such that the specific reaction-time response can be modified electronically. Figure 2.2 represents the classification between passive, semi-active and fully active suspension systems (Ikhouane and Rodellar, 2007).

System	Control (Force) Range	Control bandwidth	Power Request	Improvement compared to passive system		Control variable
				Comfort	Safety	
Passive	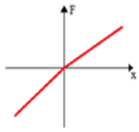	-	-	-	-	-
Semi-Active	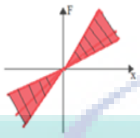	30-40Hz	10-20W	20-30%	10-25%	c (damping ratio)
Fully Active	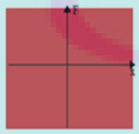	20-30Hz	5-10kW	>30%	>30%	F (force)

Figure 2.2: Classification of suspension system

Source: Ikhouane and Rodellar (2007)

Early research mainly focused on ER fluid dampers for civil applications (Ehrgott and Masri, 1992; Gavin et al., 1994). Alternatively MR fluid damper receives recognition on the significant potential (Spencer et al., 1997). Both ER and MR fluid dampers are pragmatically competing in controllable dampers development. Even though ER fluids was seen to exercise in early stages of controllable dampers, MR fluid increased on its practical usability and appeared to be more charismatic as a substitute. On magnitude derivation, a step greater was concluded for MR fluid than ER and on the operation boundary in temperature MR fluid was recorded to function from -40 ^{o}C to 150 ^{o}C with minor discrepancy of yield stress. Additional to the substance behaviour, the fluids are not vulnerable to impurities under the typical manufacturing and usage circumstances. A frail separation of particles during flow conditions is insignificant towards the performance of the damper exemplify the potential of MR fluid to be more practical. On the additives aspects, wider range of substances such as anti-ear agents and dispersants can be inserted to enhance the damper character for instance seal life, bearing, and leakage as the magneto-polarization magnetism are not affected by the electro-chemistry.

From the advantages of the MR fluid compared to ER fluid it is clear to say that the MR fluid are less perturbing in generalising an operation. Furthermore, the main concern is more on the behaviour of the damper rather than material characteristics.

2.2.2 Magneto-rheological damper characteristic

MR fluid damper is a semi-active control device that interchanges its viscosity once magnetized (Bossis et al., 2002). MR fluid comprises of oil and substantial amount of iron particle. The structure of MR fluid damper is shown on Figure 2.3. The MR fluid is lodged into the damper cylinder which allows it to flow through the orifices. Magnetisable particles submerge in the fluid actuate the MR fluid damper. This is due to magnetic field supplied from the magnetic choke prior to current supply as a consequence aligned the particles in chain-like structures perpendicular to fluid flows (Bossis et al., 2002). Subsequently the physical characteristics of the MR fluid are determined by the input current which controls the viscosity as the fluid changes to semi-solid form (Ahn et al., 2009; Ashfak et al., 2012). A change of pressure from high to low chamber through orifice contributes the change of damping ratio in conjunction with increased yield strength, hence a semi-active absorber produced.

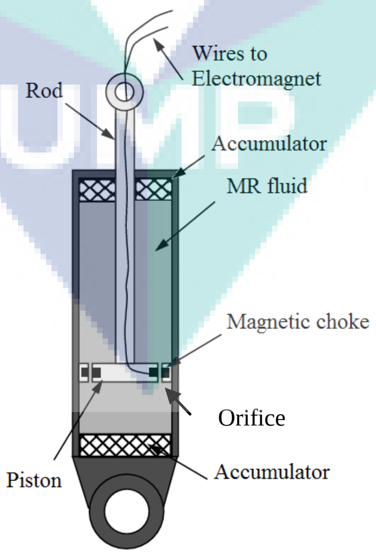

Figure 2.3: MR fluid damper schematic

Source: (Bossis, 2002)

Even so the MR fluid damper is capable of applying control mechanism; the non-linearity and representation of the response are the negative aspects that need to be look upon. Moreover, controller design comes parallel with model of the actuator resulting to greater obstacles of utilizing the MR damper. Nevertheless the two major conflicting requirements in vehicle handling of ride and comfort can be deal by the coherent solutions from MR fluid damper. However, before any realizable design of the controller to occur, it is essential that a tractable model of MR fluid damper is obtained (Jansen and Dyke, 2000).

2.2.3 MR fluid damper element and structural design

Properties of MR fluid contribute a controllable form for the shock absorber. This smart material comprises of miniscule (micro or nano) particles in the fluid that adjust the viscosity of the damper into a semi-solid form when magnetic field is applied. Meticulous steps are required particularly in designing the piston inside the MR fluid damper for tolerate the rapid viscosity regulation. Figure 2.4 illustrates the iron particles alignment during compression or rebound in magnetic choke region.

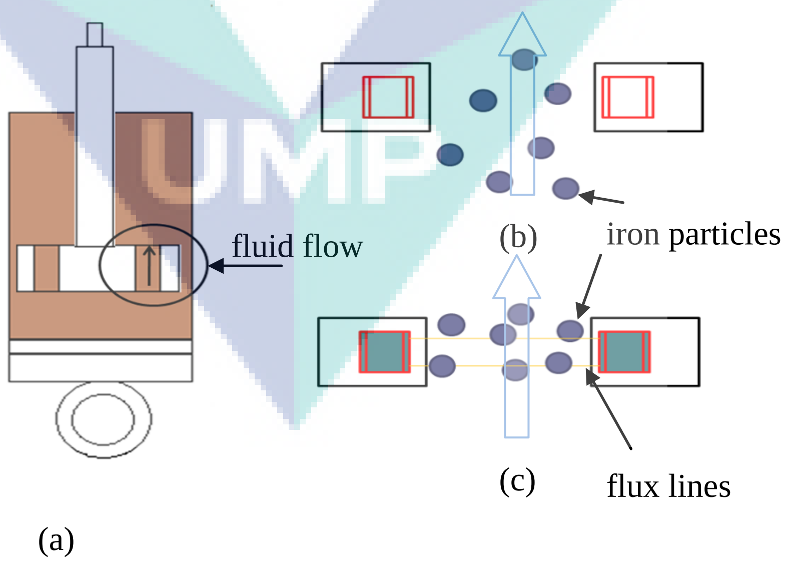

Figure 2.4: Fluid flow **(a)** Choking point flow **(b)** passive mode **(c)** magnetize mode

For Figure 2.4 (b), it illustrates the iron particles are in randomize location in which no current is exerted into the absorber. Responses of damper are identical to what is known as passive mode damper. However, initializing the magnetic field will produce an arrangement of iron particles in parallel to the magnetic flux lines. Thus, the formation that shaped through alignments of iron these particles refrained the MR fluid flow and act as a resistance.

On the progression of MR fluid flow mode, there are three practices that these modes can be enforced to. These approaches are widely known as valve, shear and squeeze mode. Valve mode are often seen in most damper application considering the flow of MR fluid are barred from the chain-line of iron particles governed by the magnetic field between two fixed plates. The valve mode is exhibited in Figure 2.5. These are where the MR fluid region is said to be covered by the magnetic flux lines and referred as the “choking points”. Altering the magnetic field strength will subsequently affect the fluid viscosity as it is inter-changeable when it increases the resistance of fluid flow until saturation point is met. It is construe as the damper resistance refuse to increase as the magnetic field yield. The fluid are often represented as a Bingham solid with variable yield strength (Lord, 1999).

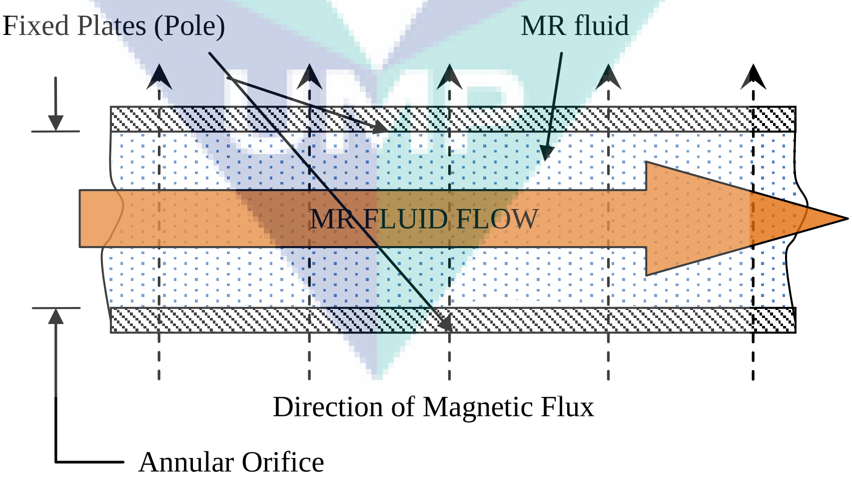

Figure 2.5: Valve mode flow

Source: (Poynor, 2001)

From the mode illustrator above, the pressure drop ΔP, can be represented by Equation 2.1, and it is the summation of both ΔP_n and ΔP_τ the viscous element and the yield stress respectively.

$$\Delta P = \Delta P_n + \Delta P_\tau \tag{2.1}$$

$$\Delta P = \frac{12\eta QL}{g^3 w} + \frac{C\tau_y L}{g} \tag{2.2}$$

where Q serve as the pressure driven of MR fluid flow, and L, g, and w are the length, fluid gap and the width of the annular orifice (area between plates) respectively. η is defined as the plastic viscosity of MR fluid and τ_y signified as the field dependant yield stress. However constant C, varies between 2 to 3 that relies on the ratio of

$$\frac{\Delta P_\tau}{\Delta P_\eta} \tag{2.3}$$

It can be deduced as following conditions;

for $C = 2$

$$\frac{\Delta P_n}{\Delta P_\eta} \leqq \sim 1 \tag{2.4}$$

and $C = 3$

$$\frac{\Delta P_n}{\Delta P_\eta} \geqq \sim 100 \tag{2.5}$$

Squeeze mode on the contrary, behaves when the MR fluid act as a thin layer (comparable to 0.5 mm) and squash between two paramagnetic poles area as shown in Figure 2.6. For the shear mode, a moving paramagnetic pole of the inner tube is magnetized with a fixed pole of the piston. This creates a resistance force confining the MR fluid flow. The resistance force can be expressed as Equation 2.6 and 2.7 where the force generated by two poles plates is F_{shear}, F_{η} govern for the viscous shear force, and F_{τ} is the magnetic field dependant shear force. To collaborate with earlier variables A and S_{shear} as the pole plate area and relative velocity between pole plates respectively (Poynor, 2001).

$$F_{shear} = F_{\eta} + F_{\tau} \tag{2.6}$$

$$= \frac{\eta S_{shear} A}{g} + \tau_y A \tag{2.7}$$

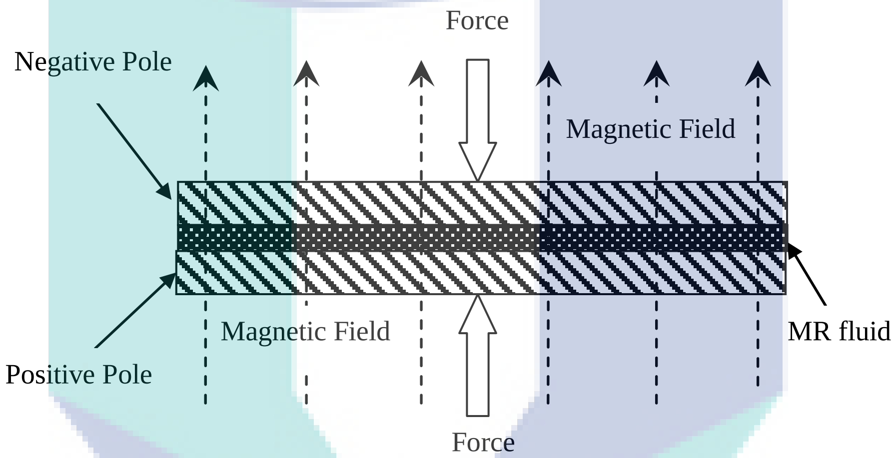

Figure 2.6: Squeeze mode MR flow

Source: Poynor (2001)

Accustomed to this, the volume of activated MR fluid, V can be extracted from equations Equation 2.1 to 2.7 an expression is given by:

$$V = k\left(\frac{\eta}{\tau_y^{\,2}}\right)\lambda W_m \tag{2.8}$$

in which the required control ratio is λ. In terms of mechanical dispersion, W_m represent the power loss hence the following equation expressed the valve mode characteristic. Thus, the parameters in Equation 2.8 for valve mode are:

$$k = \frac{12}{c} \tag{2.9}$$

$$\lambda = \frac{\Delta P_\tau}{\Delta P_\eta} \tag{2.10}$$

$$W_m = Q\Delta P_\tau \tag{2.11}$$

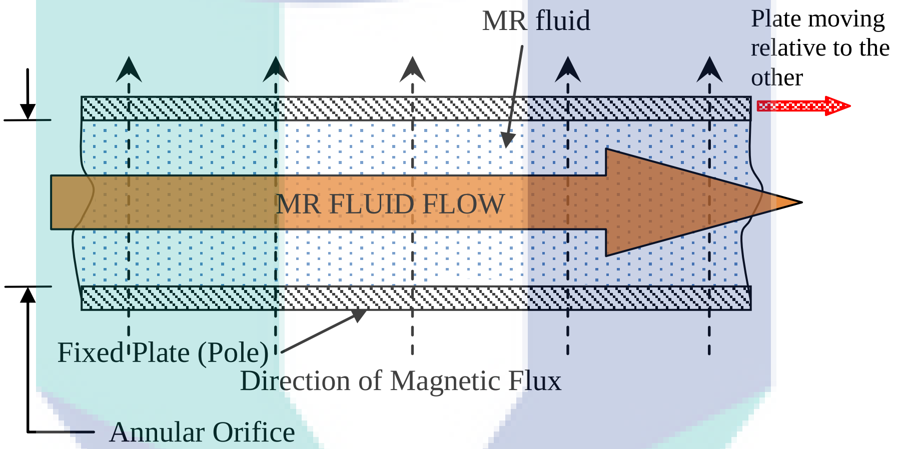

Figure 2.7: Shear Mode flow

Source: (Poynor, 2001)

Corresponding to the MR fluid device, the shear mode operates when one plate moving relatively to the other as depicted in Figure 2.7. The thin layer of MR fluid is usually range from 0.0127 mm to 0.381mm. Subsequently the counterpart motion for the fluid flow is expressed for the shear mode, conjointly as:

$$k = 1 \tag{2.12}$$

$$\lambda = \frac{F_\tau}{F_\eta} \tag{2.13}$$

$$W_m = F_\tau S \tag{2.14}$$

The additional parameter in this equation is S represented as the displacement of the valve.

In terms of magnetic circuit design, the fluid gap holds the essential barrier of designing a dependable magnetic flux transmitter that conducts it at the active magnetic region. To scrutinize the circuit, by inspecting using Kirchoff Law the magnetic circuit can be scrutinized and it is expressed by:

$$\sum H\ l = Ni \tag{2.15}$$

where H is commonly known as the magnetic field. The wire length is represented as l. The coil is supplied by an amount of current i, and to convert the total number of coil turn is represented by N. It is generally denoted that the units for magnetic field is Ampere times turns per meter and the magnetic strength of Tesla can be depicted as:

$$B = \mu\mu_o H \tag{2.16}$$

The equation above is the relation of magnetic field and strength, where the relative permeability of the material μ. It is directly proportional to μ_0 with the value of ($4\pi \times 10^{-7}$ Tm/A) the free space permeability and magnetic field.

The following equation are the conservation of magnetic flux existed in the fluid gap ϕ. It comprises of magnetic flux density for the core and wall given by B_c and B_w. For the strength at the fluid gap, the variable is known as B_g.

$$\phi = B_g A_g \tag{2.17}$$

$$B_c = \frac{\phi}{A_c} \tag{2.18}$$

$$B_w = \frac{\phi}{A_w} \tag{2.19}$$

The equations above express that the magnetic flux are indeed relate to the cross sectional areas at the fluid gap, core and cylinder wall A_g, A_c and A_w respectively. By calculating the equation in partition it will restrain the flux density from reaching a bottleneck effect or magnetically saturated. Equation 2.20 express the delivery of current input attained from the magnetic circuit equation.

$$i = \frac{1}{N}(H_g t_g + H_c l_c + H_w l_w) \tag{2.20}$$

where the number of turns N is inversely proportional to current input. The fluid gap, core length and wall length which is given as t_g, l_c and l_w respectively.

There are two types of tube design; mono-tube and twin-tube. Mono-tube has one reservoir for the fluid to flow. For the twin-tube damper, it consists of two fluid reservoirs that overlap one another. These are where the region of MR fluid that is known as “choking points” which is rendered around the magnetic lines. Changing the magnetic field strength will generate an inter-changeable state for the viscosity as the viscosity rises until the ceiling of saturation point is convened.

In this study, the type of piston used is the shear mode rather than valve mode or squeeze mode. The selection is based on the mono-tube MR damper configuration which has one reservoir on Figure 2.8. The usability of shear mode is to exploit the MR fluid and obstruct the flow transition between both paramagnetic plates.

In developing an MR fluid damper, several factors ought to be observed in order to imitate reasonable controlled responses. The MR fluid as a whole was conduct in specific array. The choice of damper itself has identified the piston element and thus relates to the paramagnetic poles movement and the restrictions created by the MR fluid. Once the selection was made, the MR damper model is second to the geometrical design, then to performance handling in search of several significant parameters. The limitations of the design rest on these parameters.

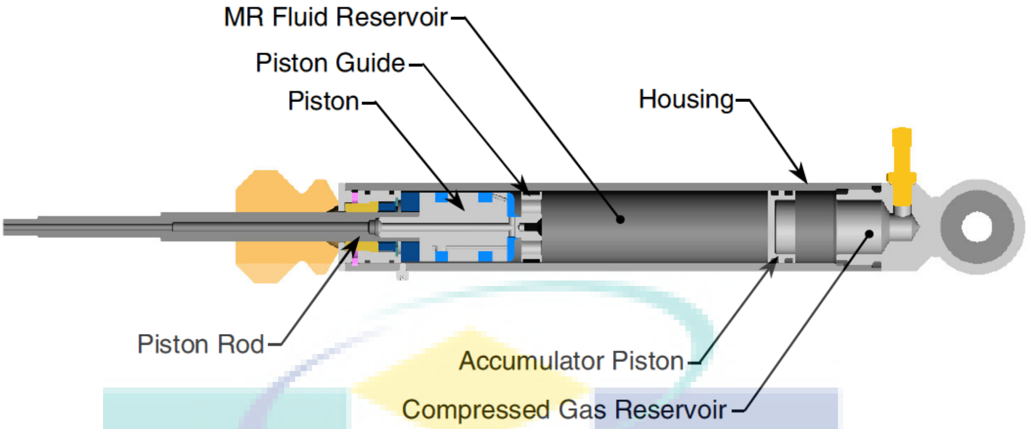

Figure 2.8: Mono-tube damper segments

Source: Ahmadian et al. (1999)

2.3 Hysteresis Model

Modelling an MR fluid damper which consists of various non-linear properties is a complicated phenomenon associated in a hysteretic system. A non-linear system can be characterized by implementing memory feature. Both instantaneous input and its precedent data contributes to the output value for specific given time. The enactment of a hysteresis system respond not proportionately instead differs from the forces applied. This component offers high flexibility to a wide scope of engineering applications. Both mathematical and non-mathematical approaches have been seen in various MR damper modelling publications (Wang and Liao, 2005, 2011; Dong et al., 2010).

In the past years, studies on MR damper model has been extensively broaden in the scope of simple dry-friction to a more intricate version sets of differential equations. Hysteresis model depict the behaviour of the damper correlates to the input/output relationship. Hysteretic semi-empirical was idealized by Bouc in 1971 and it is the further comprehended by Wen in 1976 and up until now it recognized as Bouc-Wen model (Sahin et al., 2010). In projecting the usage of hysteresis models, an assessment of hysteresis Bouc-Wen model by Ismail et al. (2009) indicated the evolution literature increases from 1971-2005.

2.3.1 Hysteresis modelling comparison and trend

Distinguish models were previously investigated along with the modification naming Bingham and Bouc-Wen model as the prominent hysteresis illustration for the MR fluid damper behaviour (Spencer et al., 1997). The distinctive effects of the trade-off between the model precision and intricacy have been the focus point throughout identification methodology. In buildings and structural engineering, a study have revealed that the robustness was affected if it based on non-linear differential equation and hinder the controller applicability in reduction of seismic response (Dyke et al., 1996). Other studies include reduction in model complexity from polynomial base (Choi and Lee, 2001), adequate results from curve-fitting model based on Hyperbolic function (Ma et al., 2002) and alternative black box method of modelling the damper (Jin et al., 2005).

Another appropriate approaches towards a resourceful modelling of MR fluid damper was soft-computing, neural networks and also fuzzy inference systems (Wang and Liao, 2001; Schurter and Roschke, 2000). It can be listed in two separate categories for modelling the dynamic behaviour of MR fluid damper through identification techniques which are; parametric and non-parametric identification. Parametric are representation of mechanical scheme by arrangement of physical qualities and its elements of spring and viscous dashpot (Dominguez et al., 2006; Spencer et al., 1997). Bouc-Wen model is an example of parameter identification technique. It is done by curve fitting of experimental results from optimizing parameters from Bouc-Wen model as a semi-empirical relationship. On the other hand, primary relationship of the input-output system model is not conjecture in non-parameter identification technique. From a given arbitrary input, the succeeding prediction of the systems are enabled subsequently identifying the prominent values of the input/output data can be stored.

Time histories of the input variables is a quality required to predict the incoming forces to produce and was reported through parametric and neural network approach

(Schutte and Groenworld, 2003). A different approach was neuro-fuzzy modelling and restoring force surface method using Chebyshev polynomial fit (Metered et al., 2009). The technique applied shows to be agile and as reliable system from its capabilities to estimate the identifying factors of force function in the terms of displacement, velocity and input voltage. However, the consistency of parameter analysis is not well elaborated as the limitations were drawn onto the various input conditions.

An extension of neural network was elaborated, initiating feed forward and recurrent neural network to enhance its findings (Wang and Liao, 2005) . It can be conducted by collecting input and output data from either experimental results or mathematical simulation to train the network. An Adaptive Neuro Fuzzy Inference System (ANFIS) method was attached to modelling of MR fluid damper (Schurter and Roschke, 2000).

As a consequent, Bouc-Wen model has been implemented throughout the years to get a well represented model of MR fluid damper. The results from previous studies have shown substantial improvement with personal advantages and drawback and an extension method to overcome particular flaws. Next section will continue discuss MR fluid damper modelling development and how this study reaches its findings to uplift the modelling technique.

2.3.2 Comparison parametric models

MR fluid damper acts as a non-Newtonian traits when it is bounded by the magnetic field and thus generate a controllable influence on the viscosity (Sahin et al., 2010). Nonetheless, the damper will act inversely instantaneous in milliseconds which the current state of Newtonian fluid can transpose the viscosity. This exclusive nature of the MR fluid damper makes the mode flow of the fluid agile.

There are many advantages of the MR fluid damper apart from the viscous manipulation, another denoted reason of using MR fluid damper is the uncomplicated design. In terms of material sustainability, it can withstand up to 150 ^{o}C with the lowest temperature as low as -40 ^{o}C and maintains to operate. With low power to generate it can produce high yield stress reaching to 100 kPa and even the material can withstand impurities as it is non toxic (Kim et al., 2009).

Effective control of an MR fluid damper mainly depends on understanding its nonlinear hysteretic behaviour under an applied magnetic field. Therefore, the development of the distinct features and consider the non-linearity behaviour of the MR damper mechanism (Spencer et al., 1997). The existing models can be categorized into two separate entities of parametric and non-parametric. Non-parametric models are able to model the MR fluid damper behaviour in such a way that the model parameters does not illustrate the physical connections of the body (Boada et al., 2008). Some of the non-parametric model are Chebyshev polynomials (Metered et al., 2009), neural networks (Wang and Liao, 2001, 2005; Du et al., 2006; Ge et al., 2007), and neuro-fuzzy (Abdullah, 2005). Non-parametric model may seem to illustrate the MR fluid damper behaviour in genuine method, however the validation for the models are highly intricate that requires vast data for model verification.

Parametric models, on the other hand, show decent representation as their parameters include physical element into replicating the hysteresis model (Boada et al., 2008). Generally the models comprises of some essential elements such as linear viscous, springs and friction. These main parameters are coupled with the physical body and the model is assessed by second with experimental data. One of the earliest parametric models is the Bingham visco-plastic model developed by Stanway which has the friction element of Coulomb that is placed parallel to a linear viscous (Stanway et al., 1987). It was demonstrated that, although this model could reasonably describe the force-displacement behaviour, it could not capture the observed non-linear force-velocity characteristic adequately. A visco-elastic-plastic model based on the Bingham visco-plastic model was proposed (Filisko and Gamota, 1991). It was constructed by adding a standard linear solid model in series with the original Bingham model. (Wereley et al., 1998) proposed a non-linear hysteretic biviscous model, which was extended into a nonlinear biviscous model by having improving the illustration of the pre-yield hysteresis (Wereley and Kamath, 1997). It was reported that this model like the previously discussed models, may interpret the force-displacement behaviour successfully, however the replication the roll-off force at low force-velocity hysteresis loops are not prompted (Abdullah and Wilson, 2005).

Identification techniques aroused to model MR fluid damper to replicate practical behavior and is categorized either parametric or non-parametric. Parametric are based on mechanical principle including interpretation by arranging springs and dashpot**.** Non-Parametric are used for direct dynamic modeling prediction of output for given inputs**,** even though the non-parametric models can efficiently depict the MR fluid damper behaviour, the complexity in validation are taxing with masses amount of data required for validation. Table 2.1 classifies the identification methods with segregation of parametric models.

Table 2.1: Parametric Identification classification

Parametric		**Non-Parametric**
Evolutionary model	**Algebraic model**	
General Bouc-Wen (BW) (Spencer et al., 1997)	Bingham (Shames and Cozzarelli, 1992)	Chebyshev polynomials (Ehrgott and Masri, 1992)
Modified Bouc-Wen (Spencer et al., 1997)	Bouc-Wen (Kwok et al., 2006)	Neural Networks (Du et al., 2006)
Voltage-Dependant modified Bouc-Wen (Spencer et al., 1997)	Modified algebraic model (Guo et al., 2005))	Neuro-fuzzy (Abdullah and Wilson, 2005)
Modified Dahl model (Zhou et al., 2006)	- -	-
Modified Lugre Friction model (Jimenezz and Alvarez, 2005)		-

A deformation state is at visco-elastic in the pre-yield region and visco-plastic in the post-yield region. They also observed that the MR fluid damper operated in the post-yield region rather in the pre-yield region (Li et al, 2000). Choi et al. (2007) proposed a polynomial model and compared the results with that model predicted the hysteresis behaviour more closely under various conditions. It was reported that the polynomial model was more of a convenient and effective method which may comprehend the contrary dynamic motion of the MR fluid damper in an analytically as well in open-loop systems in obtaining required damper force (Du et al, 2006). Nonetheless, at the low velocity area the polynomial model has neglected the pre-yield property therefore the model is not adequate enough to represent a diverse and non-linear MR fluid damper behaviour.

Gavin developed a hyperbolic tangent function to predict MR fluid damper force. They indicated that, as the model did not have a dynamic character, it could not capture the frequency-dependent visco-elastic behaviour, but the model results corresponded to the experimental results (Gavin et al., 1994). However, same case as the Bingham model, the nonlinearity factor of the force-velocity form for the Bouc-Wen model does not roll-off in the area where the acceleration and velocity are in opposing direction and the minor value of the velocity magnitude. Due to this reason, (Spencer et al., 1997) proposed a modified Bouc-Wen model (also called the phenomenological model) to better predict the damper response in this region. They estimated the parameters of the modified Bouc-Wen model and compared the results between predicted response and corresponding experimental data. The proposed model predicted the behaviour of the damper very well in all regions including the region with low velocities and the acceleration and velocity have opposite signs.

Bouc-Wen model could only estimate under certain test of MR fluid damper excitation circumstances as the parameters are not in the functions of frequency, exerted current and amplitude. Repeatability of the evaluation are required if different initial excitation were proposed and this can be unwieldy and even increase the computational efforts. In this context, to better characterize the hysteresis phenomenon of the MR fluid damper, Spencer et al., (1997) generalized their proposed modified model for fluctuating magnetic field. It’s important for developing an effective control algorithm.

Dominguez et al proposed a new hysteresis model based on the original Bouc-Wen model to incorporate not only the current excitation as done by (Spencer et al., 1997), but also frequency and amplitude. By this they enabled the designer to predict the hysteresis force more efficiently and accurately under different excitation conditions.

2.3.3 Bouc-Wen modelling development

Bouc-Wen model is widely used in mechanics primarily because it's full parametric feature. It illustrates the hysteresis non-linearity in a moderate intricacy by using differential equation. Hence, a smooth endochronic blend grants frequent usage in describing hysteretic trend.

At early discovery it was introduced by Bouc (Bouc, 1967) and was further derived by Wen (Wen, 1976). Previous researchers have demonstrated the practices of Bouc-Wen versatility in various cases. A survey was done to describe implementation of Bouc-Wen hysteretic model and with comprehensive employment for the modelling of MR fluid damper (Ismail et al., 2009; Dominguez et al., 2006; Kwok et al, 2006).

Following the model described by Bouc, Equation 2.21 and 2.22 below demonstrate the normalized equation by Wen:

$$F(t) = \alpha kx - (1-\alpha)kz \tag{2.21}$$

$$\dot{z} = Ax - \beta|\dot{x}||z|^{n-1}z - \gamma\dot{x}|z|^{n} \tag{2.22}$$

where $F(t)$ is called the restoring force, x is the displacement, k is the stiffness coefficient, α is the post-yield to pre-yield stiffness ratio and z is the hysteresis displacement. A, n, β, γ are parameters that control the hysteresis profile as shown in Figure 2.9.

Evaluating Equation 2.21 and 2.22, Ma et al., (2004) found that the redundancy of parameters occurs. The identification process for this method encounters limitations that use input-output data which could not be concluded. By fixing several parameters to certain arbitrary values, the users of Bouc-Wen model have normalized the model to eliminate redundant parameters (Ikhouane and Rodellar, 2007; Ismail et al., 2009).

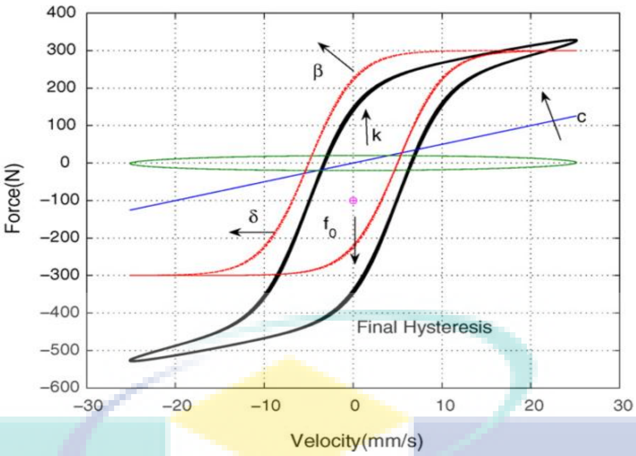

Figure 2.9: Model parameters formation

Source: Kwok et al. (2006)

Formulation of Bouc-Wen model as general derive from Newton's second law (Charalampakis and Dimou, 2010). The essence of the model can be deduced by:

$$m\ddot{u}(t) + F(t) = f(t) \tag{2.23}$$

Where *m* is the mass, *u(t)* is displacement, *F(t)* for restoring force and *f(t)* as excitation force. For the restoring force factors, it is expressed as:

$$F(t)= a\frac{F_y}{u_y}u(t)+(1-a)F_y z(t) \tag{2.24}$$

where the yield force is represented by F_y, u_y is yield displacement and *z(t)* is dimensionless hysteretic parameter in which register to the following non-linear differential equation:

$$\dot{z}(t)=\frac{1}{u_y}\left[A- |z(t)|^n\big(\beta + sgn\big(\dot{u}(t)z(t)\big)\gamma\big)\right]\dot{u}(t) \tag{2.25}$$

And an additional of signum function *sgn(•)* is observed in which the function is extracting the sign of a real number.

However, the model will tend to incline into a bilinear system for the condition of exponential parameter *n* become large and thus abrupt the transition from elastic to post elastic. For controlling the shape size of the hysteresis loop, it is governed by parameters β and γ. From Equation 2.24, it can be expressed that the ***F(t)***depicts as an elastic medium as well as hysteretic part:

$$F_e(t) = a\frac{F_y}{u_y}u(t) \tag{2.26}$$

$$F_h(t) = (1 - a)F_y z(t) \tag{2.27}$$

To elaborate the model from progression equations previously, it can be shown from Figure 2.10 below:

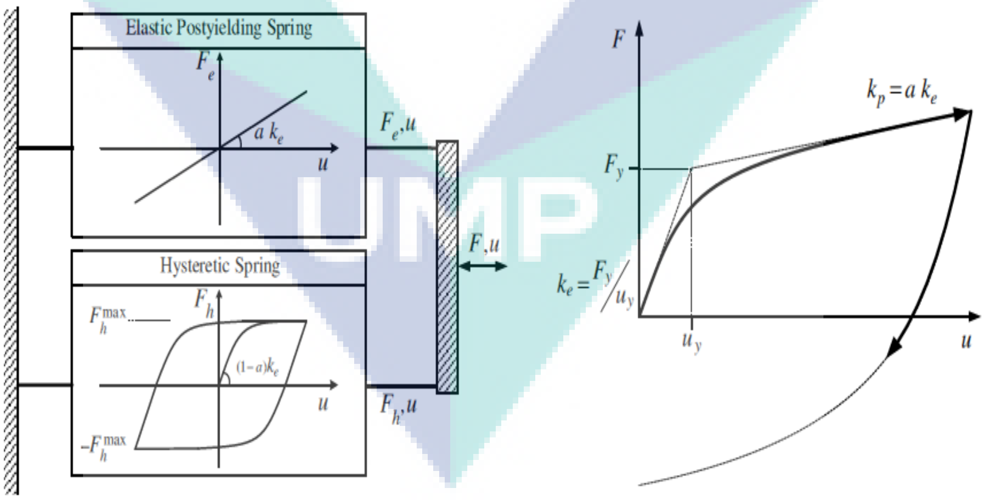

Figure 2.10: Hysteretic interpretation

Source: Charalampakis and Dimou (2010)

It can be infered that the systems shows as two springs connected in parallel form as the initial and post-yielding stiffness in Equation 2.28 and 2.29 respectively.

$$k_e = \frac{F_y}{u_y} \tag{2.28}$$

$$k_p = \alpha k_e \tag{2.29}$$

The sequences till this point has point out that development of Bouc-Wen model with normalization gives better prospect on how the hysteresis are developed. Certainties of each particular parameter were defined to play delicate role as it interrelates to one another. From this, the Bouc-Wen model chosen throughout the project is deduced by Kwok et al. (2006). A schematic model for derived equation is shown in Figure 2.11:

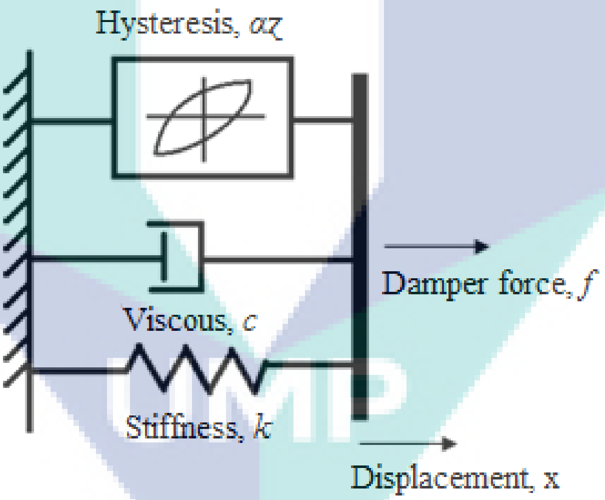

Figure 2.11: Schematic model

Source: Kwok et al. (2007)

The model is used within the following black-box method by giving a set of experimental data and tunes the model parameters as close as the measured data and described as follows:

$$f = c\dot{x} + kx + \alpha z + f_0 \tag{2.30}$$

$$\dot{z} = \delta\dot{x} - \beta\dot{x}|z|^n - \gamma z|\dot{x}||z|^{n-1} \tag{2.31}$$

where, $c, k, \alpha, \delta, \beta, \gamma$, are model parameters to be identified, z, is the hysteretic variable, f, is the damping force, c and k are the viscous and stiffness coefficient respectively. The initial condition of damper force offset, f_0, is set to be zero for experimental purposes. This will be further discussed in the following chapter.

Hysteresis response is often described from Bouc-Wen model and it has been proven to improve the modelling accuracy (Guan et al., 2011; Spencer et al., 1997; Wang and Liao, 2011). These parameters are the main concern for the identification and tuning method for PSO algorithm.

Often referred to describe the behaviour of MR or ER fluids is the stress-strain Bingham viscoplastic model (Shames and Cozzarelli, 1992). The slope ration of shear stress over strain is the measurement for plastic viscosity hence the total stress is described by

$$\tau = \tau_{y(field)} + \eta\dot{\gamma} \tag{2.32}$$

where the yield stress induced by the magnetic field is $\tau_{y(field)}$ and the viscosity of the fluid is η. Subsequently, an idealization of a mechanical model was proposed inhibits a discontinuous jump in force-velocity reaction (Stanway et al., 1987). The force is represented as for nonzero piston velocities, $\dot{x}$:

$$f = f_c sgn(\dot{x}) + c_0\dot{x} + f_0 \tag{2.33}$$

where the total force is f, and the magnitude of hysteresis is f_c or at some case is called frictional force that associated to yield stress. Owing to the presence of the accumulator, the offset f_0 is incorporated for the nonzero mean examined in the calculated force. The model generally used in uncomplicated hysteresis situation for its simplicity does not sufficiently deliver.

The model proposed by Kwok (2006) uses the hyperbolic tangent function to embody the mechanical character of viscous and stiffness corresponds to hysteresis and linear functions. The equation is submitted as below:

$$F = c\dot{x} + kx + \alpha z + f_0 \tag{2.34}$$

$$z = tanh\,[\,\beta\dot{x} + \delta sgn(x)\,] \tag{2.35}$$

where the z is the identical with other models operation except an induction of hyperbolic tangent function and the offset of the damper is the parameter of f_0. Kwok et al. (2006) claimed that the model offer efficiency in computational execution for parameter identification thus carrying out the controller design is placid from the hyperbolic tangent function institute (Kwok et al., 2006).

2.4 PSO DEVELOPMENT AND APPLICATIONS

The algorithm initially defines the design space (DS) by altering the trajectories of individuals generally known as "particles", that mobile inside the DS. The best solution draws these particles in search of their personal elucidation best solution in a swarm stochastic mode (Clerc and Kennedy, 2002). The experience gauged by these particle allows theses agent to explore the solution in less iteration and therefore make the PSO as an efficient method in parameter searching (Clerc and Kennedy, 2002).

A studied was made on the multi-dimensional PSO in the size of two dimensional (2D) and three dimensional (3D) trusses (Schutte and Greenwold, 2003). Another approach was investigated by using an enhanced variant of PSO for optimizing the air craft wing in aerodynamic structure (Venter and Sobeiski, 2004). Another optimization method were implanted into the PSO for investigating the performance with Standard Genetic Algorithm (SGA) validated via mathematical and problems arises in engineering (Dimopoulus, 2007). Implementing PSO for the estimation of the control parameters was done for permanent magnet synchronous motors (Liu et al., 2008). Binary PSO as a substitute to the conventional PSO were introduced in optimizing the truss structure and studied upon the optimal design (Dimou and

Koumousis, 2009). Biology application have aware of PSO ability to control parameters and was investigated for bacterial foraging, for the identification non-linear dynamical systems (Majhi and Panda, 2010). In civil structure specifically multi-story 2D and 3D frames, an optimal design was achieved by scaling the optimization parameters using PSO (Gholizadeh and Slajeghah, 2009).

The application conservative PSO algorithm has been seen in improving models and even efficiency. In another diverse application of various PSO was executed in constricting the parameter for computing the orbits trajectory from the velocity vector for relocate towards a desired region (Liu et al., 2006). The nonlinearity of the dynamic systems was extended by applying PSO with time varying inertia parameter with an additional similar to Genetic Algorithm (GA) mutation operator (Ye, 2006).

From the diversion of PSO algorithm examined in recent years, the effectiveness of this approach proves to be adaptable in various scenarios. Hence the method on using PSO for optimizing hysteresis model parameter is tolerable in conjunction to imitate the MR fluid damper behaviour.

2.4.1 PSO model formulation

Particles that emulate the movement of bird flocks are initially assigned with *velocities* that lead their *flight* across the solution space. After the search was made for each particles, the particle that found the best solution memorised it and transmit to the whole population for further refining search. However there are criteria for the solution to be satisfactory.

Desirable path is selected for a random search of space from the particles; hence the position and velocity of selected best particle commemorate and inform other members. Termination criterion was used to examines the temporary evolution of the fitness of the best solution hence ending the process when performance drops at a pre-defined threshold and employed for parameter estimation for MR fluid damper, (Kwok et al., 2006). The velocity vector are one of the prime variable for the stochastic behaviour and was previously investigated (Wilke and Greenwold, 2007). In evading stagnation of the PSO, criterion for the PSO algorithm was examined by using basic statistics analysis (Ge et al., 2007). To improve the convergence rate, a series of amendments was made by calculating the velocity vector of the PSO (Ali and Kaelo, 2008). PID controllers have been using the PSO algorithm in designing more stable systems (Gaing, 2004) and also in electro-magnetic application (Ciuprina et al, 2002). The PSO convergence characteristic was analyzed where the algorithm control settings were also proposed.

2.4.2 Background of Particle Swarm Optimization

Back in the days, PSO was introduced by a social psychologist name James Kennedy and was team up with Russell Eberhart an electrical engineer in the year 1995. The discovery was inspired by emulating social behaviours birds flock or school of fishes and it is widely used to interpret a widespread optimization problem ever since (Kennedy and Eberhart, 1995; Ray and Liew, 2003).

It was then studied and revolutionized by Engelbrecht (2005) whom stated that the algorithm was based on the model of psychology social influence and social learning. A particle is described as a member of the swarm that imitates the animal behaviours. The algorithm adapted from this behaviour emulates a group of communication in a population which is called a swarm. These individual set of membership particles straightforwardly imitate the success and neighbourhood of the individuals. The collective behaviour encounter discovery in an optimum design space at high dimension.

In the events of current evolution theory, PSO has interesting character to weight against other optimization methods. This include the memory that PSO algorithm has are contained in each of the particles, cooperation that builds with one another and sharing of information between particles (Kennedy and Eberhart, 1995). Besides from the theory framework simplicity to encoded and program, the PSO technique capable of generate high quality assurance in a short time (Kao et al., 2006). Besides, these stable characteristics in PSO algorithm are better relatively to other stochastic methods.

The PSO algorithm was started by implying to simulate the movement in flocks of birds. This simulation was a part of a research in biology population to investigate the relation means of "intellectual collection" (Hassan et al., 2005). The initial motive was to differentiate model social behaviour of human beings and the swarm of birds or fish. This difference is called abstraction. The swarm interchange its physical movement to avoid their predators, to find food sources and members plus adapting to environment situation including temperature and weather. On the other hand, human not only modifies their physical movements, they are also cognitive and experience manipulator (Kennedy and Eberhart, 1995).

The model simulation created by Kennedy and Eberhart chose the initial position of randomise birds (Engelbrecht, 2005). First, for a number of iteration, each particle first decides on their closest neighbours. Then, the individual change its *velocity* into their successor's *velocity*. The rhythmic movement of these birds exist from this behaviour. However, the flaw that arises from these is that the particles tend to move faster towards the final direction. To overcome this, stochastic component of "random", a form of modified velocity in random was introduced.

In addition, since the starting of the simulation, the best position is engaged based on previous individual position. While, the global best position searched by any of the particles. Both of this best position is called by 'extractor'. By extracting it, the swarm will modify their position and to swarm about around the target in less iteration. The behaviour is not affected from similar velocity or randomize component.

Engelbrecht (2005) agreed on the term of particle used in the PSO algorithm as support of individual. This is due to velocity and acceleration as relate to individual even though these individuals have no mass or volume. At the same time, the term swarm is still being used because there an occurrence of elimination at similar velocity which is the main component in swarm behaviour. Likewise, the term stays in PSO algorithm as it is suitable with primary principal of intelligent swarm having the quality, various responses, stability and adaptability.

Approximation principal on PSO are portray as multi-dimensional calculation space that is brought for each iteration while swarm particle reacts to quantity factor in the form of best position and global. The *pbest* and *gbest* will change provided the swarm follows the adaptability principal of the PSO algorithm.

2.4.3 PSO algorithm

There are two versions of PSO algorithm which are binary and continuous (Kennedy et al., 2001). Binary version can be translated as optimized algorithm qualitative and socially quantitative (De Castro, 2002). However, continuous version is the real numerical optimization algorithm. Nevertheless, both versions of the algorithm have the same ethical approach.

In the PSO algorithm, a group of particles are given randomize initial value. Then each particles in the swarm search for the best optimum position by re-enacting its generation (Hu, 2006). At a number of iteration, all of the particles update velocity and acceleration and reach towards two of the best location. The acceleration is measured by generating split randomize number to make certain of the best two best location previously (Eberhart, 2001).

The first best value is the best solution or fitness achieve at that moment only as this fitness value *pbest* is save. Another best value is the *gbest* and it is tracked by PSO global version that carries the best value from all of the particles in the population. Moreover, the local version of PSO search by using network topology in the form of a ring and regard it as *lbest* in which the size of between neighbouring particles are small. However, *gbest* is express as network social using star topology where the neighbouring for each particle is the entire swarm.

From the Figure 2.12 shows that the topology for ring type *lbest* only transmits the local information with the particle next to it, whereas the component for star type *gbest* illustrate that the information gathered are from all the particles in the swarm. They are then dynamically readjusted to their position based on the best fitted.

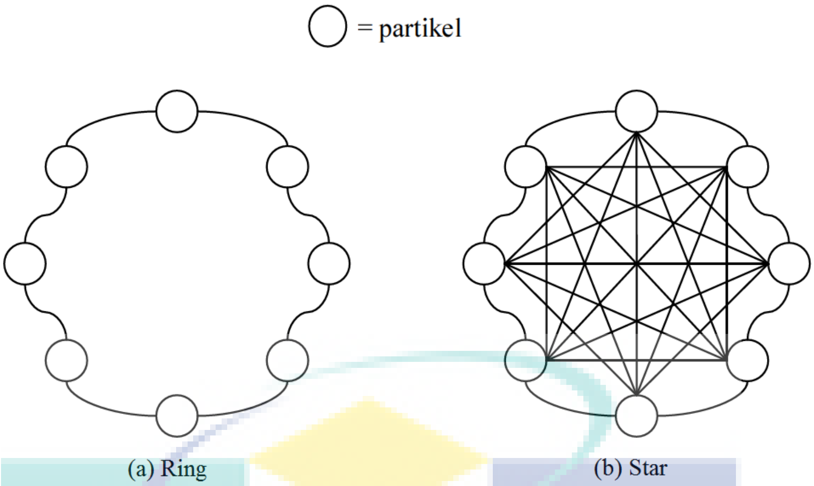

Figure 2.12: Topology of PSO social network

Source: Engelbrecht (2005)

Equation 2.36 and 2.37 express the initial swarm particles of positions and velocities, x_k^i and v_k^i, are generated randomly with boundary conditions of x_{min} and x_{max} (Priyandoko and Mohamad, 2013).

$$x_0^i = x_{\min} + rand(x_{\max} - x_{\min}) \tag{2.36}$$

$$v_0^i = \frac{\text{position}}{\text{time}} = \frac{x_{\min} + rand(x_{\max} - x_{\min})}{\Delta t} \tag{2.37}$$

Uniformly distributed random variable, *rand*, is valued from 0 to1. Vector format is translated to describe velocity and position denoted by *i*th particle at given time *k*. The best global value, p_k^g, is to be determined from the fitness function value of a particle in the running swarm. Hence, the best position *pbest* is selected from each particle correlate with all previous groups for best global *gbest*. In Equation 2.38, summation mode is associated to reposition the direction of combining swarm influence, particles' memory and current motion. Consequently Equation 2.39 explains the velocity vector which is applied to update the position of the particle.

$$v_{k+1}^{i} = wv_{k}^{i} + c_{1}rand\frac{\left(p^{i} - x_{k}^{i}\right)}{\Delta t} + c_{2}rand\frac{\left(p_{k}^{g} - x_{k}^{i}\right)}{\Delta t} \tag{2.38}$$

$$x_{k+1}^{i} = x_{k}^{i} + v_{k+1}^{i}\Delta t \tag{2.39}$$

where w is the inertia weight, p^i is the initial position, p_k^g best global position, c_1 and c_2 are the constant acceleration.

2.4.5 Parameter control in PSO

In the PSO algorithm, there are only a few parameters that need to be managed. There are two categories of parameters, explicit and implicit parameters. Explicit parameters are the maximum velocity, constant acceleration, population size, and number of iteration or generation. The implicit parameters are the inertia weight. The performance of PSO algorithm can be improved by manipulating theses parameters.

The maximum velocity *vmax* determines the resolution or fine space between the current position and the searched target position. In the midst of avoiding the system to explode from additional particles oscillating, it is the *vmax* that plays an important role. The application of *vmax* is to contain the particle at a limited speed for that the particles are tight down to the speed of *vmax.*

The value of *vmax* is pre-set at the early process and stays constant until final iteration. Critically if the *vmax* is set to high, it may cause the particle to soar pass over the best solution. However the exploration of the particles to find the best local value will be constrained if *vmax* is too small. The dynamic range variable for *vmax* is suggested to be between 10 % -20 % for each dimension.

Constant acceleration (φ *or* c) is the explicit parameter to control the PSO algorithm. Learning factor of acceleration coefficient is the other substitute term related to constant acceleration. The type of trajectory movement for the particle is determined by the constant acceleration.

There are two factors of constant acceleration which is $c_1$and c_2. Self confidence factor in a particle is translated as $\boldsymbol{c_1}$whereas the swarm confidence factor represents the confidence stage of particle towards their neighbours. Both constant controls the stochastic influence of the particles' cognitive and overall social velocity.

For the particles to be attracted equally towards *pbest* and *gbest*, both of the constant acceleration has to be equivalent (c_1 and c). The designation of c_1 and c_2 at low value from 0 to 4 is to certify the particles trajectory in a smooth transition and allows it to reach further than the good design space before retracted to previous searched location. If the constant values are high, hence great deals of acceleration with abrupt direction change are getting closer or further from the area that has a good value. A number of researchers have mended the constant acceleration value to 2.0 for various applications.

Population size or number of particles used in a system is a type of explicit parameter that is required to control in PSO algorithm. A large overall number of particles in a swarm will endorsed diversity for the starting population system and acknowledge the design space to maximise the exploration for given iteration. However, the bigger the population size the complexity to account per iteration is higher as well as lowering the process stages into a mere series of random search.

There are no concrete evident in any research literature regarding the appropriate size of swarm in PSO algorithm. The size of the population depends on the problem that needs to be solute.

When it was first introduced, it was recorded between 15 to 30 particles used to employ the PSO algorithm. Latter sighting suggested that in the range of 20 to 30 was sufficient to utilize the algorithm. An adequate solution can be achieved by just using small population size compared to size that were used in other smart algorithm.

Another explicit parameter listed to control the PSO algorithm is the iteration number. Nonetheless, there has not been any exact amount on what number iteration to be used. However, to achieve the best solution for the population size condition, the iteration number will also depends on the type of problem to resolve. If the iteration number is small, it will lead to premature process calculation and early stoppage time. On the other hand, the larger the iteration number, it will place the system in an insignificant complex cumulative condition. This occurs since the iteration number functions as a termination condition for the algorithm.

Inertia weight *w* is fall under implicit parameter category. It was introduced as a mechanism to explore and exploit the swarm control capability. The value of *w* is to gauge and manage the momentum of particle attribute from previous velocity to a new velocity.

The optimum value of *w* is crucial to instil sensible behaviour of focus and inter-changeable between exploration and exploitation. Bigger value of *w* leads to increasing process of diversity in exploration while smaller *w* assists in local exploitation. However, a number that is too small for *w* may terminate the potential of particle exploration.

As a reference, (Eberhart and Shi, 2001; Kennedy et al., 2001) implement the inertia weight at the value of 0.4 to 0.9 at reducing time mode. Thus, the inertia weight will provide stability between global and local search and agitate the factoring process from exploration mode to exploitation mode in the event to search optimum solution.

Another alternative for the inertia weight is the narrow factor, however it is not covered under the scope of this research yet the literature can be found in (Eberhart and Shi, 2000).

2.5 SUMMARY OF THE REVIEW

The review has shown extensive summary on this research from the MR fluid damper development to parametric identification with an optimization method using PSO. The background of MR fluid damper was initially discuss along with the internal structure. Then the dissertation extends to parameter identification method, existing hysteresis model and the parameters concern for the formation of MR fluid damper behaviour. Elaboration of the hysteresis model parameters regulation technique by implanting PSO was also presented.

As a conclusion, modelling an agreeable representation of MR fluid damper is a major setback as the nonlinearity restricts the model and makes it far more complex to replicate. The implementation of an artificial intelligent approach of PSO algorithm is essential to denote the parameters of hysteresis model. These optimized parameters of the hysteresis model generated by PSO will supply a better performance for the reaction to imitate the MR fluid damper. This basis has the relation with the research objectives to optimize the hysteresis model parameters to achieve a higher similarity of the MR fluid damper performance. Recent studies have not shown the correlation between the hysteresis parameters and MR fluid damper model in terms of sensitive variables that has influential character to distribute the mapping of depicting the MR fluid damper behavior.

On the next chapter, the theory discussed previously will be realized and structure in methodological manner for the development of MR fluid damper and integration between hardware and simulation is presented which forecasted the research objectives.

CHAPTER 3

RESEARCH METHDOLOGY

3.1 INTRODUCTION

On the previous literature review chapter, MR fluid damper development has been discussed. It conceals the design aspects of parameter and magnetic design collaborating into a functional MR damper. However, the integrated phase from experimental and simulation are obliged to accomplish the refining model and optimization. Therefore this resolute to the decision for research methodology commenced in this research.

An inclusive flowchart of the research methodology was elaborated to underline the entire element process of the purported research project in the next section. The distinctive stages of procedures depict the extensive function for each allocated task coupled with the supplementary means. In principal, the stages are divided into two categories starts with the process of experimental than the simulation. Both sections mutually progress in series to conform the absolute findings by evaluating the compared data. This chapter rationalizes the research methodology and conducts the corresponded sections customarily.

3.2 EXPERIMENT FRAMEWORK

Figure 3.1 illustrates the compliant flowchart alongside the explicit sections for the research methodology. Prior to the advancement of the flowchart, literature review was pragmatically studied to pledge a definite apprehension from the various standpoints into a contracted significance consequently allow the procedures to be apparent concerning the research.

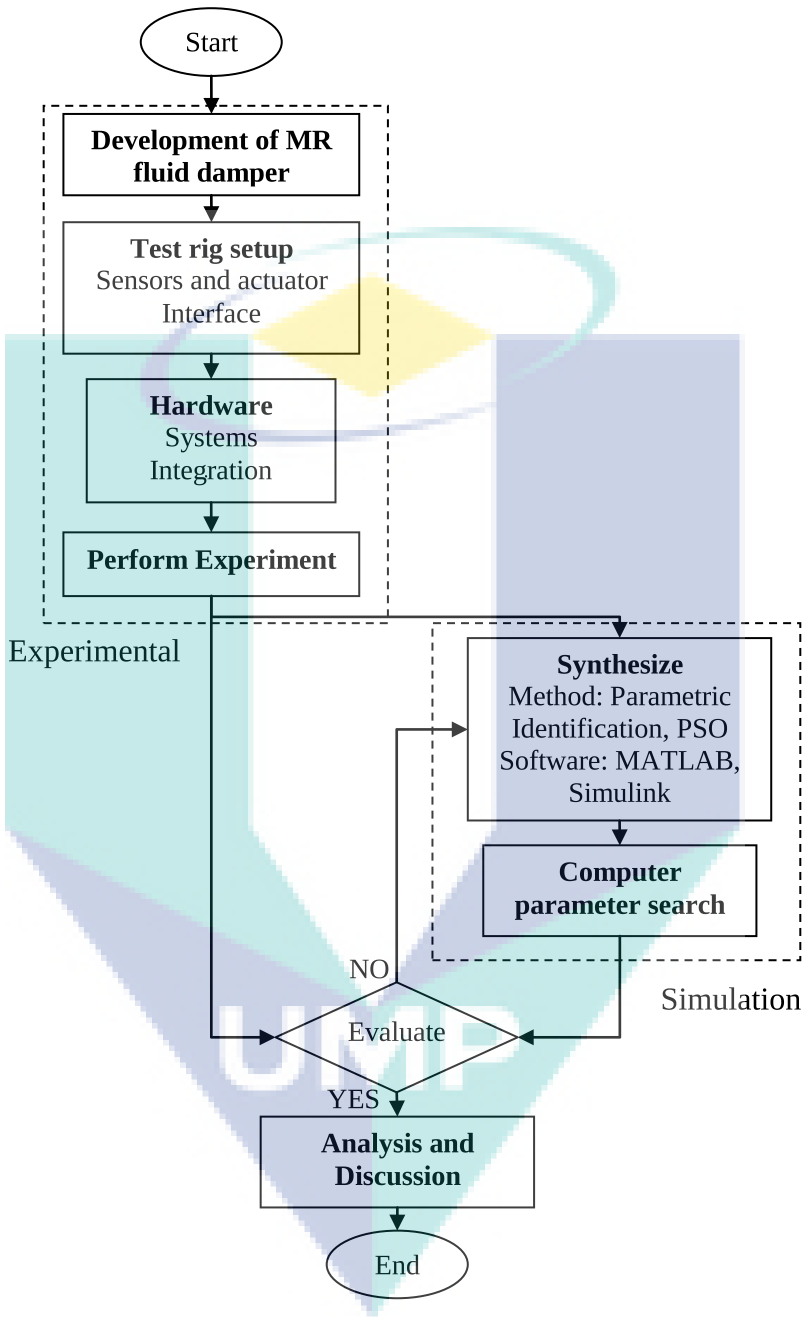

Figure 3.1: Flowchart of research methodology

The experiment assortment starts with developing the MR fluid damper, covers the parts pertaining in the shock absorber, measurements and the initial performance. Geometric and magnetic design ensue the final fabrication of the absorber. Then, a thorough set-up on the test rig convened based on the performance requirements. This includes the specification of the item implemented on the rig. Once the rig is finalized, the hardware systems integration justifies the retrieving data from the rig. Decisively, the experiments are performed to gather the experimental data and are set to be evaluated corresponding to simulated data.

The simulation phase requires substantial understanding on the MR fluid model which corresponds to hysteresis system. The model was done by creating a set of functions through SIMULINK. This function has an import block to extract the experimental data and thus generate into a parameter identification plant. Then, MATLAB generates these processes with the sub-function of PSO block that optimize each parameters of hysteresis model. An evaluation takes place after the simulation has completely run by overlapping the simulated data with experimental data. Lastly, the results are being deliberated and analyse for higher precision and detect any improvements required to the model.

3.2.1 Development of MR damper

Primary objective on developing the MR damper is to fabricate an MR fluid damper that has the order of generating the outcome in terms of bounded forces and the average operating current. The bounded force is in fact stated by the original equipment. However once the damper is magnetized for instance an assured ranged value of current is inserted, the cause of observed forces changes. This observed force is the bounded resultant by the operating current.

An original equipment of shock absorber was employed as an orientation in developing the MR fluid damper model. Proton Waja's shock absorber was elected as a reference due to its specifications and unsophisticated operation sets of assembly. However, installation of MR fluid damper model into the Proton Waja's model will elevate constrictions in terms of design as the factors of parameters for instance the shock absorber tube's diameters and stroke length are in place. To comprehend the described parts and elements, Figure 3.2 and 3.3 are illustrated elaborating the absorber in extended degree.

Figure 3.2: Original absorber of Proton Waja

A conventional damper mainly consists of a piston rod, bearing and seal. However, an MR fluid damper comprises several additional medium essentially accumulator and electromagnet. Nonetheless, MR fluid of Hydrocarbon-based MRF-122EG was employed into the damper cylinder with the purpose of implying an electromagnetic behaviour on the damper. It is exhibited as in Figure 3.3, where the diagram illustrates the sequence of assembly events of the MR fluid in the damper. Figure 3.3 (a) starts with unclamped damper, then the MR fluid is inserted as Figure 3.3 (b) before the absorber is fasten as Figure 3.3 (c)

The flow of MR fluid in this damper is from the higher to lower pressure chamber through and orifice. The behaviour of MR damper is volatile by means of electromagnet's input current. Magnetic fields exerted from the current input are controlled to facilitate the amount of yielded strength, consequently supply a continuous variable damping. The current is supplemented to the magnetic choke and produces a magnetic field. Viscosity of the fluid altered into a semi-solid form by virtue of magnetic fields that aligns the particles perpendicular to fluid flows

(a) Unclamped damper (b) Fluid insertion (c) Clamped damper

Figure 3.3: MR fluid damper assembly

Nonetheless, after deliberating the noteworthy parameters through geometric and magnetic design, the parameters are ascertain and given as in Table 3.1 and Figure 3.4.

Table 3.1: Shock absorber measurement

Feature	*Dimension (mm)*
Stroke (min and max)	150 (±75)
Piston rod length	350
Extension stroke stopper	65
Thickness (Inner tube)	2
Diameter (Inner tube)	35
Height (Inner tube)	302
Gaps (Inner and outer tube)	5

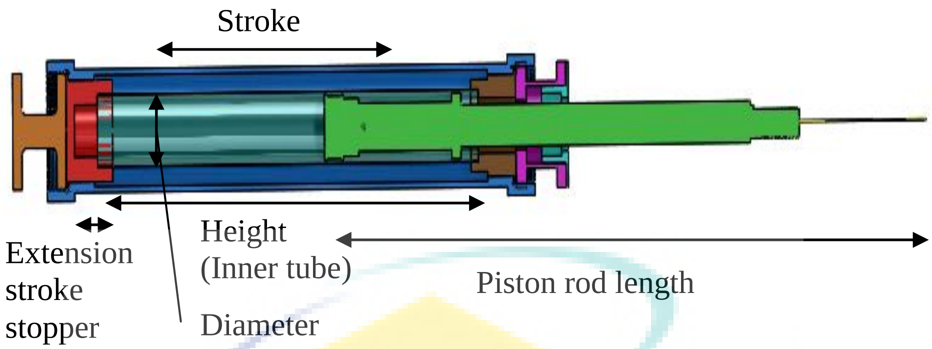

Figure 3.4: Shock Absorber Measurement

As for the performance of the damper, Figure 3.5 illustrates the force against velocity for the original equipment. The performance of this damper is used as a point of reference in designing the damper. This was tested using Material Testing System (MTS) Machine.

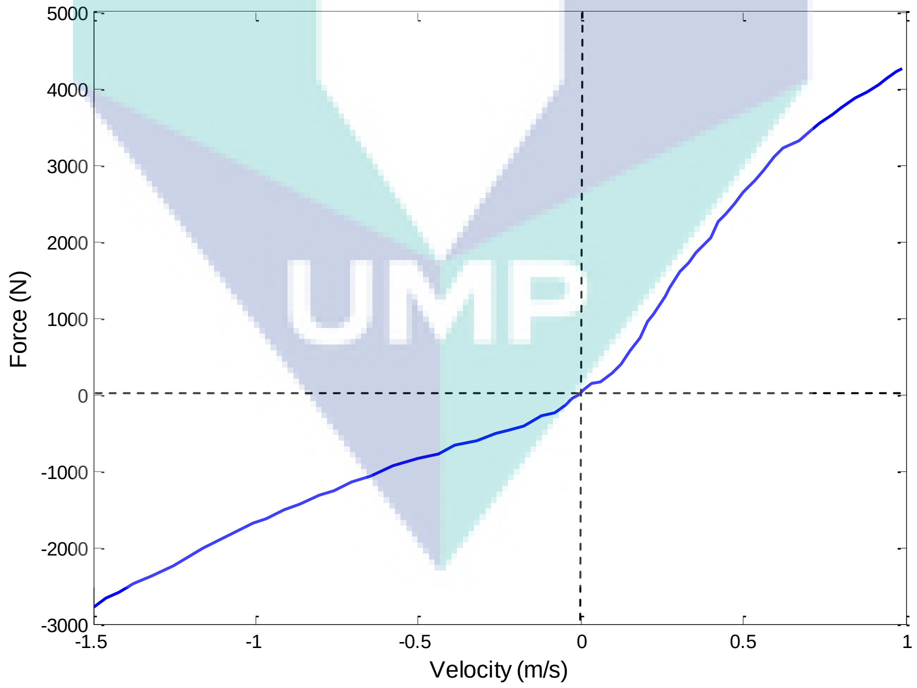

Figure 3.5: Force-velocity plot of original Proton Waja absorber

Figure 3.6 is where the designing factors that interjacts the resultant forces for the absorber and generally known as “choking points”. The design of parameters were based on the choking points and the copper wire coil is placed as in Figure 3.6:

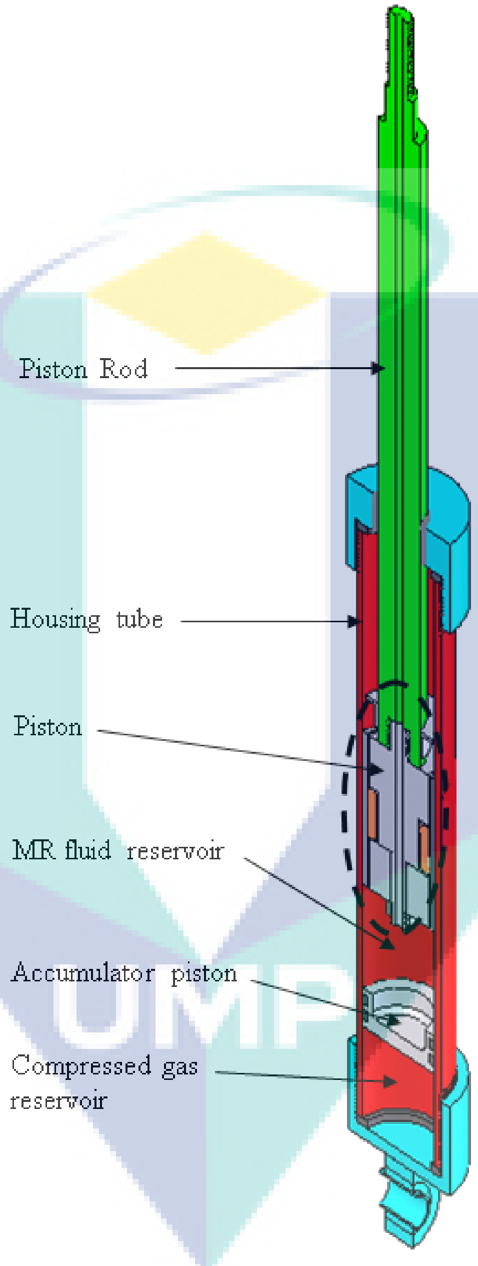

Figure 3.6: MR damper valve mode of the shock absorber

The performance suggest a passive behavior of the damper, this is when zero current is supplied to the coil. The consequence of geometric and magnetic circuit design commence from developing a feasible MR fluid damper. Thus, the modeling of a recognizable damper can be promptly implemented subsequent to the gathered parameter design data. Figure 3.7 indicates the location of electromagnetic coil inside the damper. Magnetic fields are generated once the current is supplied. Hence, the restriction of the oil flow investigated as the restriction force.

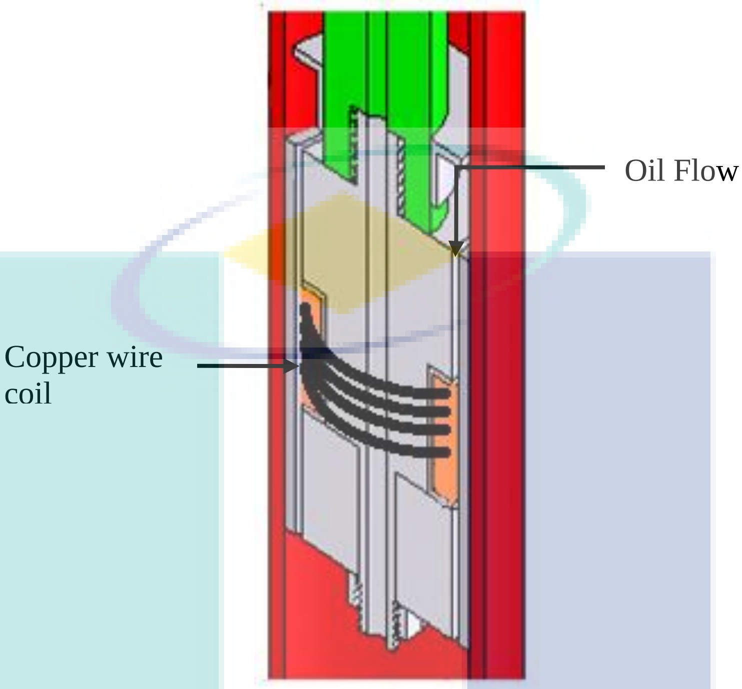

Figure 3.7: Electromagnetic coil inside damper "choking points"

The parameter of this set determines operating current for the damper. This can be distinguished in Table 3.2 where the alleged sets were chosen on accord of Average Amp output. On retrieving the required value from the preferences suggested that the proposed magnetic circuit design parameters were indicated from average ampere as the maximum supplied current are at least 150 % in excess of the original equipment shock absorber performance. This is done during the on-state operation and on top of that less than 50 % is required upon off-state condition. Therefore, MR damper possess the aptitude to endow resisting forces for both account including the original equipment shock absorber (Poynor, 2001).

Table 3.2 has concluded the average current value required to progress the MR development. There are certain parameters which identified beforehand by the designer and predetermined prior to developing the MR damper. Figure 3.8 are extracted from the “choking points” in segments to further elaborate the parameters design. The parameters that required attention are *D1*, *D2*, *D4*, *G*, and *W*, as respective to the wire hole inside the hollow shaft, internal diameter of the piston ring, outer diameter of piston ring, fluid gap and flange thickness. Piston overall length is also considered to be resolve amongst previous parameters.

Table 3.2: MR damper parameters of geometric and magnetic design

Wire Gauge	Wire Diameter (mm)	Total turns	Length (m)	Resistance (Ω)	Average Current (A)
25	0.455	2780	7.19	0.76	15.71
26	0.404	3526	8.10	1.09	11.01
27	0.361	4416	9.06	1.53	7.85
28	0.320	5619	10.23	2.19	5.48
29	0.287	6986	11.40	30.4	3.95
30	0.254	8919	12.88	4.38	2.74
31	0.226	11266	14.48	6.22	1.93
32	0.230	13964	16.12	8.57	1.40
33	0.180	17760	18.18	12.27	0.98
34	0.160	22478	20.45	17.53	0.68
35	0.142	28538	23.04	25.00	0.48

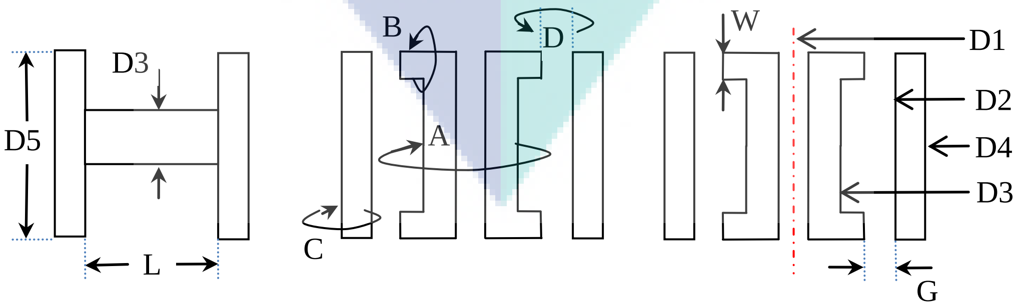

Figure 3.8: Design of parameters in choking points

There are several respective prerequisite parameters to opt in fabricating the MR fluid damper. These specifications must be adequate enough to be manufactured. Table

3.3 indicates the suggested parameters and the respective values according to practical manufacturing demands.

Table 3.3: Input parameters and output data

Input Parameters		**Output Data**	
D1 (mm)	4.000	Area A (mm^2)	405.429
D4 (mm)	46.000	Area B (mm^2)	405.429
D2 (mm)	40.000	Area C (mm^2)	405.429
G (mm)	0.500	Area D (mm^2)	62.071
Piston overall length	40.000	D5 (mm)	39.000
W (mm)	3.000	D3 (mm)	5.151
Supply voltage (V)	12.000	L (mm)	34.000
Groove depth	16.925		

As the requirements recommends, wire hole *D1* of the hollow shaft must tolerate the wire to be inserted inside. The internal diameter original equipment shock absorber tube advocates the size of outer diameter of piston ring *D4*. To select the proper value of fluid gap *G*, consideration on fail-safe behavior relates to magnetic flux density. Thus avoid saturation to the flux lines.

The development of MR fluid damper trails from deciding on the shock absorber, choking points parameters and magnetic design. The conclusive damper should generate a satisfactory damper behavior for and the retrieve data are practical to be evaluated with simulation study.

3.2.2 Test rig

The test rig was previously developed in the case of non-parametric study. It was designed based on the original damper equipment used in a conventional passenger vehicle. The parameters of the shock absorber are fixed in sense of exclusion towards the research findings.

Once the MR fluid damper is assembled, it is placed on the test rig shown in Figure 3.9. A load cell is employed on the top of the damper. This will collect the amount of forces generated by the damper. On the bottom half of the damper is the road profile element. The cam is designed to generate disturbances to the damper as an act of sinusoidal wave. Subsequently, velocity and displacement are measured with an accelerometer; Linear Variable Differential Transformer (LVDT) sensor Micro-Epsilon, WPS-MK series; 0.05 m - 7.50 m measurement, 0.05 % Full Scale Output. It is placed between the damper and the road profile.

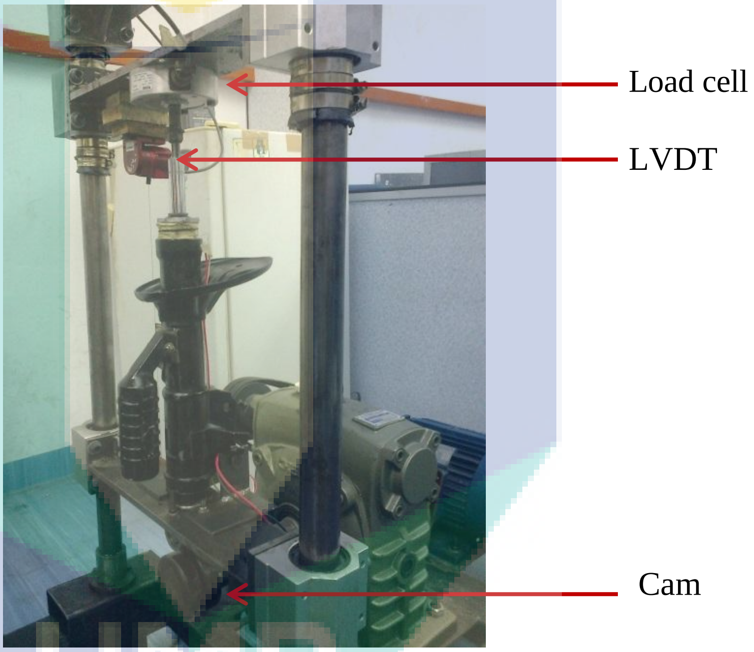

Figure 3.9: MR fluid damper employment

3.2.3 Hardware and system integration

Previously the test rig setup has been employed, in order to receive data from sensors and commencing the actuators, the hardware assembly and hardware integration are required to fit seemly. A power inverter is installed in order to surpass sufficient amount to the power supply and induce respective current to sensors, Data Acquisition (DAQ) and cam. By inducting turbulences to the system, suitable amount of current are applied to the damper as suppose inflicting the force and velocity behaviours. The collection of these data are transmitted to a Data Acquisition (DAQ) system using NI PCI-6221 (37-Pin) 16-Bit, 250 kS/s, 16 Analog inputs with 37-Pin D-Sub, by electing the signals sample from the physical forces into digital numeric values. In the manner of test rig setup, the context of equipment arrangement is display in Figure 3.10.

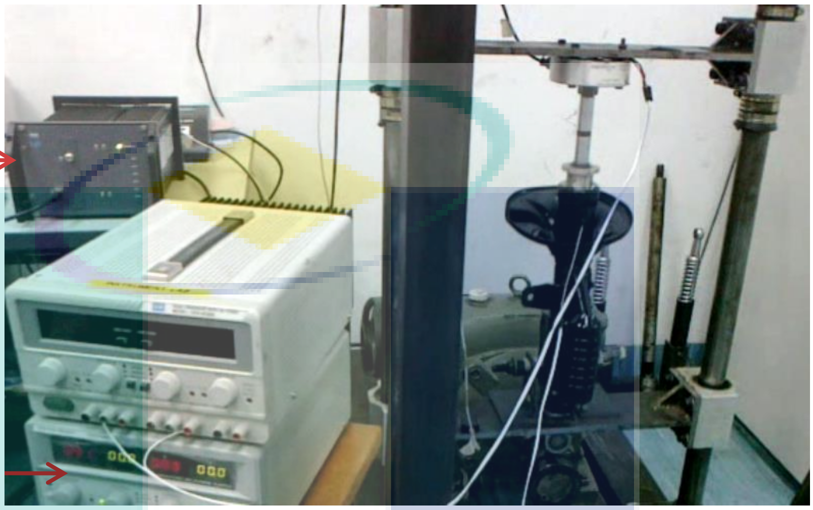

Figure 3.10: MR fluid dampers Equipment

3.2.4 Perform experiment

Referring to the methodology flowchart, preparation of the test rig setup permits to performing the experiment. There are several conditions needed to be justified before handling to simulation phase.

The responses of the damper are collected based on the test rig with different given conditions. A set of current input is given from 0.0 A to 2.0 A with an increment of 0.5 A. The range of current inputs were previously based upon the MR fluid damper design which tolerate the mean operating current of 1.93 A. In addition, the maximum input is taken before the coil reached saturation input current before exposing the coil to high current that may leads to melting point. The frequency and amplitude are fixed and defined by 1.1 Hz and 3 cm respectively which is the preset dimension from the cam that acts as a disturbance or exciter. After storing these data, sets of diagram were projected. The significant sets are displacement against time, force over time, force against displacement and lastly force versus velocity.

The non-linearity of the MR damper is considered as a major setback, to an evident on the relation between displacement, force and velocity. The overall outcome of this research is to mitigate the measured data graph from and optimized model data. In accordance to enhance the performance of the hysteresis model, the collected data are the benchmark on which the simulation study is based on.

On the next segment, thorough investigation on developing the model is alleviated. The objective in optimizing the significant parameters are examined, concurrently to the computer search followed by evaluation stage. The question remains vague up to the process of several optimization reruns and back to synthesizing method.

3.3 SIMULATION STRUCTURE

The simulation section comprises of MR damper modelling that involve coherently with the software application and method integrated within by assimilate both to replicate behaviour of MR damper. The software programming is done by creating codes that emulate method of study in which the parametric identification conjointly with PSO.

3.3.1 Method of parametric identification and PSO configuration

The modelling of MR damper event has scrutinized certain assumptions for the simulation study to administrate in the course of the proposed research. It specifies primarily on the model of a quarter car suspension system inferred to singular shock absorber component. It indicates that the construction of the hysteresis model is conjoint to the viscosity and stiffness. The parametric identification was earlier discussed in Chapter 2 and listed in Table 2.1. Nonetheless in this study, the model that is compared to is Bouc-Wen (BW), Bouc-Wen (Kwok) and Bingham model.

After deliberating these models, as shown in Figure 2.12 the schematic model of Bouc-Wen, the hysteresis behaviour are ought to be discovered hence replication of MR fluid damper behaviour is achieved. However, the sets of parameters for instance the essential parameters for Bouc-Wen (BW) in Equation 2.30 and 2.31 harvest the hysteresis behaviour. As mentioned earlier, the definitive changes on the imperative parameters will yield the hysteresis graph as shown in Figure 2.10.

As the main purpose of PSO is to optimize the parameters value of hysteresis models, PSO itself has its own parameters and factors to be ascertained beforehand. But these parameters are kept constant and are believed to trigger the best possible value for the Bouc-Wen model parameters.

Parametric Identification for Bingham and Bouc-Wen model was done by using SIMULINK block as the model requires call back from certain parameters. For Bouc-Wen model by Kwok is generated by m-script function of MATLAB coding. The models are then optimized by calculating the parameters from hysteresis models. These can be seen in Appendix A for PSO programming and Appendix B for hysteresis models. Both codes are generated through a main window that calls experiment data and compared to simulated data as referred in Appendix C. On the next chapter the layout and process of implementing PSO into hysteresis model is described.

3.3.2 Software Application

As part of communicating with the experimental data, a proper structure and understanding of optimization method is vital as it might cause unstable model. From the reciprocal modelling of hysteresis and its parameter limitation condition, MATLAB coding and Simulink plan were articulated. The coding is derived to implant a state of initial values and subsequent product for the PSO and SIMULINK mainly to describe the Bouc-Wen model and most importantly as a platform to compare the experimental data and simulated data. The programming map follows the instruction phase as in Appendix C.

3.3.3 Computer Parameter search

Once the model for both Bouc-Wen and PSO had come to an agreement, the computer parameter search is simulated. These data are later compare to the experimental data collected previously.

The form of hysteresis models are satisfied by meeting at the predecessor model, align with the parameters considerations. In all, synthesizing is pleased when the model of Bouc-Wen is conjugated with PSO. Nevertheless, simulated model is confirmed when the evaluation stage confirm its theory. This is elaborated on the next chapter for verification of the hysteresis model and simulation.

3.4 EVALUATION, RESULTS AND DISCUSSION STRUCTURE

Formerly, the simulation section have met the conditions of modelling the hysteresis with associated software approach. These data are compared to the experimental data. The evaluation must meet the condition of reducing the marginal error at each extracted points. For each test condition the case is repeated by keeping the model parameters search constant together with the PSO algorithm.

Furthermore, the verification for measuring both performances are by judging through the average error from the examined test conditions. The lower average error suggests that the model has revealed appropriate results of reproducing the MR fluid damper behaviour. The following chapter will illustrate the procedure that has been governed from this methodology stage. A number of results from evaluation stage is granted however in deliberating the optimum results of hysteresis model searched by using PSO algorithm an elemental statistic is embedded to justify in numerical representation hence portray in diagram for visual perceptive.

3.5 SUMMARY

This chapter has converse the stages of the research methodology in realizing the finding of modelling an MR fluid damper by enhancing the parameters of Bouc-Wen model by Kwok using PSO algorithm. The methods were segmented in two main criteria; experiment and simulation stage.

For experiment part, it started out by developing the MR fluid damper. The structural and magnetic designs of the absorber were initially decided upon the outcome and operating performance to carry out the experiment. Once the damper had completely fabricated, the test rig setup was assembled through various indication for the absorber specification to meet requirement in order for the collection data to accomplish. The sensors and actuators that are required for realizing the data collection were placed in distinctive location. Then, collaborates these elements into digital version were done by system integration stage. To close the experimental phase as a render for simulation to attained, performing the experiment was done in various test condition. Once the appropriate results were conferred, the data were stored for comparison with simulation stage.

The simulation fraction is mainly to identify the result carried out by the proposed hysteresis model with PSO algorithm are restrained and acceptable for further analysis. Synthesizing between parametric models and software integration were explained and can be observed on the process of delivering the result with respect to experimental data. Comparison of existing models were carried to justify the proposed model are reliable to depict the MR fluid damper. In conclusion both experiment and simulation data were coordinated to ensure in evaluation process the outcome are satisfactory for further analysis. The next chapter will investigate thoroughly on the results and deliberate whether the results from parametric modelling with the support of PSO method can depict the behaviour of MR fluid damper.

CHAPTER 4

RESULTS AND DISCUSSION

4.1 INTRODUCTION

The description on previous methodology was demonstrated to apprehend the stages of promoting analysis apprehension in this chapter. This is done by divulging a comprehensive narration on developing MR fluid damper, examination of hysteresis model and the application of parametric identification method.

MR fluid is claimed as a material with intelligence behaviour that has the capability to change its properties once magnetized. A pragmatic solution in developing the MR fluid damper modelling is considered prominence in the parametric study where the challenge lies on the prediction of relationships between input and output. MR fluid dampers' elemental structure was presented affiliated with geometric consideration and performance. The subsequent accounts are then exploited with appropriate hysteresis model. A curve-fitting method of hysteresis modelling was expounded from various existing model in an inclusive comparison of parametric identification.

PSO is introduced as a parameter search in adjusting the best fitting model relatively to the developed MR fluid damper. The analysis is configured in a trail to execute parameter findings hence determine the best hysteresis model adequate to the MR damper. Simulation results of optimized hysteresis model and reference MR fluid damper was conferred and the validation for both experimental and validated data are discussed.

Then, a comparison of noteworthy hysteresis model was deliberated to obtain and justify the selected model for this research. An elementary statistical analysis is presented for unveiling the resolution for nominated models. Once the selection is fulfilled, the various test conditions for elected model is illustrated comparing the experiment and simulated data. Next, a thorough analysis on the marginal and percentile error was deliberated to enhance the declaration of finest optimized hysteresis model. The parameter values are examined to extent the understanding of significant changes that leads to forming the curve.

4.2 MR FLUID DAMPER CHARACTERISTIC

From the previous chapter, the MR fluid damper has been developed and employed onto the test rig. Hardware integration was successfully done and extracted to DAQ and saved as experimental results. The conditions of the experimental test were evaluated under a set of assessment as measured earlier. First the response is excited by the cam or the frequency of disturbance gauged by 1.1 Hz and the amplitude of 3 cm.

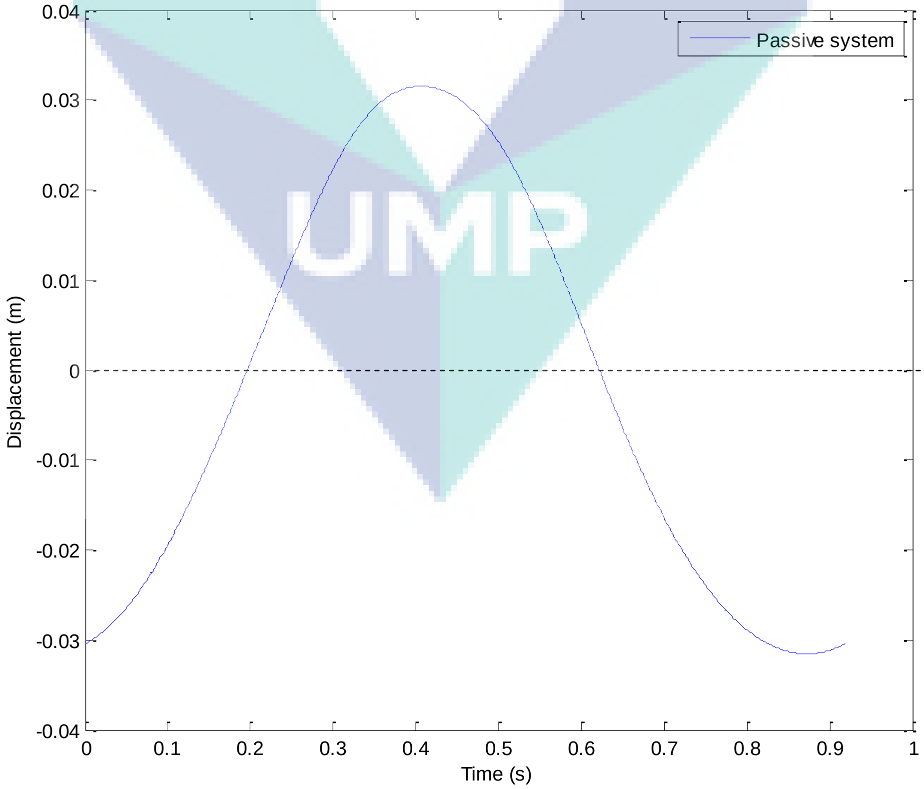

Figure 4.1: Displacement over time for passive absorber

Figure 4.1 reveals the MR fluid damper as in passive state in which no current was supplied onto the MR fluid damper. From this it confirms the behavior of MR fluid damper operates well even without any external input. As a fail-safe mode for the damper, it has sustained the effect and yet acts as a passive damper.

Then test conditions of current were inserted ranged from 0.0 A to 2.0 A with incremental value of 0.5 A. After the data were collected, the findings are examined in terms of hysteresis model; displacement over time, force over displacement and force versus velocity. Figure 4.2 demonstrates the evident from these practices.

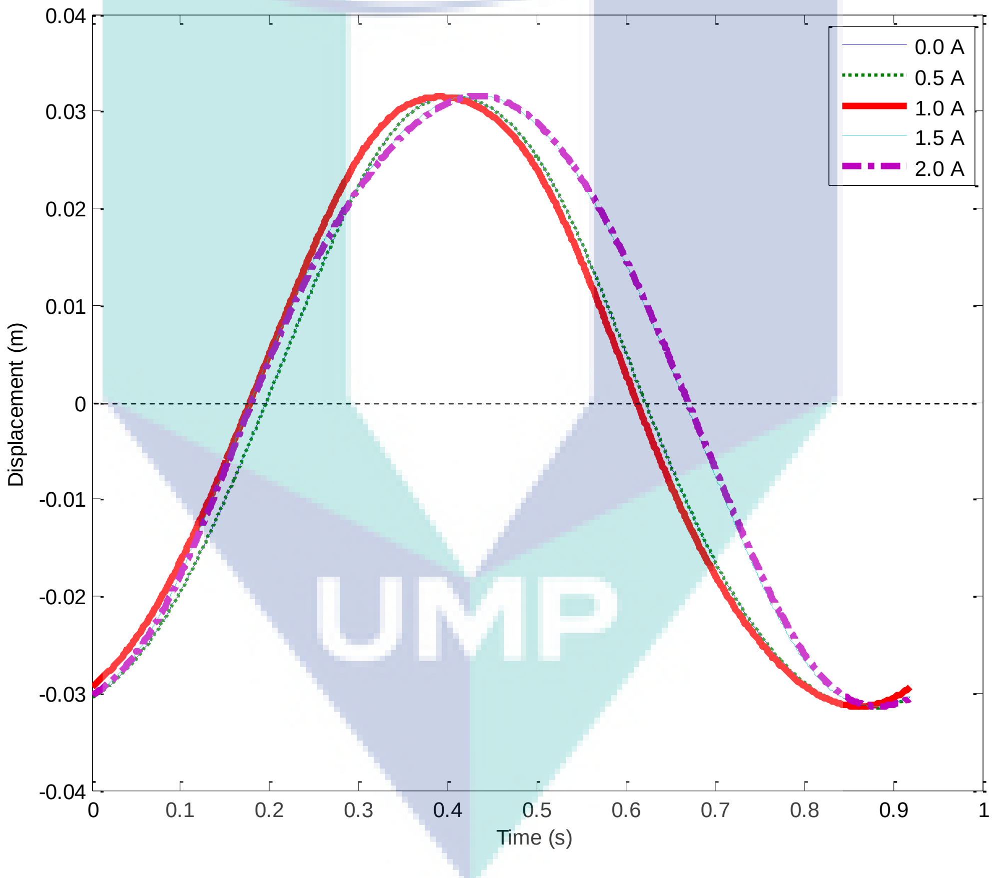

Figure 4.2 Displacement over time of test conditions

From evaluating the responses by the MR fluid damper, it can be noticed that the effect of changing the current input does affect the damper behaviour. As perceived on the diagram, the outcomes of 0.0 A and 0.5 A differ in miniscule value that are considered negligible change. But once the current is supplied to 1.0 A, a marginal shift is observed. As the test conditions raise its current of 1.5 A and 2.0 A, the reaction elongated, hence the reaction time for increase has upsurge to over 4.0 s compared to previous test of 0.0 A to 1.0 A. This is acknowledged by the resistive force generated from the MR fluid damper and the damper resists to act upon swiftly.

To perceive the force reactions of the damper, Figure 4.3 was extracted from the test conditions. An evident from this implies that as the current input increases the force accesses with respective input. As a retracting force, the direction changes as so for the force value, thus the graph depicts behaviour of the damper being in a motion of compression and rebound. Anyhow, the time taken for each action to meet at interjection (transition from compression to rebound) suggest distinctively. For 0.0 A and 1.0 A the time taken to transit are faster than 0.5 A along with 1.5 A and 2.0 A as it requires longer time to shift. As mentioned earlier to justify this similarity, the cause of non-linearity of the damper brings off peculiar result of the outcome. Nevertheless, the performance of MR fluid damper is adequate and acceptable for further analysis in the following process.

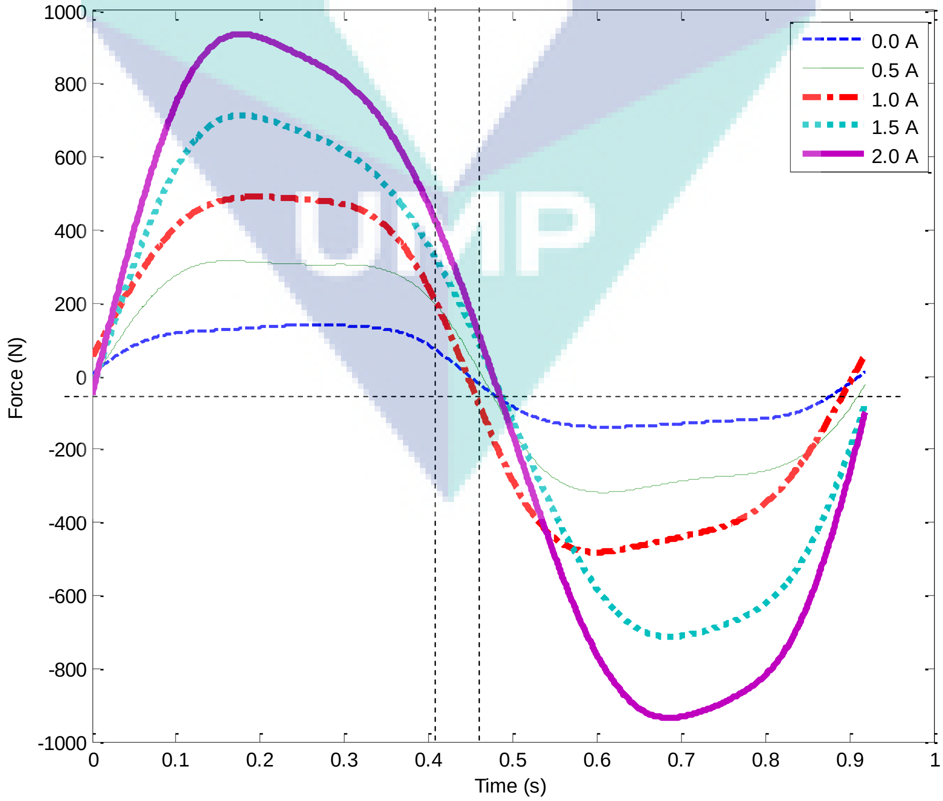

Figure 4.3: Forces over time current input comparison

On the contrary, Figure 4.4 represents the magnitude of the MR fluid damper for force against displacement. At initial state, the damper is situated at -0.03 cm in which the damper is said to be on a 'rest' state. By visual observation of the graph, it express that the damper gain respective forces from the current input given hence demonstrate the reaction of the absorber as it increases gradually from 0.0 A to 2.0 A. This is due to the restrictive force exerted by the iron chain particles perpendicular to the flow MR fluid. As the input current increases, the force reads higher value as it required more strength to compress the damper. Adversely, when the absorber is retracted, the rebound forces trails back to its original position. The forces recited negative value as it being on the opposite direction. From retracting bearing it suggest diverse curves as it can be seen that the gradients for 0.0 A, 0.5 A and 1.0 A have almost similar form at displacement 0.02 cm to 0.03 cm. However, a steep gradient was observed for 1.5 A and 2.0 A for repealing force at displacement of 0.01 cm to 0.03 cm for the reason of larger forces wielded by the MR damper. As consequence the response rebound time was influenced and an abrupt pace was detected during transition phase.

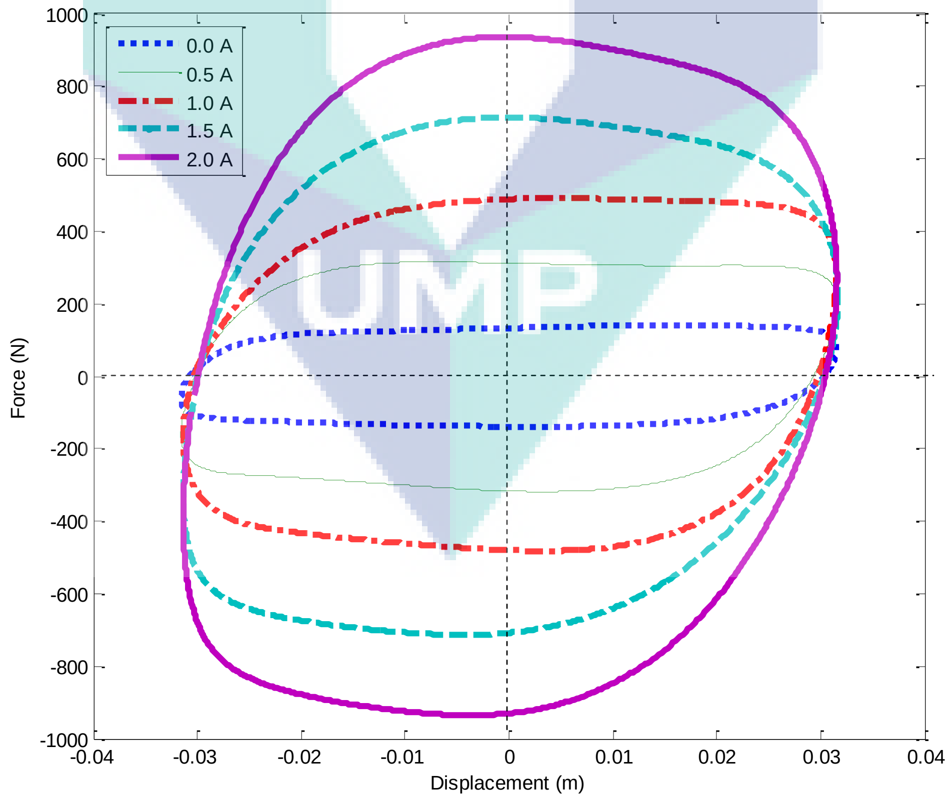

Figure 4.4: Force against displacement for various test conditions

In terms of force over velocity characteristic, it is exemplified on Figure 4.5 below where the hysteresis model is recognized. The gradient inclinations ascent for all succeeding conditions, and as specified earlier in Chapter 2 the significant parameters in hysteresis model that spur the model to form in respective manner. The noteworthy parameters will be discussed as progresses to model comparison. The next stage is to replicate the hysteresis model as closest to the experimental results portray by the MR fluid damper.

To consummate the MR fluid damper characteristic from the stage of developing the damper down to performing the experiment, the accumulated data was amiable. The results prove to be tolerable thus it is admissible to proceed with parameter identification.

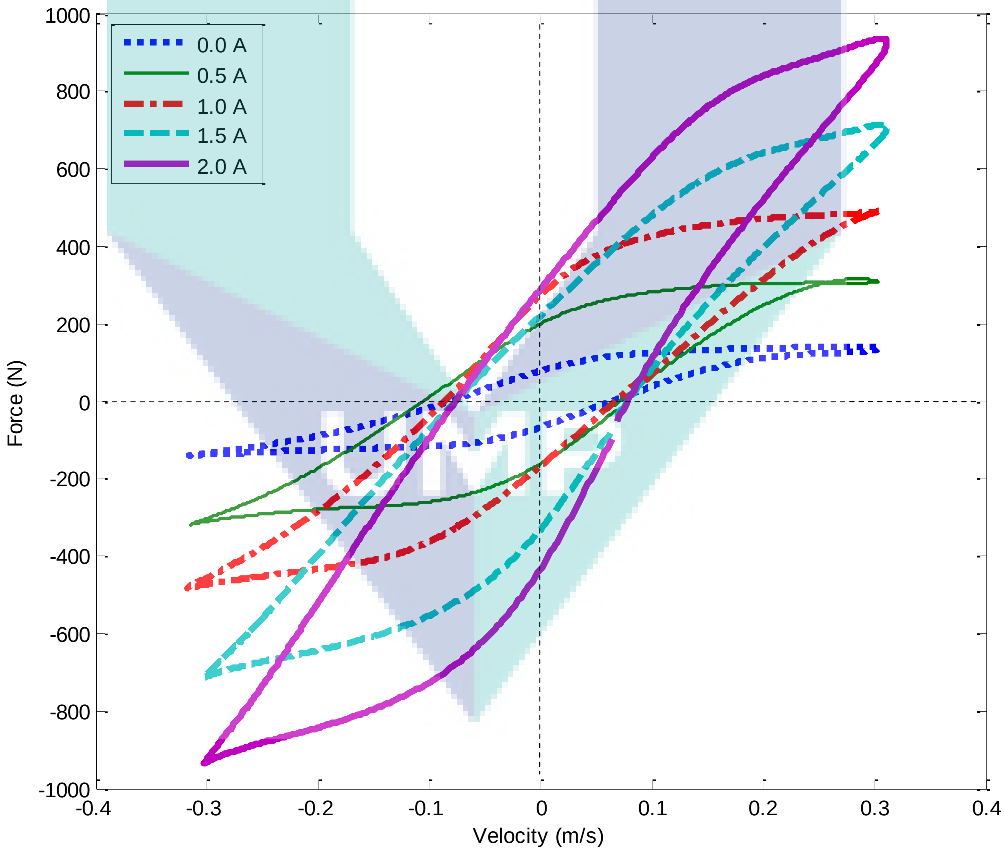

Figure 4.5: Force against velocity for various test conditions

4.3 EXPERIMENT VALIDATION ON PARAMETRIC MODEL COMPARISON

Formerly, the representative of MR fluid damper at various condition performances were elaborated and discussed on dissimilarity for each test. The outcome reveals comprehensive findings that allow the supplementary validation by imposing parametric identification method. In this subsection, a phase of comparing the algebraic equation is utterly prepared to justify the best fit hysteresis model to the experimental data. This is done by managing the model in MATLAB and SIMULINK program. As a remark from Chapter 2, the decided parametric models were Bingham, Simple Bouc-Wen, and Bouc-Wen by Kwok. These models exhibit less complication during the synthesis process.

Accordance on selecting the model for this research, a comparison of existing model is established. The objective is to recognize the best fit model to the experimental conditions. Other studies have measured the realistic findings on the best model, however their claims only valid for exclusive condition according to their specifications (Sahin et al., 2010). Nonetheless, the model examined here is singled out on the achievement of calibrating between hardware test rig conditions and simulation using MATLAB and SIMULINK.

An evaluation method was exploited to gauge the differences between experimental and simulated data. A basic scheme for justifying the measurement is illustrated as Figure 4.6 and referred to Appendix C. Firstly, the Input Data (collected from experiment) are submitted into Synthesize Program for valuation with the programming code.

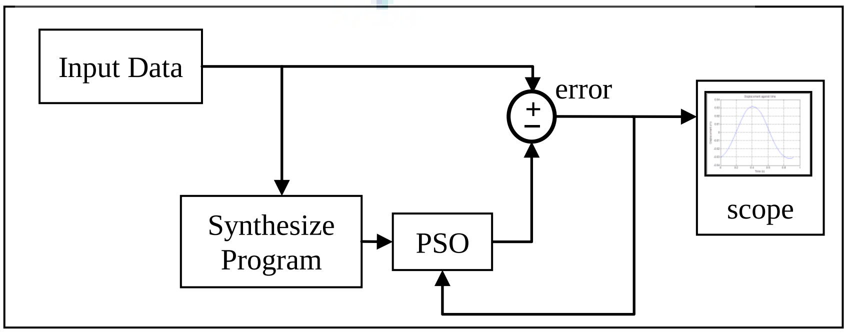

Figure 4.6: Error comparison gauge measurement

The hysteresis models have been incorporated in the Synthesize Program beforehand, the reason is to clarify significant parameters that required optimization prior to disparity investigation with experimental data. Subsequent to altering the relevant parameters, PSO was applied to enhance the performance of simulated hysteresis graph and compared to the Input Data. Then, an evaluation was made to ensure the error between both Input Data and the resultant optimize result is satisfactory. To end with the appraisal, a visual of both set result is drafted as Figure 4.7. It draws the graph for Bingham model of experimental and simulated data for the current input of 0.0 A to comprehend on the curve divergence.

As presume by the mechanical simplicity of Bingham model, it could not ideally conduct the representation of experimental data. This can be highlighted at the leap nudge at 0.4 s and 0.88 s as the lines fall short to resume on the subsequent course.

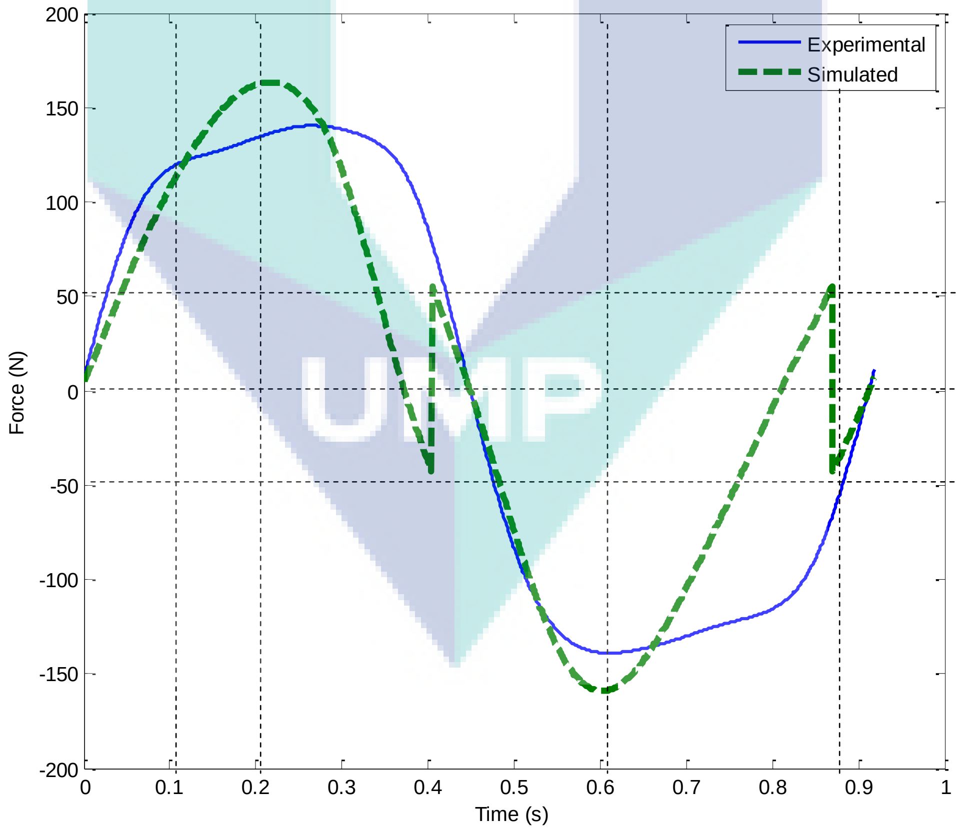

Figure 4.7: Comparison of data for Bingham model with 0.0 A

To rationalize the hitch pertaining the deficiency of Bingham model identification, it can construe that the number of the model parameters necessitate for demonstrating a best fit model were limited. As the sequence for experimental data casted, the simulated curve starts to surpass the region of 0.12 s to 0.2 s. A steep declination witnessed after it reaches maximum peak disregard to attempt on trailing the original reference point. Yet again the similar occurrence of neglecting the primary line has subdued the simulated line from lowest end at 0.6 s up till 0.88 s. It is confer that this model requires supplementary adjustment to achieve suitable fitting to the experimental bend.

Next is the simple Bouc-Wen model to be compared with the original performance of MR fluid damper. Unique features of the Bouc-Wen model formulation has oblige the use of Simulink to detain its operation in synthesizing the software program. Figure 4.8 as per Appendix D of Simulink blocks insinuates the formulation into minimal computational complexity like so manage to match the experimental order.

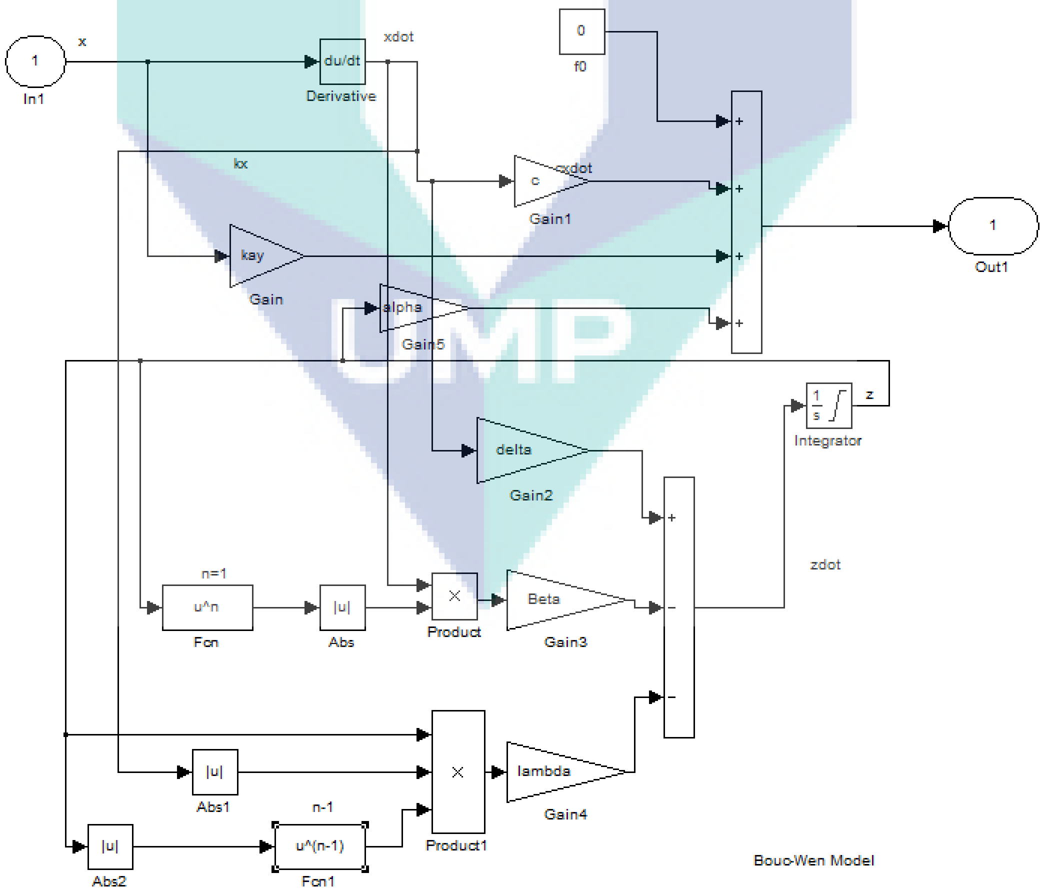

Figure 4.8: Simulink circuit of Bouc-Wen model

From Equation 2.30 and 2.31, the parameter of *z* as the hysteresis variable ought to incorporate with the total force as a product with α. By utilizing SIMULINK function, the model formulation for Bouc-Wen model was accomplished. Hence, the required parameters to optimize have undergone a phase of iteration in PSO in search of best possible fitting into experimental diagram.

Once, the PSO has reached its verdict on the finest selection of parameters value, the figure is printed out with respect to the experimental graph. It can be seen in Figure 4.9 that both data have been illustrated onto the figure. Although the simulated curve shows decent approximation to the reference, it has slight variation throughout the manner. The serrated appearance between 0.6 s to 0.7 s is evidence of restriction in command initiated through SIMULINK for Bouc-Wen model. Nonetheless, it was a good estimation as regards to the MR fluid damper and requires a fair amount of enhancement to duplicate finer replication.

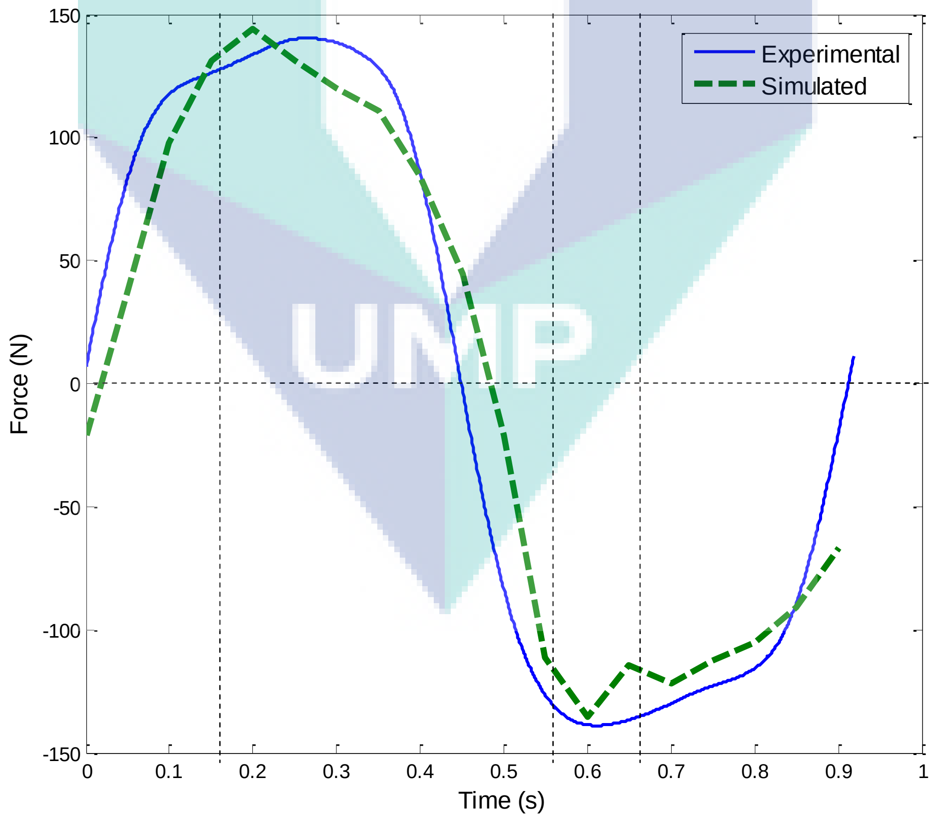

Figure 4.9: Comparison of data for Bouc-Wen model with 0.0 A

From list of hysteresis model comparison, the Bouc-Wen model proposed by Kwok et al. (2006) is the remaining procedure to establish a reasonable resemblance towards the MR fluid damper. It was done computationally using MATLAB coding as Appendix B and dispatch to PSO for optimization as shown in Figure 4.6. The results of this process prove to verify that this model has the best solution in imitating the MR fluid damper behaviour.

Examining the response constructed by simulated data, it is admissible to justify that Bouc-Wen model establish more robust gesture towards the MR fluid damper performance. The Figure 4.10 has spotted the delicate phase of reproducing hysteresis model mainly at the site of 0.2 s and 0.6 s. Although there is a gap error at these points, it is deem to accomplish the best solution out of the previous model that has been deliberated.

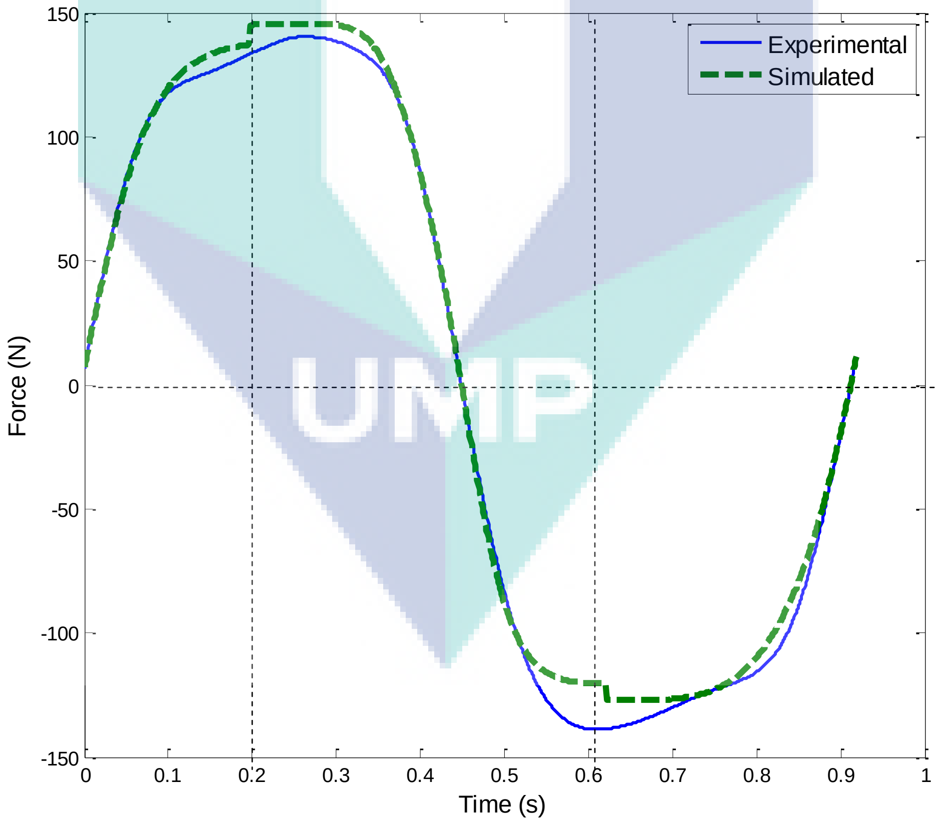

Figure 4.10: Comparison data for Bouc-Wen by Kwok et al. (2006) model with 0.0 A

Revising the performance of these three models, the test conditions for various current input were commence to gauge how the result either alleviate or aggravated as the current increases. The following figures demonstrate implication of this test.

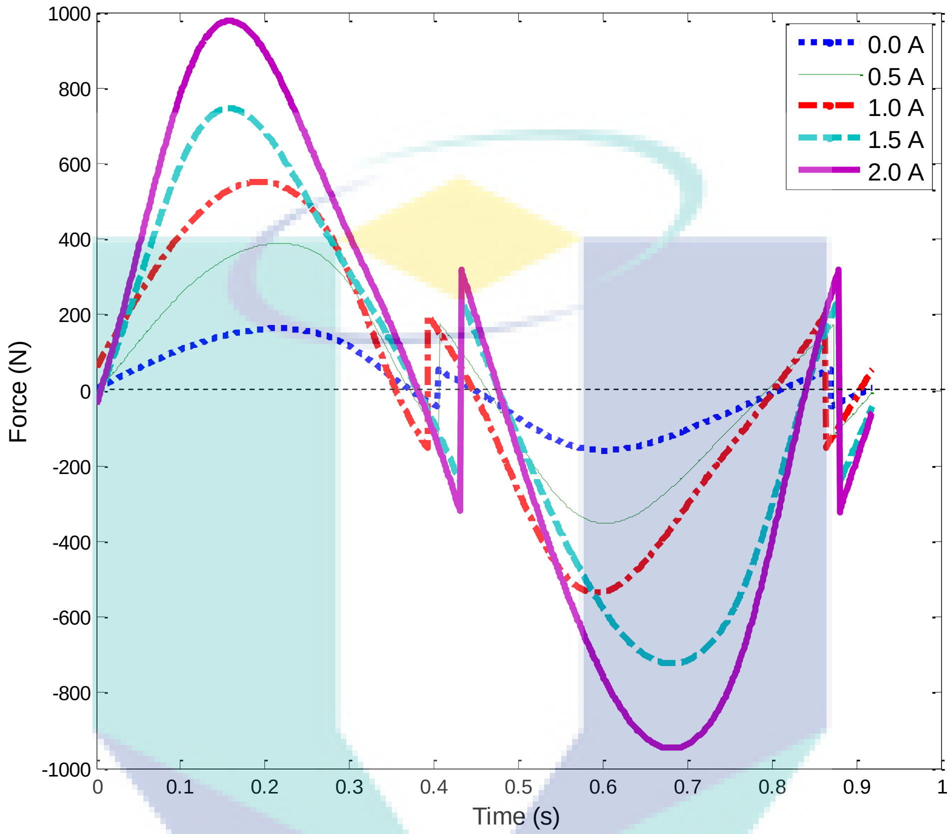

Figure 4.11: Bingham model comparison for various test conditions

To state the lucid remark from Figure 4.11, 4.12 and 4.13 was the discrepancy in projecting a fixture corresponding to the experimental value as the test conditions current intensify. In Figure 4.11, the range of aberration is detected at the juncture between compression and rebound with the largest gap during input current of 2.0 A with nearly 550 N of discrepancy. In contrast to Figure 4.12 for Bouc-Wen model, the dispute is not at the instant transition, but at the trajectory fitting as it is inaccurate and seems miscarry the original form. The intention to achieve maximum and minimum curve were appalling in which has distorted the hysteresis form. This might be the cause of internal noise spawn during computational search using Simulink. Shortage of defining the boundary and appropriate filter may cause the model to provide suitable outcome. Nonetheless, the model manages to overcome the passing form compress and rebound phase, yet further adjustment requires obtaining plausible results. In response to former models, the Bouc-Wen model by Kwok et al. (2007) displays logical interpretation on hysteresis model.

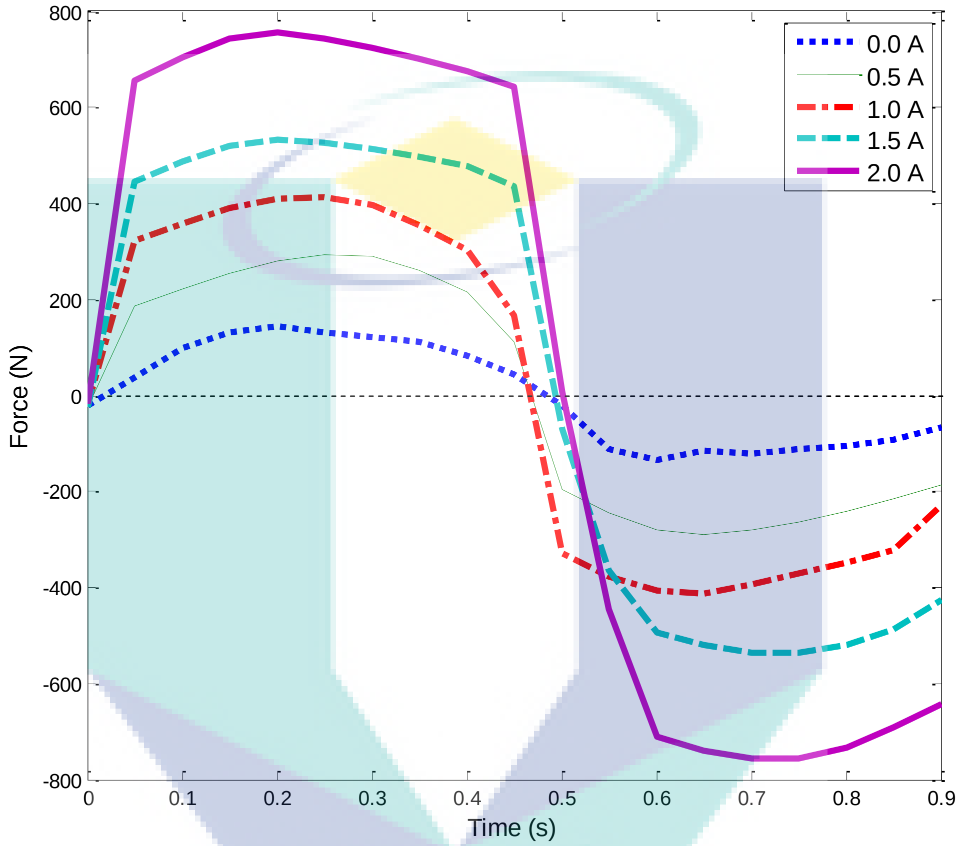

Figure 4.12: Bouc-Wen model comparisons for various test conditions

However, to highlight the mishap on Figure 4.13, at time 0.19 s and 0.65 s indicate the similar case as Bouc-Wen model wherein translating the fitting curve at maximum and minimum trajectory is arduous. The severity of this cause does not affect the representation of hysteresis model considering Bouc-Wen by Kwok et al. (2006) at most points delivered the best possible solution. To apprehend the comparison aforementioned, Figure 4.14 exposes the distinction of each models and by visual prove the leading hysteresis model amongst them.

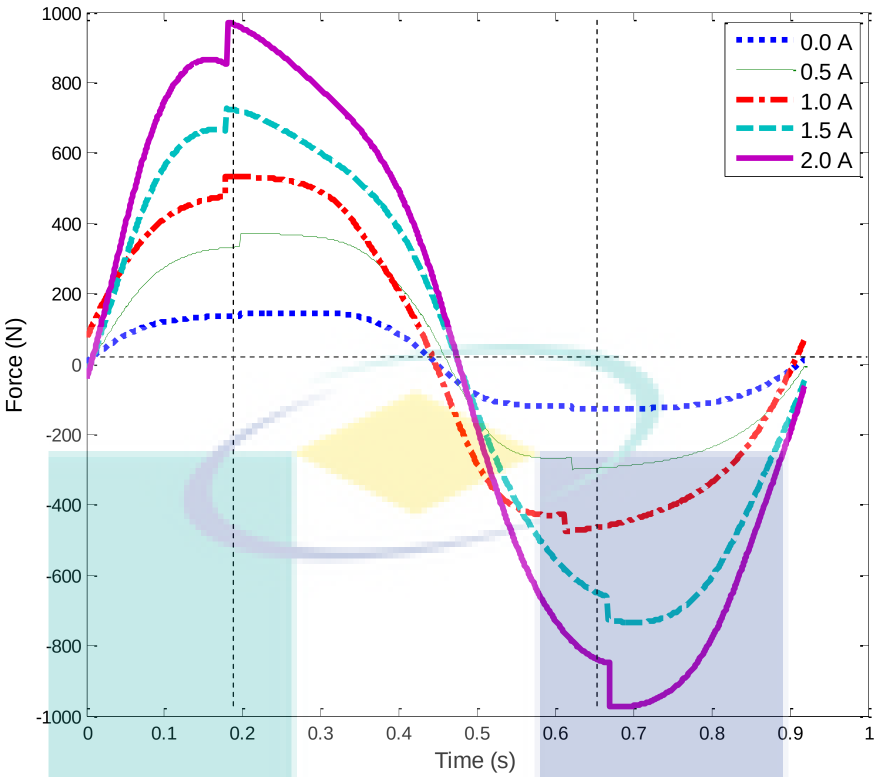

Figure 4.13: Bouc-Wen model by Kwok et al. (2006) comparisons for various test conditions

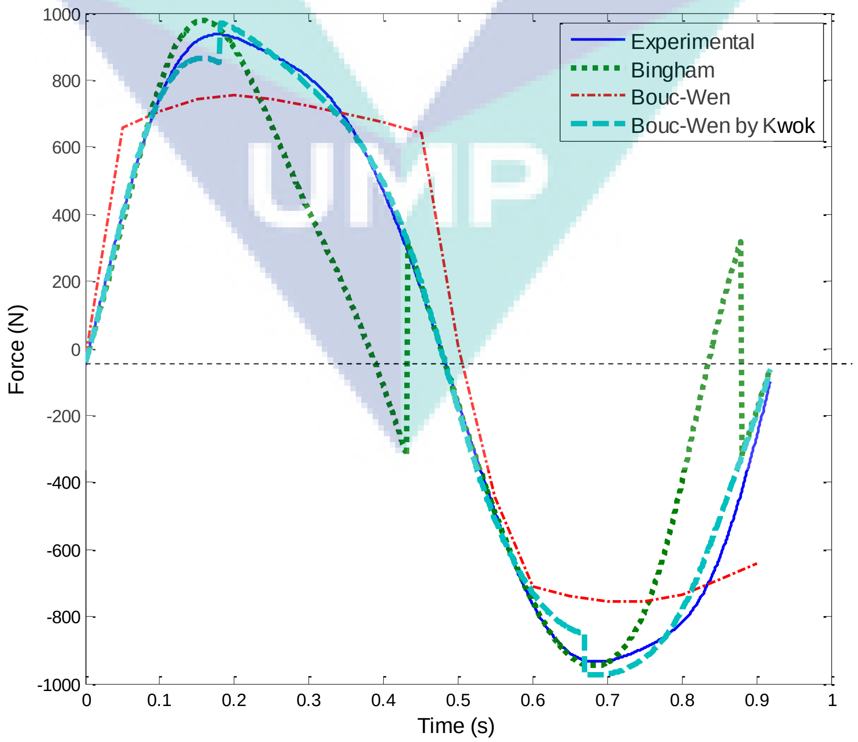

Figure 4.14: Comparison of hysteresis models performance for 0.0 A

As speculated earlier, Bouc-Wen model by Kwok proposes the adequate representation of MR fluid damper. To justify the comparison results, a transparent statistical analysis approach was adopted to further clarify the variance from these models. Equation 4.1 resolve the approach of mean average error:

$$\text{Mean error} = \sum_{1}^{N} \left(F_{exp} \text{-} F_{sim} \right) \tag{4.1}$$

Where F_{exp} is the experimental data and F_{sim} stands for the results project by simulation. This approach is to gauge how much difference the forces are relatively to original damper behavior. Table 4.1 polls the respective findings ensuing with the test conditions input.

Table 4.1: Mean of parametric models force error (N)

Test condition *Current input (A)*	***Parametric model error (N)***		
	Bingham	Bouc-Wen	Bouc-Wen Kwok
0.0	35.917	20.094	5.452
0.5	87.068	30.752	20.601
1.0	110.347	75.829	18.142
1.5	139.181	119.175	23.013
2.0	182.453	150.557	33.201
Mean average	**110.993**	**79.281**	**20.082**

Trends of rising force error were observed for all models as the current input ascends. The largest increment is clearly distinguished from Bingham model in range of 30 N to 50 N as the test input extents. With a demeaning mean average of 111 N it placed the Bingham model as an unseemly form for replicating the MR fluid damper behaviour. The Bouc-Wen model on the other hand demonstrates slight improvements in the marginal error with impartial results of 79.3 N. Nonetheless, this irregularity outcome is still inconsistent in parameter identification. Ultimately, the Bouc-Wen model by Kwok presents an astounding inference on MR fluid damper performance. The divergences between the test conditions were minimal with less than 15 N and significant mean average of 20.1 N marginal errors. Concluding these facts by diagram illustration will enhance the comprehension of best parametric identification motive. Figure 4.15 depicts the mean deviation of force error against test conditions for supportive evident on the findings.

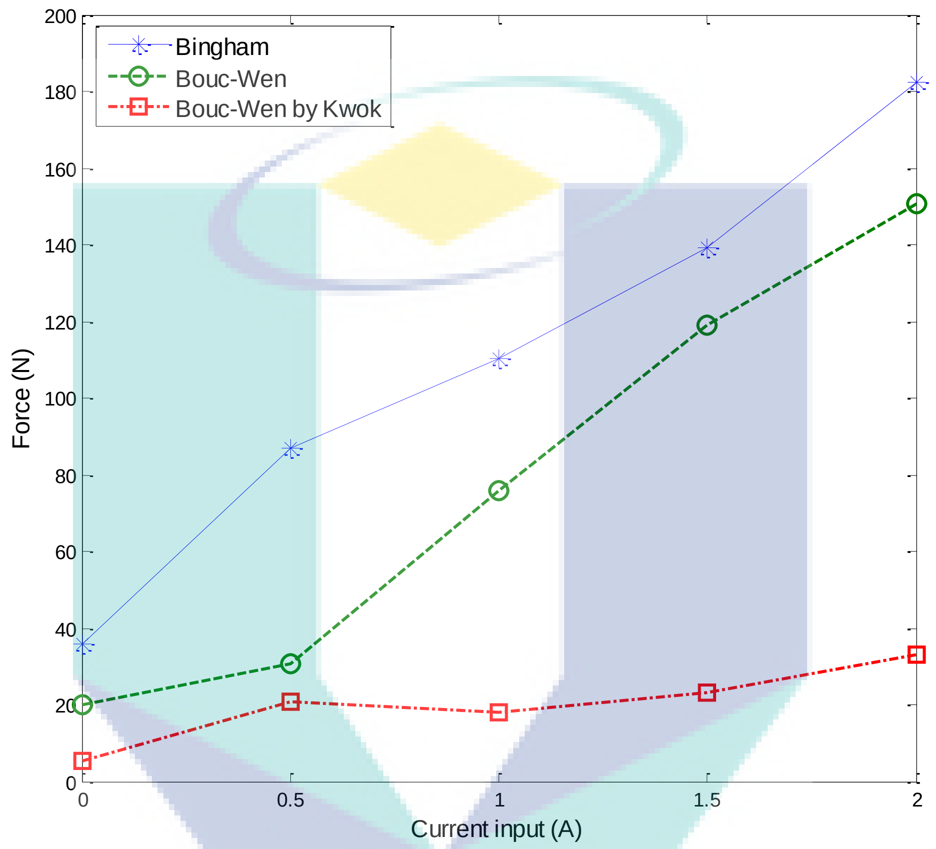

Figure 4.15: Model comparison of mean deviation force error

Justification from the figure has concluded that hysteresis Bouc-Wen model proposed by Kwok delivers the best out come from the other models. Hence, this model was selected for extensive analysis of parametric identification. Next subtopic is to discuss on the consequence verification of implanting Bouc-Wen Kwok model into parameter search to determine the resolute parameter values of hysteresis model.

4.3.1 Consequent findings on Bouc-Wen model by Kwok

This subsection is purely the findings of extrapolating the simulation data from experimental behaviour of MR fluid damper. The figures sorted out into respective graph of force over time, force over displacement and force over velocity for various test conditions. An additional figure was computed to assess the force error across the experiment test. It was plotted in segregated manner for each condition as the objectives is to imitate the MR fluid damper for given current input.

The initial step on testing the experiments are to apply a current input of 0.0 A. As mention earlier, the behavior is comparable to passive damper due to zero current exerted hence the MR fluid acts as a typical fluid damper excluding the resistive force by unmagnetized particles. Figure 4.16 is the trait that how the findings is demonstrated as the act of scrutinizing the simulation data achievement towards the measured value.

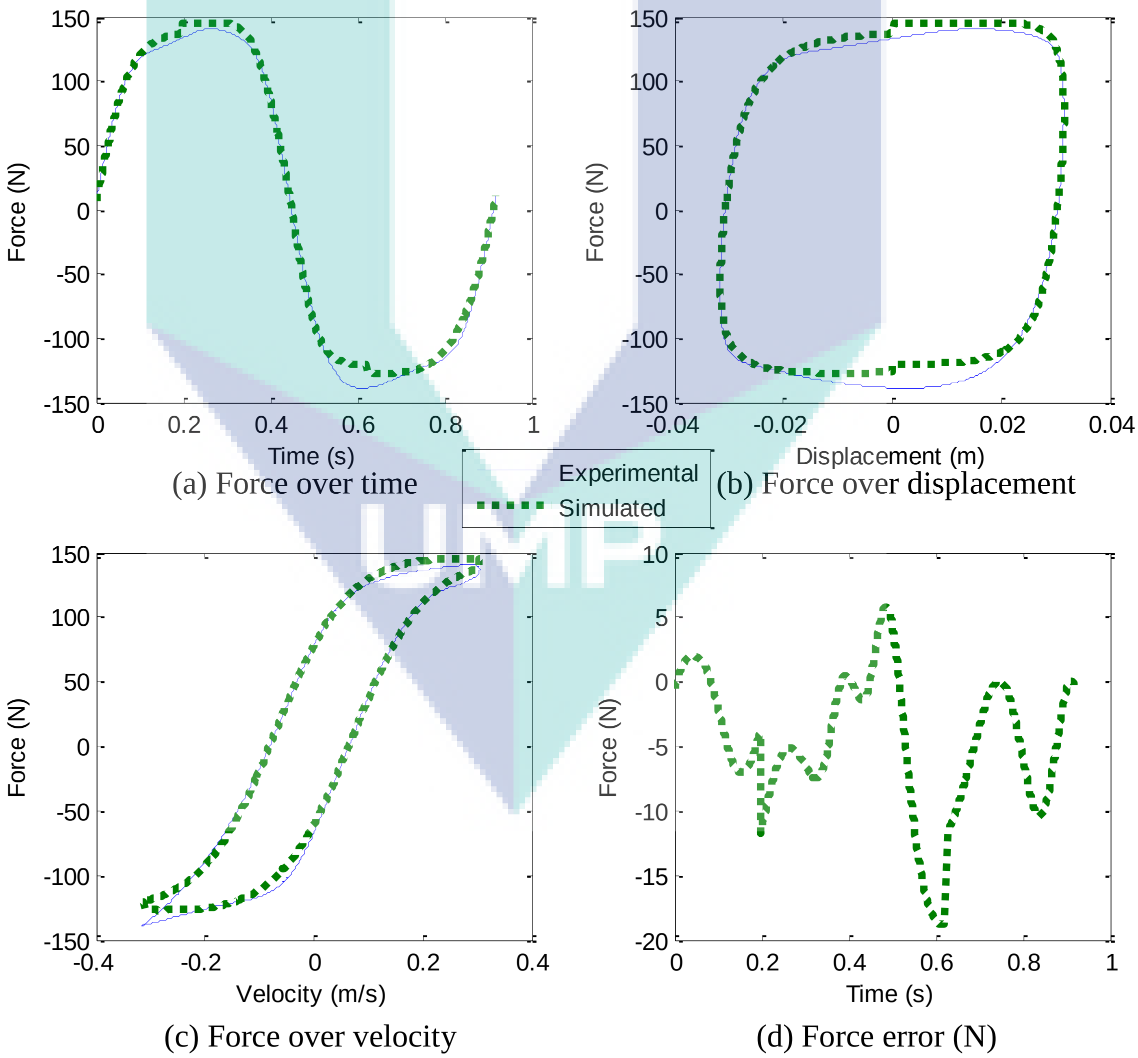

Figure 4.16: Data comparison of Bouc-Wen by Kwok (2007) model for 0.0 A

The exhhibitions of respective figures were assigned in arrays as in Figure 4.16. The force over time graph has been formerly examined similar to Figure 4.10. Nonetheless it was mere justification on the force against time only without evaluating with force over displacement and velocity. With supporting figures as Figure 4.16 (b) and (c), the judging and realization are much attain as it relates to the corresponding hysteresis model. To second the findings, the marginal error in term of force as Figure 4.16 (d) was elaborated as discussed reffrering from Equation 4.1. In this manner, the inspections of the findings are done in parallel for straightforward verdict. Taken as a whole, the reponse emulated from test condition 0.0 A presents a credible results and as a decisive model for parametric identification. Next condition to be examined is the input current of 0.5 a as shown in Figure 4.17.

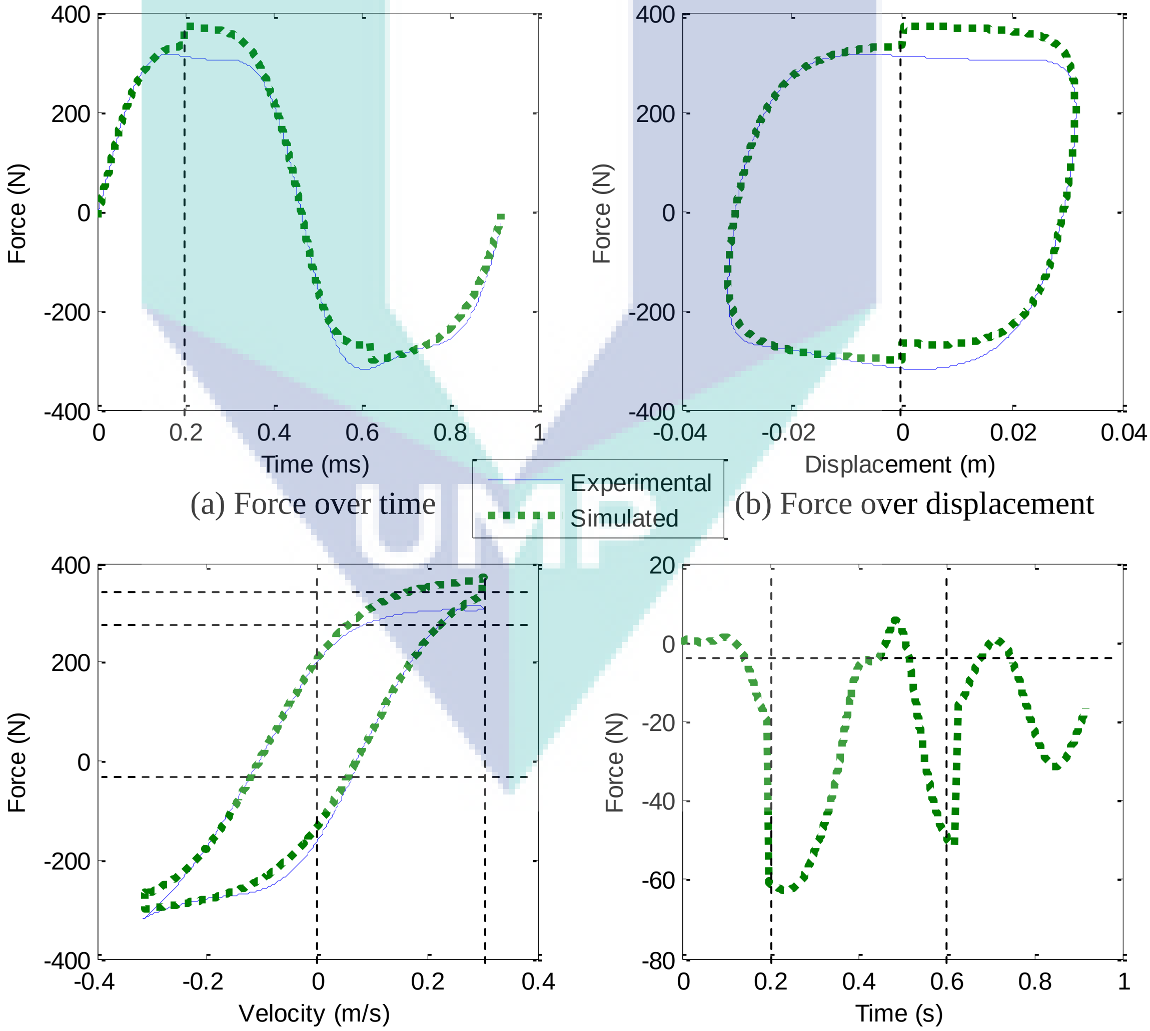

(a) Force over time (b) Force over displacement

(c) Force over velocity (d) Force error (N)

Figure 4.17: Data comparison of Bouc-Wen model by Kwok (2007) for 0.5 A

The results suggest diversely from previous test, the simmilarity of measured and calculated data were rather disfigured. Figure 4.17 (a), (b) and (c) depict the insignificant defect. In force over time graph has pointed out perceptible slit at time 0.2 s. As a consequence, Figure 4.17 (b) was affected mainly at displacement 0 m in which the magnetized particles undertook the impact to restrict the absorber by increasing the damping coefficient. The status of marginal error reports the highest remote with 60 N. The rationale of this is clearer on the hysteresis graph of force against velocity between 0 ms^{-1} and 0.3 ms^{-1}. Simulated graphs were inflated over the measured graph as the velocity increases due to the edge of retracting the absorber. However at -0.3 ms^{-1}, the halt of rebounding graph shows promising balance in the impression to measured data successively verify that this model is ascertain. Current input of 1.0 A is deliberated on Figure 4.18.

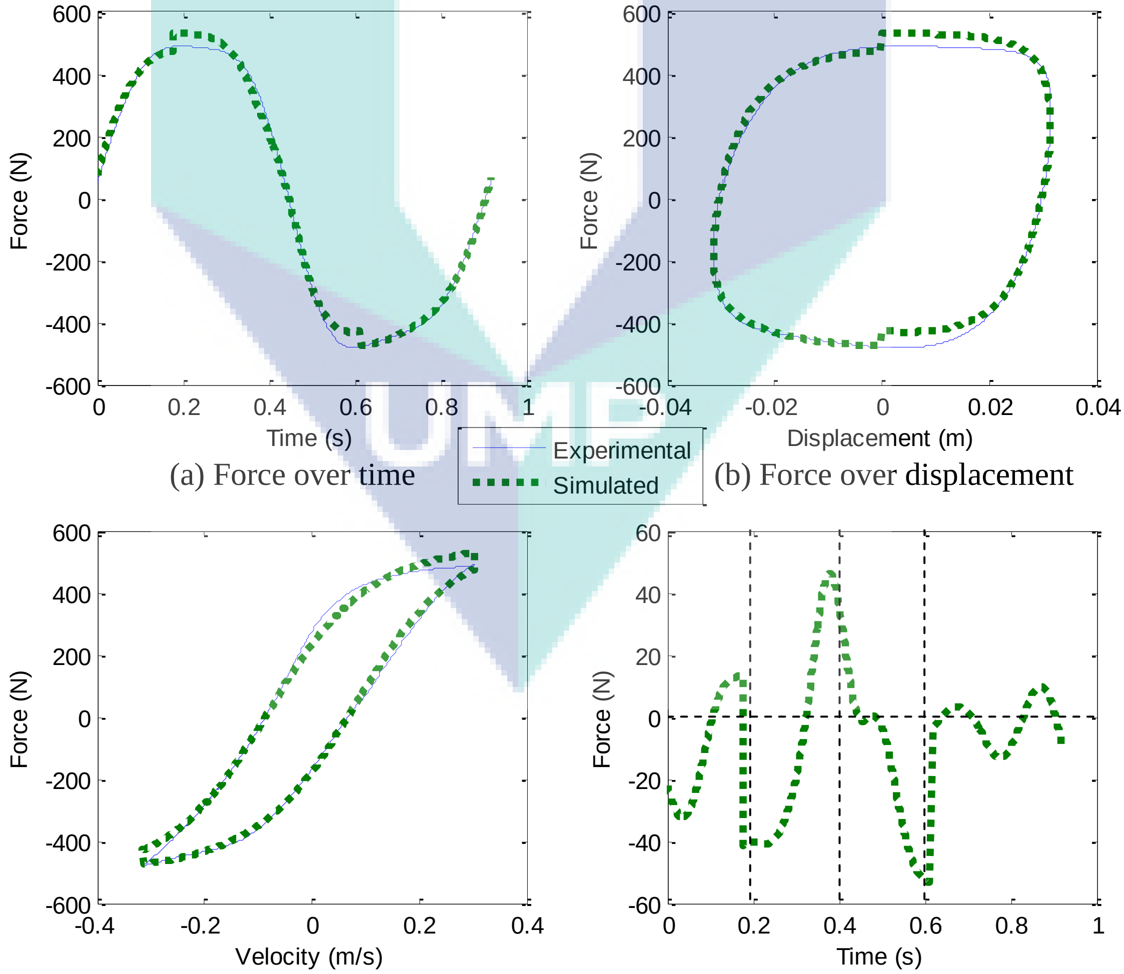

(a) Force over time
(b) Force over displacement
(c) Force over velocity
(d) Force error (N)

Figure 4.18: Data comparison of Bouc-Wen model by Kwok (2007) for 1.0 A

It is much convincing to witness that as the current input rises the response does not deflect further from experimental curve. It has illustrated for all three Figures 4.18 (a), (b) and (c) validated admirable outcome. Concentrating on the force error diagram, the time where eminent difference was recorded at time 0.2 s and 0.4 s with 40 N, and at 0.6 s with 55 N. These are the crucial transitions for the simulation to mimic however the justification for suitable model has concurred that this model manages to sustain its performance so far. Resuming with the analysis, the next test conditions to be investigated were the illustrations for 1.5 A current input as in Figure 4.19.

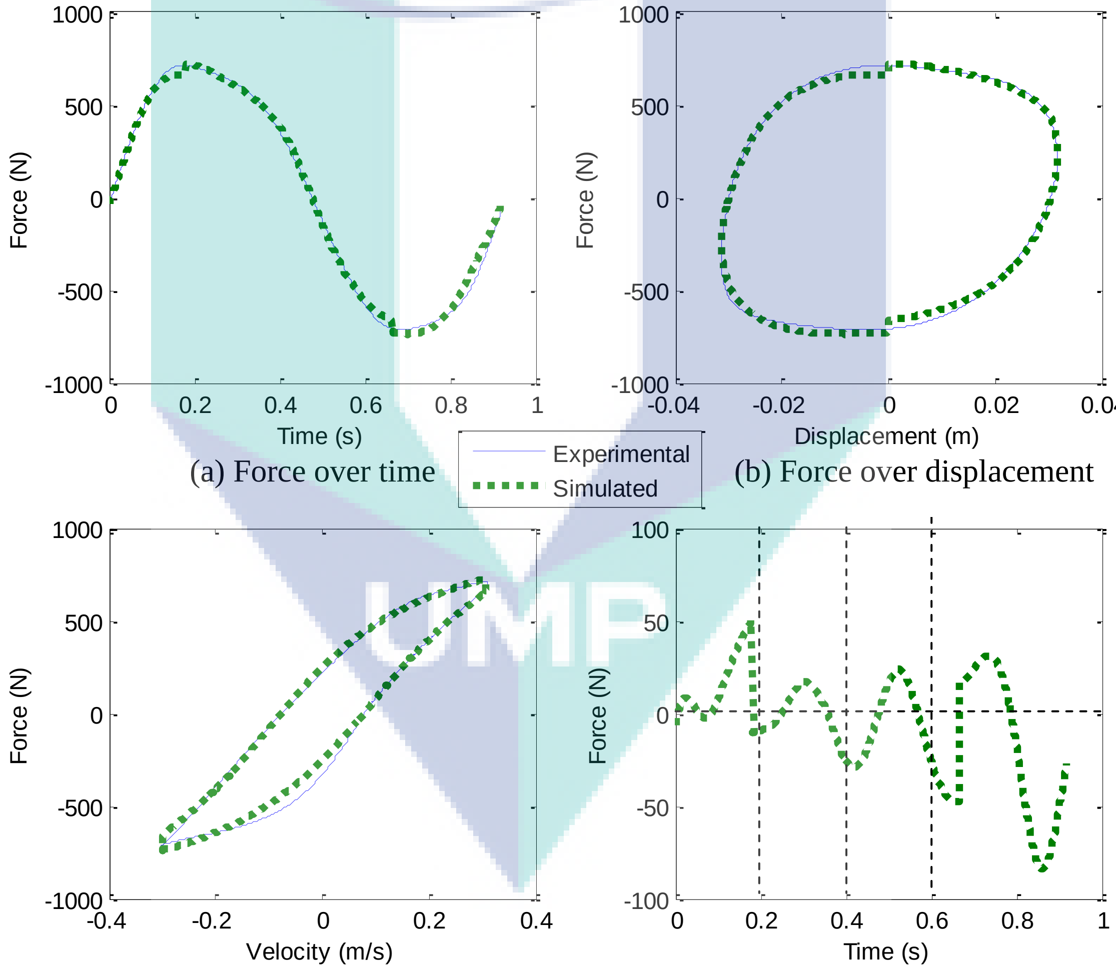

Figure 4.19: Data comparison of Bouc-Wen model by Kwok (2007) for 1.5 A

It is well aware that the higher the current input on MR fluid damper will generate greater resistive force, in subsequent it was more delicate to reproduce the absorber reaction with a thin despair will affect substantial amount of marginal error. Figure 4.19 exhibits the standard plotting arrays, and to focus on the force error graph it reveals a maximum error mounted up to 80 N which has raised 25 N from previous test. In spite of this, the simulation did conserving the hysteresis model profile exceptionally even so with enlarged force boundaries. Collectively the pattern from tests input thus far have left traces of the fragile area, primarily detects at time 0.2 s and 0.6 s. Then again the figure above has identified another remark on the crucial area after 0.8s in which the absorber was drawn to the initial position. This phase is the retracting motion before coming to the starting point and to emphasize this incident, Figure 4.19 (c) withdraws the transitions at -0.03 ms^{-1} as the source for fragile point. Current input of 1.0 A is deliberated on Figure 4.18.

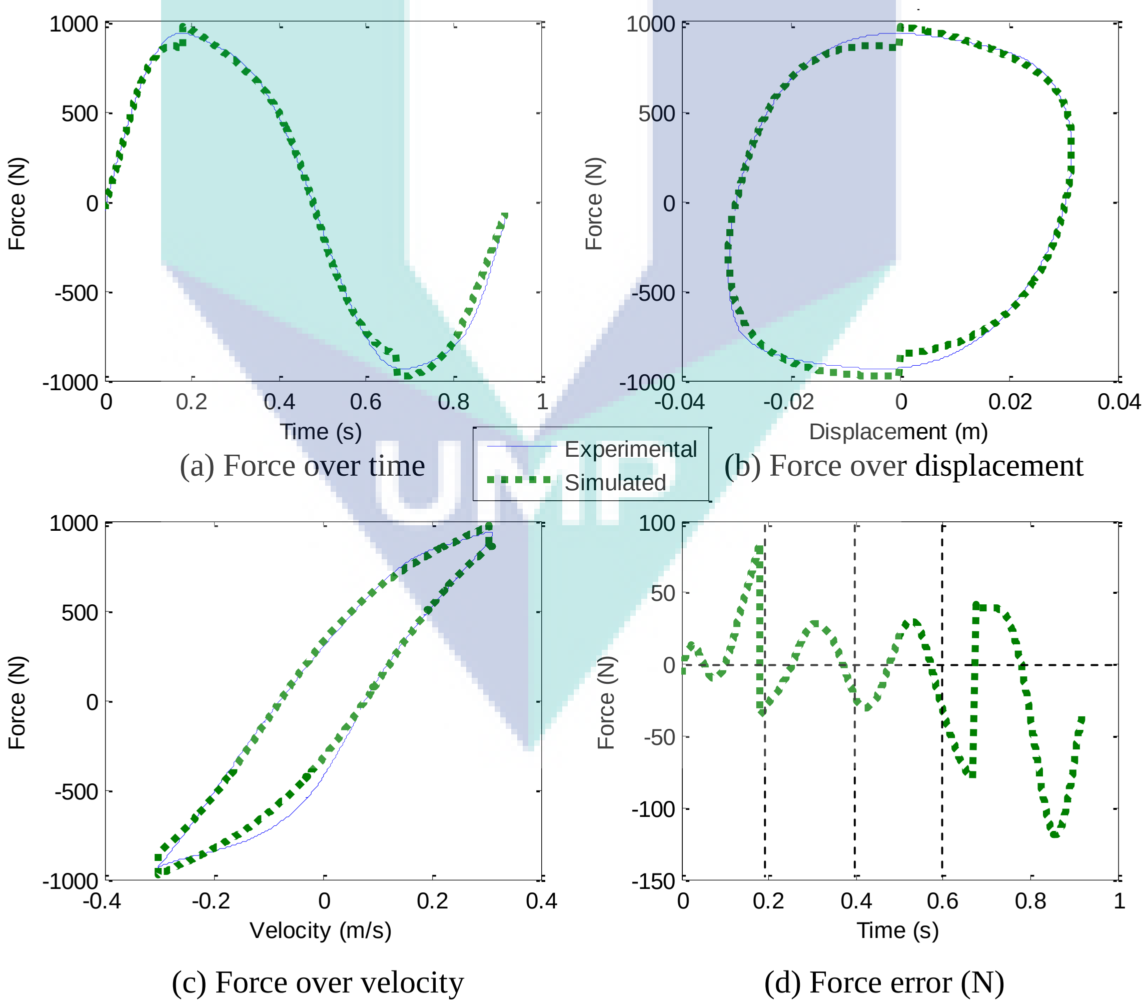

Figure 4.20: Data comparison of Bouc-Wen model by Kwok (2007) for 2.0 A

However, it is yet to be concluded after realizing the outcome from last test condition of 2.0 A that is obtained as in Figure 4.20. Resembling to previous test results, the crucial area as predicted has stated the disproportion at time 0.2s, 0.6s and 0.8s. The nonlinearity of MR fluid absorber is inevitable although the responses from Figure 4.20 (a), (b) and (c) that was predicted by this model has shown substantial outcome in evading the external noises during simulation and parameter search.

In general, the entire results from the test conditions forecasted by using Bouc-Wen model by Kwok et al. (2006) were endurable despite having minor setback that was insignificant with respect to the MR fluid damper characteristic. As an alternative, supplementary analysis were taken to commit into final verdict of verifying the parametric model as a substitute for modeling MR fluid damper.

4.4 SUPPLEMENTARY ANALYSIS

Prior to the deliberated results, this subsection is the complementary findings from previous outcome. Proceeding to the test condition errors, a comparison of their divergence are dispense for unambiguous verification. Then, percentage error graph is conferring to make an estimation of the deviation. The values for parameters in accordance from Bouc-Wen Kwok model are manifests subsequently. The assumptions that were made earlier can be justified herein from visual and numeric interpretation.

Notifying the fragile section at time 0.2 s, 0.65 s ± 0.5s and 0.8 s, it has clarified that there is an existence of border at these points displayed on Figure 4.21. For the first three current inputs it suggests that the errors are in the range less than 60 N. The consistency of this model to maintain its form was impressive until input current of 1.5 A was inserted. The graph plummeted at time 0.85 s precisely which includes the curve for 2.0 A. It is explicable to claim that the elevation is due to higher range of force in short given space. Nonetheless the probability of extended error is logical from conducting bigger range forces.

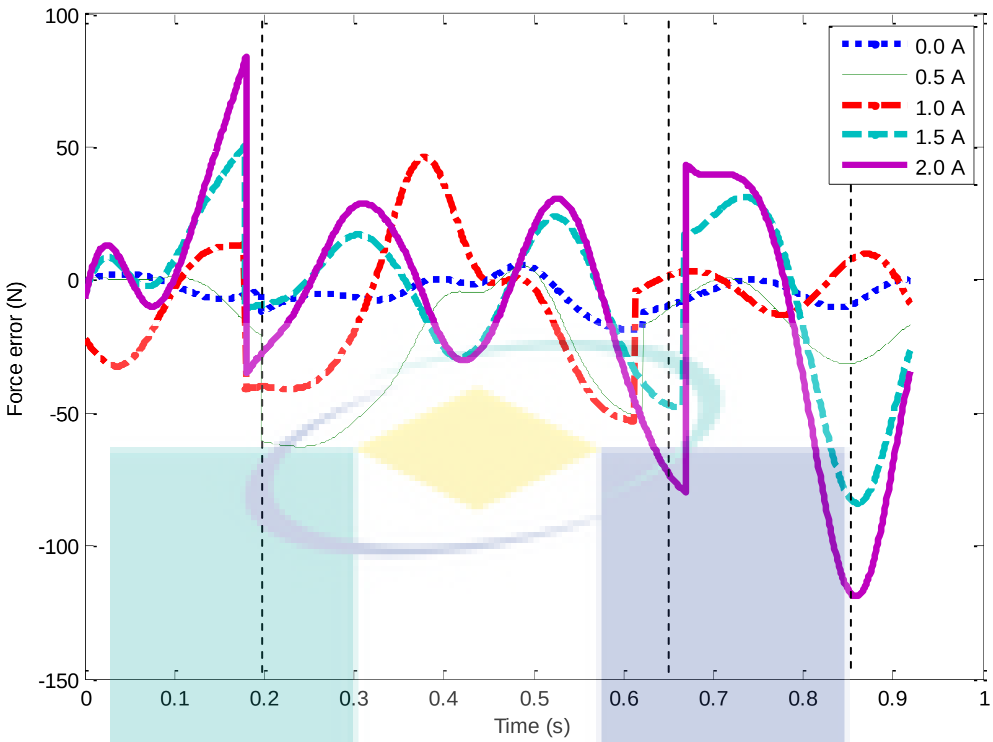

Figure 4.21: Force error comparisons for various test conditions

A constructive method was carried out to conserve the statement for best fitting solutions by the model. This was done by measuring the percentage error of each simulated point with reference to experimental data. By addressing it comparatively by percentile, the correlation with given test inputs are sensible considering that different test inputs have peculiar force range. Equation 4.2 below interprets the evaluation of percentage error in force unit:

$$\text{Percentage error } \% = 100 \times \sum_{1}^{N} \left| \frac{F_{exp} - F_{sim}}{F_{exp}} \right| \tag{4.2}$$

where F_{exp} is the experimental value and F_{sim} is the simulated data for the forces respectively. The conclusive results were charted as in Table 4.2 underlining the maximum and mean percentage error.

From the Table 4.2 lists down the tally between test input and percentage error of maximum and mean value. The highest maximum value is 39.0 % by test input of 0.5 A and the leading mean error was provided from 0.5 A condition. These results suggest the nonlinearity exists in MR fluid damper and the parametric identification results may alter along replicating the behavior. However, the findings from percentage error have listed the mean values to be consistent in the range of 5 % to 9 % error throughout the parameter search in curve fitting and modeling of MR fluid damper. Figure 4.22 illustrates the percentage error comparison for pictorial analysis.

Table 4.2: Percentage of force error for various test conditions

Test Input	***Maximum %***	***Mean %***
0.0A	13.6	5.11
0.5A	39.0	8.47
1.0A	24.1	6.12
1.5A	35.6	6.45
2.0A	35.3	6.72

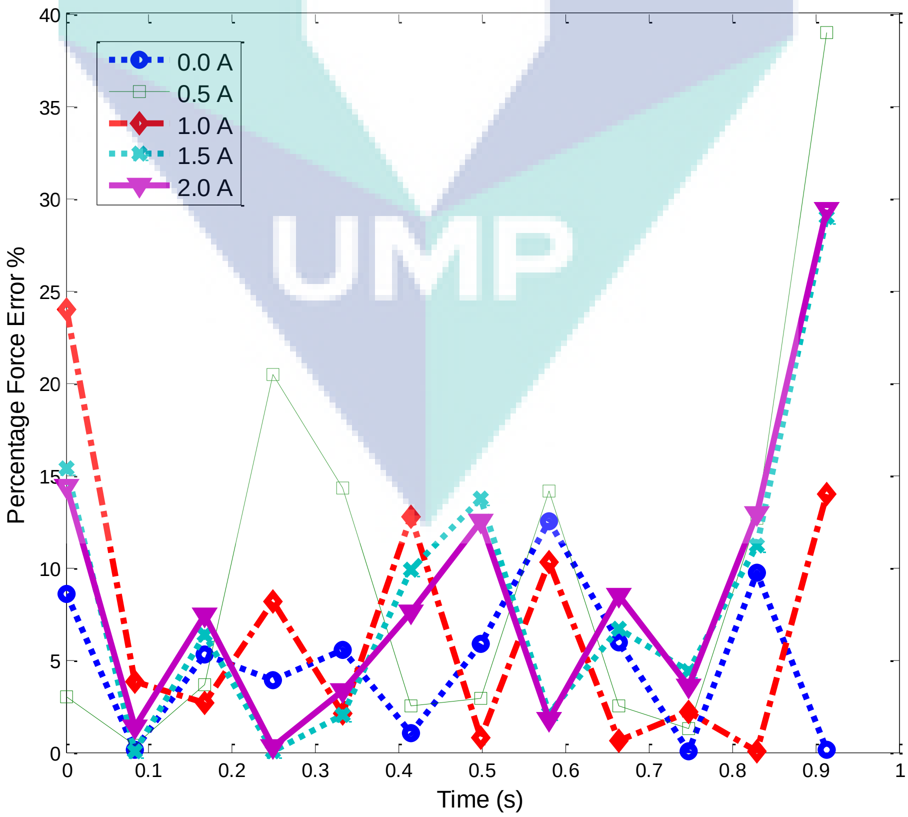

Figure 4.22: Percentage error comparisons for various test conditions

In the previous comment had declared the unruly nonlinearity impact on parametric identification. An apparent outliner was perceived for test input of 0.5 A at time 0.2 s as it elevated to 20 % error whereas others kept the composure to sustain their performances. As foreseen for the fragile point at time 0.8 s, it validates the error as for most test condition upsurge nearly 30 % to 35 % and reaches maximum percentage error. Nonetheless the overall operation of optimizing parameters was noteworthy. The consequence of these results were mainly founded by the parameters value and the indices are list in Table 4.3.

Table 4.3: Parameters value for various test conditions of Bouc-Wen by Kwok at al. (2007) model

Parameters	***Test conditions (A)*** **0**	**0.5**	**1**	**1.5**	**2**
Viscous coefficient, c	-19.03	20.07	160.75	956.04	1092.49
Stiffness coefficient, k	25.51	-321.96	4.21	1453.66	13.55
Scaling factor of hysteresis, α	142.85	333.96	463.38	445.53	658.72
Damper force offset, f_0	9.10	36.71	28.93	-2.60	-3.36
Hysteresis parameter, β	7.38	6.41	5.83	5.60	5.28
Hysteresis parameter, δ	0.52	0.59	0.47	0.50	0.53

From the list of parameter values indicates that the parameters diverse as the test input conditions changes. Noting the damper viscous coefficient c, it increases as the test input progresses. Whereas the remaining parameters have implied that the output varies primarily for the stiffness k. For parameter α, the estimation values are as anticipated while it develops to achieve re-enactment of hysteresis model. For the remaining parameters of f_0, β and δ, the amounts resides at a minimal range recommending that these parameters are oblivious towards the hysteretic model. In contrast the table endorsed the sensitive parameters are c and k as it fluctuates from one test condition to another. By deducing these parameters, it reveals that the instabilities were the effect of amending the simulation hysteresis model into the best possible fitting of MR fluid damper.

Root-mean square-error (RMSE) analysis was obtained in comparison with the hysteresis models of Bingham and Bouc-Wen model for concretise the selection of Bouc-Wen model by Kwok et al. (2007) as the best fitting model. The equation is given as:

$$\text{RMSE} = \sqrt{\frac{1}{n}\sum_{i=1}^{n}\left(F_{exp} - F_{sim}\right)^2} \tag{4.3}$$

in which the number of data points in n, F_{exp} and F_{sim} are the forces from experimental and simulated data respectively. The corresponding results are shown in Figure 4.23.

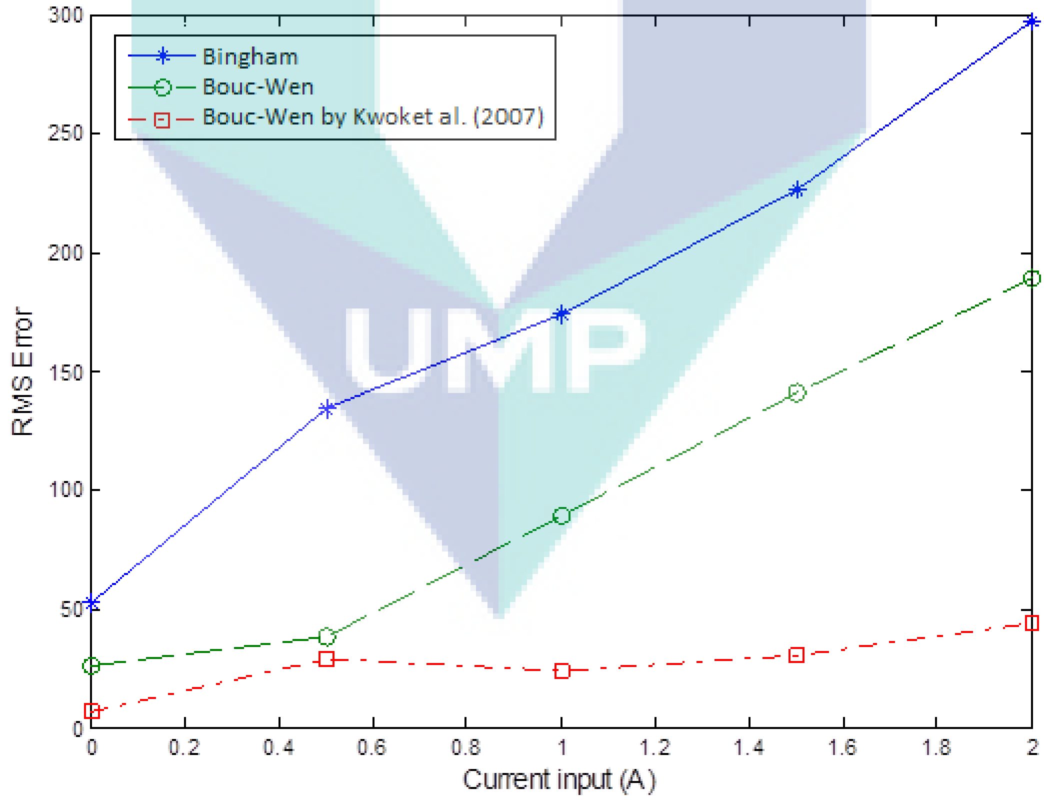

Figure 4.23 RMSE comparison of hysteresis models

4.5 SUMMARY

This chapter has reflected the hysteresis model as a whole in terms of curve fitting, statistical analysis of error and the optimized value for each parameter. The selection of the eminent hysteresis model is the Bouc-Wen by Kwok et al. (2007). It has indicated the remarkable consistency on applying the optimization phase for all test condition. The errors perceived were explicably diverse by the known fact of MR fluid damper nonlinearity, however the model defensibly appear to be reliable and robust concerning the identification. The parameter values fluctuated for certain, the sensitivity is rational by means of larger boundary imposed from MR fluid damper. This means that parameters of c and k plays large role in maintaining the model in a stable condition. Nonetheless the stability of Bouc-Wen model by Kwok (2007) was truly virtuous and it is factual to claim that this model is suitable for modelling the MR fluid damper.

CHAPTER 5

CONCLUSION

5.1 INTRODUCTION

In this chapter, the research summary, conclusion and proposed future research works was presented. The accountability from the results and analysis have aggregate to the extent of presumption.

5.2 SUMMARY OF THE THESIS

The main objectives of this research are to emulate a developed MR fluid damper behavior that is functional and operational to withdraw the performances by modeling via optimizing the parameters segmented in the hysteresis model.

Modeling an MR fluid damper has shortcomings prior to non-linearity features that comprises in the absorber behavior. The hysteresis model utilizes the parameters in distinctive manner to replicate the performance of the damper and with sustenance from PSO algorithm the hysteresis model is ample and robust to avert the non-linearity. Bouc-Wen model proposed by Kwok et al. (2007) has made the reproduction of MR fluid damper venerable with the provision of PSO algorithm that refines distinctive parameters of the hysteresis model impeccable.

This research has underlined considerable recommendation on inflicting approaches for future work in improving the current state of findings. For hysteresis model cases in obtaining more agile model, identified parameters that are not sensitive towards the hysteresis model are given a boundary value and for the delicate parameters a set of perceptive ration of their values is thoroughly allocated and specified.

In the development of a mono-tube MR fluid damper, the benchmark design was met according to the experiment requirements in allocating suitable data retrieval for simulation integration phase. The structural design of the damper has met the requirements for experiment purposes. The design comprises dimension of the magnetic choke device model and the operating current for various conditions were successfully fabricated. Furthermore, the behavior of MR fluid damper did illustrate a practical performance based on the research scope for the experiment.

Subsequent to the hysteresis parameters, the algorithm of PSO is analytically investigated before implanting to search and optimize the parameters for hysteresis model. The condition and cognitive function within the PSO are recognized beforehand along with simulation structure deduced by the programming codes. Nonetheless, the modeling for the hysteresis model must allocate the coherency between the practical data from experimental results and parameter identification method.

The results from comparing existing parametric models with the proposed Bouc-Wen model by Kwok et al. (2007) were done by computer simulation. Then the selected model is optimized through imposing PSO algorithm in assigning the significant parameters into best fitting model with respect to MR fluid damper. From the analysis it reveals that the average percentage error for the simulation to depict the MR fluid damper's behavior is approximately 6.0 % to 8.3 % marginal error. The estimation of this is presumed to be adequate recognizing the facts that several constraints were obliged during the process of this research.

Furthermore, the physical experimental results prove to provide tolerable response for the proposed structural and magnetic design of the absorber. This can be verified by the number of experiment taken with various test conditions. The collected data was mapped according to the test input and compared with simulation results. The simulation succeeds to project respective diagrams via MATLAB and Simulink hence advanced to optimizing the hysteresis model parameters using PSO algorithm.

The improvements portrayed by using Bouc-Wen model by Kwok et al. (2007) suggests that the parameters value fluctuate for high sensitive parameters and for the less significant variable were stagnant. Nevertheless the diversion value of each parameter implies that the model is agile to accommodate interchangeable state from the MR fluid damper behavior. If the implementation of the optimization method for the hysteresis modeling was to employ onto a real semi-active system, the small marginal error and robustness of this model can be accomplished. This is primarily to compensate the non-linearity of MR fluid damper and most importantly to gauge and predict the behavior in fast respond time.

Moreover, the results from simulation testimony for the control algorithm system of the PSO are much more efficient in search of best possible value for hysteresis model parameters. The proposed method has the advantages to amplify the model ability in parameter searching.

5.3 RESEARCH CONCLUSION

This research has succeeded to develop a practical mono-tube MR fluid damper for simulation investigation in modeling the behavior of the absorber by parametric identification of Bouc-Wen model by Kwok et al. (2007) method by optimizing the hysteresis parameters value using PSO algorithm.

This research has proved the competence of PSO algorithm in searching of the best credible value for Bouc-Wen model proposed by Kwok et al. (2007) to increase the modeling reliability of the MR fluid damper by associating between experiment and simulation process.

The significant contribution of this research is that the proposed method of applying the PSO algorithm to search the optimum value of Bouc-Wen hysteresis model parameters manage to depict the developed MR fluid damper for various test conditions and suitable for semi-active modeling.

5.4 FINDINGS AND CONTRIBUTION

The findings were accumulated and deliberated from the stage of experiment and simulation with the support of evaluation process. It suggests that several parameters of the hysteresis systems requires boundary and by imposing the known sensitive variables to the model can be emulated into near perfect model.

From realizing the hysteresis into and optimize platform it has indicated that the methods are reliable and thus managing the hysteresis parameters as independent product are acceptable. Hence, by imposing boundaries for each parameter can be accomplished.

5.5 SUGGESTION FOR FUTURE WORK

There are two main suggestions for the extension of future work in modeling the MR fluid damper:

The first suggestion is to find the boundary of hysteresis parameters and their relation specifically c, and k and the coherent parameters α, β and δ. In this research, these parameters were not given any specific range and relationships for the purpose of inflicting a behavior based on MR fluid damper. Hence the reason of fluctuated value occurs for the sensitive parameters whereas the stagnant parameters depict insignificant changes. Therefore, if these parameters were given specific instructions the model may behave in inventive manner as how the hysteresis model must perform.

For the MR fluid damper to increase accuracy on the modeling, the dynamics limitations of the damper behavior must be broadened. External sensors are required and by widening the frequencies exerted to the damper can demonstrate a realistic behavior of suspension systems during car motion with peripheral conditions is to be introduced.

REFERENCES

Abdullah, M. and Wilson, C.M.D., 2005, *Structural vibration reduction using fuzzy control of magnetorheological dampers* ASCE Structures Congress , 1-12

Ahmadian, M., Poynor, J.C. and Gooch, J.M., 1999, *Application of magneto rheological dampers for controlling shock loading*. American Society of Mechanical Engineers, Dynamic Systems and Control Division (Publication) DSC 67, 731-735.

Ahn, K., Truong, D. and Islam, M., 2009, *Modeling of a magneto-rheological (MR) fluid damper using a self tuning fuzzy mechanism*. Journal of Mechanical and ScienceTechnology 23, 1485-1499.

Ali, M.M. and Kaelo, P., 2008, *Improved particle swarm algorithms for global optimization*. Applied Mathematics Computing 196, 578-593.

Ashfak, A., Abdul, J.J. and Abdul, R.K.K., 2012, *Magneto-rheological (MR) Damper based vehicle suspension.* International Journal of Applied Engineering Research 7, 613-626.

Boada, M.J.L., Calvo, J.A., Boada, B.L. and Diaz, V., 2008, *Modelling of a Magnetorheological damper by recursive lazy learning*. International Journal of Non-Linear Mechanics 46, 479-485

Bouc, R., 1967. *Forced vibration of mechanical systems with hysteresis.* In: Proceedings of the fourth conference on non-linear oscillations, Prague, Czechoslovakia, p. 315.

Bossis, G., Lacis, S., Meunier, A. and Volkova, O., 2002, *Magnetorheological fluids.* Journal of Magnetism and Magnetic Material 252, 224-228.

Charalampakis, A.E. and Dimou, C.K., 2010, *Identification of Bouc–Wen hysteretic systems using particle swarm optimization*. Computers and Structures 88, 1197-1205.

Choi, S.B. and Lee, S.K., 2001, *A hysteresis model for the field-dependent damping force of a magnetorheological damper*. Journal of Sound and Vibration 245, 375-385.

Ciuprina, G., Loan, D. and Munteanu, I., 2002, *Use of intelligent-particle swarm optimization in electromagnetics*. IEEE Tranactions on Magnetics. 38, 1037-1040.

Clerc, M. and Kennedy, J., 2002, *The particle swarm - explosion, stability and convergence in a multidimensional complex space*. IEEE Transactions on Evolutionary Computation. 6, 58-73.

De Castro, L.N., 2002. *Immune, swarm and evolutionary algorithm part i: basic models. In: Proceeding of the international conference on Neural Information Processing*, pp. 1464-1468.

Dimopoulus, G.G., 2007, *Mixed-variable engineering optimization based on evolutionary and social metaphors*. Computer Methods in Applied Mechanics and Engineering 196, 803-817.

Dimou, C.K. and Koumousis, K.V., 2009, *Reliability based optimal design of truss structures using particle swarm optimization*. Journal of Computing in Civil Engineering - ASCE 23, 100-109.

Dominguez, A., Sedaghati, R. and Stiharu, I., 2006, *A new dynamic hysteresis model for magnetorheological dampers*. Smart Materials and Structures 15, 1179-1189.

Dong, X.M., Yu, M., Liao, C.R. and Chen, W.M., 2010, *Comparative research on semi-active control strategies for magneto-rheological suspension*. Nonlinear Dynamics 59, 433-453.

Du, H, Lam, J. and Zhang, N., 2006, *Modelling of magnetorheological damper by evolving radial basis function networks*. Engineering Applications of Artificial Intelligence 19, 869-881.

Dyke, S.J. and Spencer, Jr. B.F., 1997. *A comparison of semi-active control strategies for the MR damper*. In: Intelligent Information Systems, 1997. IIS '97. Proceedings, 8-10 Dec1997, pp. 580-584.

Dyke, S.J., Spencer, Jr. B.F., Sain, M.K. and Carlson, J.D., 1996, *Modelling and control of magnetorheological damper for seismic response reduction*. Smart Material nad Structures 5, 565.

Eberhart, R.C. and Shi, Y., 2000, *Comparing inertia weights and constriction factors in particle swarm optimization*. Proceedings of the Congress on Evolutionary Computation, 81-86.

Eberhart, R.C. and Shi, Y., 2001. *Particles warm optimization: developments, and applications and resources*. In: Proceedings of the Congress on Evolutionary Computation, pp. 81-86.

Ehrgott, R.C. and Masri, S.F., 1992. *Studies of a Controllable Electrorheological Vibration Damper*. In: First International Conference on Motion and Vibration Control, Yokohoma, Japan, Sept 7-11, pp. 356-361.

Engelbrecht, A.P., 2005, *Fundamentals of computational swarm intelligence*, John Wiley and Sons, Sussex.

Filisko, F.E. and Gamota, D.R., 1991, *Dynamic mechanical studies of electrorheological materials: moderate frequencies*. Journal of Rheology 35, 399-425.

Gaing, Z.L., 2004, *A particle swarm optimization approach for optimum design of PID in AVR system*. IEEE Trans. Energy Conversion 19, 384-391.

Gavin, H.P., Hose, Y.D. and Hanson, R.D., 1994. *Design and Control of Electrorheological Dampers. In: First World Conference on Structural Control, Pasadena*, CA, pp. WP3-83 through WP83-92.

Ge, H.W., Liang, Y.C. and Marchese, M., 2007, *A modified particle swarm optimization based dynamic recurrent neural network for identifying and controlling non-linear systems*. Computers and Structures 85, 1611-1622.

Gholizadeh, S. and Slajeghah, E., 2009, *Optimal design of structures subjected to time history loading by swarm intelligence and an advanced metamodel*. Computer Method in Applied Mechanics and Engineering 198, 2936-2949.

Guan, X.C., Guo, P.F. and Ou, J.P., 2011, *Modeling and Analyzing of Hysteresis Behavior of Magneto Rheological Dampers*. Procedia Engineering 14, 2756-2764.

Guglielmo, E, Sireteanu, T., Stammers, C., Ghita, G. and Giuclea, M, 2008, *Semi-active suspension control: Improved vehicle Ride and road friendliness*. London.

Guo, D and Hu, H., 2005, *Nonlinear-stiffness of a magnetorheological fluid damper*. Nonlinear Dyanimcs, 40, 241-249

Hassan, R, Cohanim, B., deWeck, O. and Venter, G., 2005. *A comparison of particle swarm optimization and the genetic algorithm*. In: Proceedings of 46th AIAA/ASME/ASCE/AHS/ASC Structures, Structural Dynamics & Material Conference, pp. 1-13.

Hrovat, D., 1997, *Survey of Advanced Suspension Developmnts and Related Optimal Control Applications*. Automatica, Vol 33, no 10, 1781-1817.

Hu, X., 2006. *Particle swarm optimization (PSO) tutorial*, http://www.swarmintelligence.org/tutorials.php/index.php

Ikhouane, F. and Rodellar, J., 2007, *Systems with Hysteresis: Analysis, Identification and Control using the Bouc-Wen model*. Wiley, West Sussex, England.

Isermann, R., 2003, *Mechatronic system: Fundmentals*. Springer-Verlag

Ismail, M., Ikhouane, F. and Rodellar, J., 2009, *The Hysteresis Bouc-Wen Model, a Survey*. Archives of Computational Methods in Engineering 16, 161-188.

Jansen, L. and Dyke, S., 2000, *Semiactive Control Strategies for MR Dampers: Comparative Study*. Journal of Engineering Mechanics 126, 795-803.

Jin, G., Sain, M.K. and Spencer, Jr. B.F., 2005, *Nonlinear blackbox modelling of MR dampers for civil structural control*. IEEE Transactions in Control Systems Technology 13, 345-355.

Jimenezz R and A Alvarez-Icaza L., 2005. *LuGre friction model for a magnetorheological damper*. Structural Control Health and Monitor. 12, 91-116

Kao, C.C., Chuang, C.W. and Fung, R.F., 2006, *The self-tuning PID control in a slider-crank mechanism system by applying particle swarm optimization approach*. Mechatronics 16, 513-522.

Kennedy, J and Eberhart, R., 1995. *Particle swarm optimization*. In: Proceedings of IEEE international conference on neural networks IV, Perth, Australia. Piscataway, NJ, pp. 1942-1948.

Kennedy, J., Eberhart, R.C. and Shi, Y., 2001, *Swarm Intelligence*. New York: Morgan Kaufmann

Kim, Y., Langari, R. and Hurlebeus, S., 2009, *Semiactive nonlinear control of a building with magnetorheological damper system*. Mechanical Systems and Signal Processing 23, 300-315.

Kwok, N.M., Ha, Q.P., Nguyen, T.H., Li, J. and Samali, B., 2006, *A novel hysteric model for magnetorheological fluid dampers and parameter identification using particle swarm optimization*. Sensors and Actuators A 132, 441-451.

Kwok, N.M., Ha, Q.P., Nguyen, T.H., Li, J. and Samali, B., 2007, *Bouc–Wen model parameter identification for a MR fluid damper using computationally efficient GA*. The International Society of Atomation ISA Transactions 46, 167-179.

Li, W.H., Yao, G.Z., Chen, G., Yeo, S.H. and Yap, F.F., 2000, *Testing and modelling of a linear MR damper under sinusodial loading*. Smart Materials and Structures 9, 95.

Liu, B, Wang, L., Jin, Y.H., Tang, F. and Huang, D.X., 2006, *Directing orbits of chaotic sytems by particle swarm optimization.* Chaos Soliton Fract 29, 454-461.

Liu, L, Liu, W. and Carters, D.A., 2008, *Particle Swarm Optimization - Based parameter identification applied to permanent magnet synchronous motors*. Engineering Applcations of Artificial Intelligence 21, 1092-1100.

Lord, Corporation, 1999, *Designing with MR fluids*. Lord Corporation Engineering note, Thomas Lord Research Center, Cary, NC.

Ma, F., Zhang, H., Bockstedte, A., Foliente, G.C. and Paevere, P., 2004, *Parameter analysis of the differential model of hysteresis*. Journal of Applied Mechanics ASME 71, 342-349.

Ma, X.Q., Wang, E.R., Rakheja, S. and Su, C.Y., 2002, *Modelling hysteretic characteristics of MR-fluid damper and model validation*. Proceedings of the 41st IEEE Conference on Decision and Control, Las Vegas, Nevada, 1675-1680.

Majhi, B. and Panda, G., 2010, *Development of efficient identification scheme for nonlinear dynamic systems using swarm intelligence techniques*. Expert System Application 37, 556-566.

Metered, H., Bonello, P. and Oyadiji, S., 2009, *Nonparametric Identification Modeling of Magnetorheological Damper Using Chebyshev Polynomials Fits*. SAE International Journal of Passenger Cars - Mechanical Systems 2, 1125-1135.

Poynor, J., Chaired by Ahmadian, M., 2001, *Innovative Designs for Magneto-Rheological Dampers*, Masters of Science in Mechanical Engineering thesis, Faculty of Virginia Polytechnic Institute and State University, Blacksburg Virginia

Priyandoko, G. and Mohamad, Z.B., 2013, *PSO-optimised adaptive nero-fuzzy system for magneto-rheological damper modelling*. International Journal of Applied Electromagnetics and Mechanics 41, 301-312.

Rabinow, J., 1948, *The magnetic fluid clutch*. American Institutes of Electrical Engineers Transactions. 67, 1308-1315.

Ray, T. and Liew, K.M., 2003, *Society and civilization: an optimization algortihm based on the simulation of social behaviour*. IEEE Transactions of Evolutionary Computation 7, 386-396.

Sahin, I, Engin T. and Cesmeci, S., 2010, *Comparison of some existing parametric models for magnetorheological fluid dampers*. Smart Materials and Structures 19. 035012 1-11.

Schurter, K.C. and Roschke, P.N., 2000. F*uzzy modelling of magnetorheological damer using ANFIS*. In: Proceedings of the Ninth IEEE International Conference on Fuzzy Systems, San Antonio, Texas, May 2000, pp. 122-127.

Schutte, J.F. and Groenworld, A., 2003, *Sizing design of truss structures using particle swarms*. Structural and Multidisciplinary Optimization 25, 261-269.

Shames, I.H. and Cozzarelli, F.A. 1992. *Elastic and Inelastic Stress Analysis*, Hall, P., ed. (Englewood Cliffs, New Jersey), pp. 120-122.

Spencer, Jr B.F., Dyke, S.J., Sain, M.K. and Carlson, J.D., 1997, *Phenomenological model of a magnetorheological damper*. ASCE Journal of Engineering Mechanics 123, 230-238.

Stanway, R., Sproston, J.L. and Stevens, N.G., 1987, *Non-linear modelling of an electrorheological vibration damper*. Journal of Electrostatic 20, 167-184.

Venter, G. and Sobieski, S.J., 2004, *Multidisciplinary optimization of a transport aircraft wing using particle swarm optimization*. Struct Multidiscip Optim 26, 121-131.

Wang, D.H. and Liao, W.H., 2011, *Magnetorheological fluid dampers: A review of parametric modelling*. Smart Materials and Structures 20. 023001, 1-34.

Wang, D.H and Liao, W.H., 2001. *Neural Network modelling and controllers for magnetorheological fluid dampers*. In: Proceedings of the 2001 IEEE International Conference on Fuzzy Systems, Melbourne, Australia, December 2001, pp. 1323-1326.

Wang, D.H. and Liao, W.H., 2005, *Modelling and Control of Magnetorheological Fluid Dampers Using Neural Networks*. Smart Materials and Structures 14.

Wen, Y.K., 1976, *Method for random vibration of hysterestic systems*. Journal of Engineering Mechanics American Society of Civil Engineers ASCE 102, 249-263.

Wereley, N.M. and Kamath, G.M., 1997, *A nonlinear visco-elasti-plastic model for electrorheological fluids*. Smart Materials and Structures 6, 351-359.

Wereley, N.M., Pang, L. and Kamath, G.M., 1998, *Idealized hysteresis modelling of electrorheological and magnetoreheological*. Journal Intelligent Material System Structures 9, 642-649.

Wilke, D.N, Kok, S. and Groenwold, A.A., 2007, *Comparison of linear and classical velocity update rules in particle swarm optimization: notes on diversity*. International Journal of Numerical Methods in Engineering 70, 962-984.

Winslow, W.M., 1947. *Method and means for translating electrical impulses into mechanical force.* Patent Num US2417850 A.

Winslow, W.M., 1949, *Induced Fibration of Suspensions.* Journal of Applied Physics 20, 1137-1140.

Ye, M., 2006. *Parameter identification of dyanmial systems based on improved particle swarm optimization.* In Intelligent Computing, Lecture notes in control and information sciences, Huang De-Shuang, L.K., George William Irwin, ed., pp. 351-360.

Zhou Q, Nielsena S R K and Qu W L, 2006. *Semi-active control of three-dimensional vibrations of an inclined sag cable with magneorheological dampers.* Journal of Sound and Vibrations. 296, 1-22

APPENDIX A

PSO PROGRAMMING CODE

```
%% clear all data
clc, clear, close all
%% load data
load data_hydraulic_50ms.mat
%% This data represent the values from from experimental input from
%% 0.0A to 2.0A in the form of force, velocity, acceleration and time

totalTime= length(ident_input.time);
%% ident_input.time is the length of experiment time taken of 920 data

for i=1:1:totalTime
    input_Ident(i)=ident_input.signals.values(1,1,i);
end
%% assignning input and output data
tIN = ident_input.time;
input_Ident = input_Ident';

tOUT = ident_output(:,1);
output_Ident = ident_output(:,2)*(10/40);

%% temporary plotting input & output data
subplot(211)
plot(tIN,input_Ident,'r'), grid on;

subplot(212)
plot(tOUT,output_Ident), grid on;

%% data isolation (between training data & validation data)

% selecting input data up to 40 s
inTrain = input_Ident(1:length(input_Ident)*40/100);
outTrain = output_Ident(1:length(output_Ident)*40/100);
tTrain = tIN(1:length(tIN)*40/100);

% assigning training input-output to variable
TrainInput.time = tTrain;
TrainInput.signals.values = inTrain;

TrainOutput.time = tTrain;
TrainOutput.signals.values= outTrain;

% assigning validating input-output to variable
ValidateInput.time = tIN;
ValidateInput.signals.values = input_Ident;

ValidateOutput.time = tOUT;
ValidateOutput.signals.values = output_Ident;


figure (2)
plot(tTrain,inTrain,tTrain,outTrain), grid on;
```

APPENDIX B

HYSTERESIS PARAMETER CODING

```
%% clear all data
clc, clear, close all
%% load data
load data_mrdamper.mat
%% This data represent the values from from experimental input from
%% 0.0A to 2.0A in the form of force, velocity, acceleration and time

totalTime = length(time);
%% time is translated from loading mr damper file

for i=1:1:totalTime
    input_Identd(i)=d15(:,i);
    output_Ident(i)=f15(:,i);
end

%% assignning input and output data
tIN = time;
input_Identd = input_Identd';

tOUT = time;
output_Ident = output_Ident';


%% temporary plotting input & output data
subplot(211)
plot(tIN,input_Identd,'r'), grid on;

subplot(212)
plot(tOUT,output_Ident), grid on;


%% data isolation (between training data & validation data)

% selecting input data up to 40 s
tTrain = tIN(1:length(tIN));
inTrain = input_Identd;%(1:length(input_Ident));
outTrain = output_Ident;%(1:length(output_Ident));

% selecting input data up to 40 s
inTrain = input_Identd(1:length(input_Identd));
outTrain = output_Ident(1:length(output_Ident));

% assigning training input-output to variable
TrainInput.time = tTrain;
TrainInput.signals.values = inTrain;

TrainOutput.time = tTrain;
TrainOutput.signals.values= outTrain;
```

APPENDIX C

MAIN SIMULINK

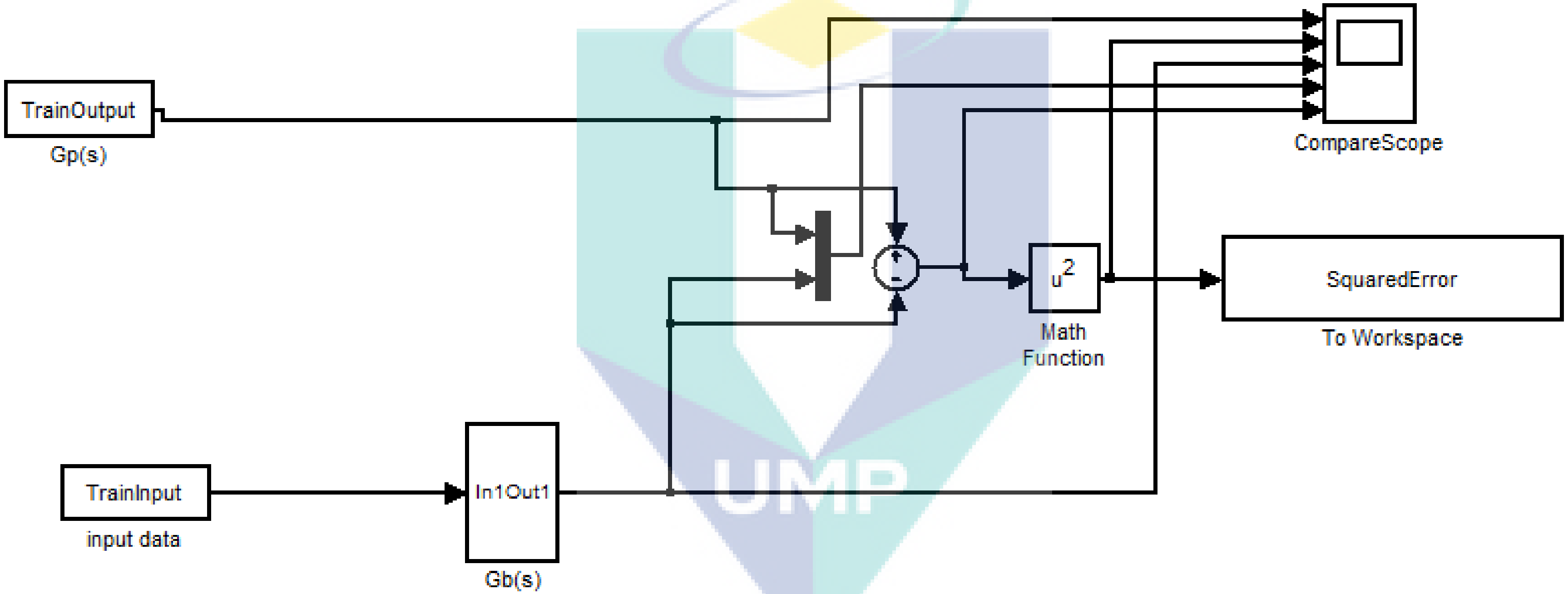

APPENDIX D

LIST OF PUBLICATIONS

Mohd Azraai Razman, Gigih Priyandoko, Ahmad Razlan Yusoff. (2014). *Bouc-Wen Model Parameter Identification For A MR Fluid Damper Using Particle Swarm Optimization*. Advanced Materials Research Vol. 903(2014) pp 279-284. Trans Tech Publications, Switzerland. doi:10.4028/www.scientific.net/AMR.903.279

Mohd Azraai Razman, Gigih Priyandoko, Ahmad Razlan Yusoff, Mohd Fadzil Rashid, *Optimization of Bouc-Wen model parameters identification of magneto-rheological fluid damper using Particle Swarm Optimization*. International Journal of Applied Electromagnetics and Mechanics (Submitted)

Advanced Materials Research Vol. 903 (2014) pp 279-288
Online available since 2014/Feb/27 at www.scientific.net

Doi:10.4028/www.scientific.net/AMR.903.279

Bouc-Wen model parameter identification for a MR fluid damper using particle swarm optimization

Mohd Azraai Razman[1, a], Gigih Priyandoko[2, b], Ahmad Razlan Yusoff[1, c]
[1]Faculty of Manufacturing Engineering, University Malaysia Pahang, 26600, Pekan, Malaysia
[2]Faculty of Mechanical Engineering, University Malaysia Pahang, 26600, Pekan, Malaysia
[a]azraai@ump.edu.my, [b]gigih@ump.edu.my, [c]razlan@ump.edu.my

Keywords: Bouc-Wen, Magneto-rheological, optimization, parametric identification

Abstract
This paper presents parameter identification fitting which are employed into a current model. Irregularity hysteresis of Bouc-Wen model is colloquial with magneto-rheological (MR) fluid damper. The model parameters are identified with a Particle Swarm Optimization (PSO) which involves complex dynamic representation. The PSO algorithm specifically determines the best fit value and decrease marginal error which compare to the experimental data from various operating conditions in a given boundary.

Optimization of Bouc-Wen model parameters identification of magneto-rheological fluid damper using Particle Swarm Optimization

Mohd Azraai Razman*[1], Gigih Priyandoko[2], Ahmad Razlan Yusoff[1], Mohd Fadzil Rashid[2]

[1]Faculty of Manufacturing Engineering, University Malaysia Pahang, 26600, Pekan, Malaysia
[2]Faculty of Mechanical Engineering, University Malaysia Pahang, 26600, Pekan, Malaysia

*Corresponding author, Tel: +60176454151
Email: azraai@ump.edu.my (M. Azraai)

Keywords: Bouc-Wen, Magneto-rheological, optimization, parametric identification

Abstract

The modelling of Magneto-rheological (MR) fluid damper for the control device has been a major focus throughout the decades as semi-active systems is deem to be efficient in vibration suppression for various application. MR fluid damper is abide by the behaviour of hysteresis model that not just predict the subsequent impact, but have the ability to retract the motion by the model internal memory. Acquiring a suitable model come a setback from the natural existence of non-linearity from the MR fluid damper as the parameters of the hysteresis model may requires tuning as the response time for the absorber to response are in milliseconds. Hence, Particle Swarm Optimization (PSO) was introduce for altering significant parameters for hysteresis model to replicate the MR fluid damper performance in real-time. Validation by physical experiment and simulation was conducted to enhance the justification of the present model. These performances are measure in force against displacement and force against velocity for the hysteresis model to depict MR fluid damper behaviour. The average marginal error was presented to strengthen the model along with analysis and discussion in deliberating the outcome.